7-24-2014

Selection of a Nanoparticle Stabilizer for a Calcium Phosphate Drug Delivery System

Jessica L. Woodman
University of Connecticut, jessica.woodman@uconn.edu

Selection of a Nanoparticle Stabilizer for a Calcium Phosphate Drug Delivery System

Jessica Lea Woodman, Ph.D.

University of Connecticut, 2014

Overall cancer survival rates steadily decline each year following diagnosis and side effects of chemotherapy restrict its use. The chemotherapeutic cis-diamminedichloro-platinum (cisplatin, CDDP) is poorly soluble and has dose limiting side effects. Nanoparticle delivery systems can deliver a higher dose of drug directly to the tumor by both active and passive targeting, holding promise of fewer side effects and greater anti-tumor efficacy. To date, few nanoparticle systems have been FDA approved for the treatment of cancer due to complicated physicochemical characterization, drug inactivation by the delivery system, scale-up challenges, and lack of demonstrated *in vivo* safety and efficacy. Further research is needed in this area.

This dissertation examined a naturally biocompatible carrier for delivery of CDDP: calcium phosphate (CaP). Three molecules were tested to stabilize CaP nanoparticles (nCaP) and increase injectability: sodium polyacrylate (D), sodium citrate (CIT) and carboxymethyl hyaluronic acid (CMHA). $nCaP^{D}CDDP$ and $nCaP^{CIT}CDDP$ were examined against a head & neck cancer (HNC) model, because HNC patients could greatly benefit from localized chemotherapy prior to surgical resection. Triple negative breast cancer (TNBC) with a $CD44^{high}/CD24^{-/low}$ cell phenotype has emerged as an important new target for chemotherapeutics. CD44 is the major receptor for hyaluronic acid, targetable with CMHA. These studies showed all three molecules stabilized nCaP as measured by light scattering, zeta

potential, x-ray diffraction and transmission electron microscopy, and released biologically active CDDP as measured by *in vitro* release studies and *in vitro* cytotoxicity testing. However, intratumoral (IT) delivery of nCaP^{D}CDDP or nCaP^{CIT}CDDP was not as effective as CDDP IT *in vivo* against murine and human HNC tumor models, due stabilizer inhibition of CDDP. Surface plasmon resonance proved CMHA and nCaP^{CMHA}CDDP bind CD44. CMHA didn't inactivate CDDP and nCaP^{CMHA}CDDP had comparable activity to free CDDP *in vitro*. Local delivery of nCaP^{CMHA}CDDP did not demonstrate a benefit over local delivery of CDDP in a human TBNC mouse model, due to lack of even distribution of nanoparticles throughout the tumor where CDDP alone could freely diffuse. These studies show that localized delivery of CDDP remains a promising strategy to increase drug effectiveness while decreasing drug side-effects that negatively impact cancer patients.

Selection of a nanoparticle stabilizer for a calcium phosphate drug delivery system

Jessica Lea Woodman

B.S., Rensselaer Polytechnic Institute, 2006

A Dissertation

Submitted in Partial Fulfillment of the

Requirements for the Degree of Doctor of Philosophy

At the

University of Connecticut

2014

APPROVAL PAGE

Doctor of Philosophy Dissertation

Selection of a Nanoparticle Stabilizer for a Calcium Phosphate Drug Delivery System

Presented by

Jessica Lea Woodman, B.S.

Major Advisor_____
Liisa T. Kuhn

Associate Advisor_____
A. Jon Goldberg

Associate Advisor _____
Diane J. Burgess

Associate Advisor _____
Aliassghar Tofighi

University of Connecticut

2014

Acknowledgements

I would like to begin my thanking my parents, whose love and guidance though out my life allowed me to achieve all I have today. From when I was very young, I was instilled with the value of hard work and determination. My parents have always led by example, whether we were doing yard work or volunteering at our church. My father believes if you are going to do something, it must be done the right way, otherwise there isn't purpose. I believe this simple rule is what has driven me throughout my life. They overcame much adversity in their own lives, which has only made them stronger, better people and parents. It is difficult to express how thankful I am for their love, support and guidance.

My family has served as a great source of support. My brother is my counterbalance. I cannot imagine my life without him growing up by my side. I have wonderful, loving Grandmothers and Aunts, who have always helped me in times of need. I was lucky enough to have three sets of great grandparents, who were sources of inspiration and perseverance. They represent strength and the ability to overcome the most challenging of situations. Lastly, my fiancé, Frank Iacono, has been and will continue to be the most amazing partner to traverse life with. His love and support propelled me in times I lagged and picked me up any time I fell.

Lastly, I would like to thank my major advisor, Dr. Liisa Kuhn, as well as my committee members, Dr. A. Jon Goldberg, Dr. Diane Burgess and Dr. Aliassghar Tofighi. Together they have been a great resource of knowledge. Over the years they have helped me develop my skills as a scientist. I am grateful for their instruction, patience and support during my graduate education.

Table of Contents

List of Figures

List of Tables

List of Abbreviations

A2780cis	human cisplatin-resistant ovarian carcinoma cells
Aq CDDP	aquated cisplatin, made via reaction with $AgNO_3$ to precipitate AgCl, thus removing Cl^- ions from the cisplatin molecule leaving it with a net positive charge
BC	breast cancer
BT-474	human epithelial breast cancer cells from the mammary gland
BT-474m	human mesenchymal-like breast cancer cells, transformed from BT-474 cells
CaP	calcium phosphate
CDDP	cis-diamminedichloro-platinum, cisplatin
CIT	sodium citrate
CMHA	carboxymethyl hyaluronic acid
D	Darvan® 811, sodium polyacrylate
ER	estrogen receptor
FaDu	human squamous cell carcinoma of the head and neck
FDA	Food and Drug Administration
HER-2	human epidermal growth factor receptor 2
HNC	head and neck cancer
IC50	Inhibitory concentration of drug that causes 50% cell death
ICP-OES	Inductively coupled plasma optical emission spectroscopy
IP	intraperitoneal injection, systemic
IT	intratumoral injection
IVIVC	in-vitro-in-vivo-correlation
LMS	luminal –to – mesenchymal switch cells, transformed from MCF-7 cells

MCF-7 human epithelial breast cancer cells derived from a metastatic site, luminal type A

microCaP calcium phosphate microparticles precipitated without a stabilizer

MTS (3-(4,5-dimethylthiazol-2-yl)-5-(3-carboxymethoxyphenyl)-2-(4-sulfophenyl)-2H-tetrazolium), a one-step MTS assay: Promega CellTiter 96® AQueous One Solution Cell Proliferation Assay

nCaP^{CIT} calcium phosphate nanoparticles, stabilized with sodium citrate

nCaP^{CIT}CDDP calcium phosphate nanoparticles, stabilized with sodium citrate carrying cisplatin

nCaP^{CMHA} calcium phosphate nanoparticles, stabilized with carboxymethyl hyaluronic acid

nCaP^{CMHA}CDDP calcium phosphate nanoparticles, stabilized with carboxymethyl hyaluronic acid, carrying cisplatin

nCaP$^{D/2}$CDDP calcium phosphate nanoparticles, stabilized with Darvan® 811, sodium polyacrylate, carrying cisplatin

nCaP^{D} calcium phosphate nanoparticles, stabilized with Darvan® 811, sodium polyacrylate

nCaP^{D}CDDP calcium phosphate nanoparticles, stabilized with Darvan® 811, sodium polyacrylate, carrying cisplatin

nCaP^{x} calcium phosphate nanoparticles, stabilized with X, where X is one of the stabilizers examined

nCaP^{x}CDDP calcium phosphate nanoparticles, stabilized with X, where X is one of the stabilizers examined, carrying cisplatin

NCI National Cancer Institute

NT near tumor injection

PR	progesterone receptor
SCCVII	mouse squamous cell carcinoma of the head and neck
subcut	subcutaneous injection
TEM	transmission electron microscopy
TNBC	triple negative breast cancer, tumor lacks expression of progesterone receptor, estrogen receptor and human epidermal growth factor receptor -2
UCHC	University of Connecticut Health Center
USP	United States Pharmacopeia
XRD	X-ray diffraction

Chapter 1

Specific Aims and Background

1.1 Specific Aims

Despite a combination of surgery, radiation and/or chemotherapy overall survival rates for a majority of cancers steadily decline each year following diagnosis, with an estimated 1,600 deaths per day in 2013[1,2]. Chemotherapy has many debilitating side effects because it kills normal replicating cells while killing cancer cells. Nanoparticles can deliver a higher dose of drug directly to the tumor by both active and passive targeting, with the goal of fewer side effects and greater anti-tumor efficacy[3–5]. However, few nanoparticle systems have been FDA approved for the treatment of cancer due to complicated physicochemical characterization, scale-up challenges[6], and lack of demonstrated *in vivo* safety and efficacy[7]. Stabilizer molecules are often needed to prevent nanoparticle aggregation but may negatively interact with the drug[8–10]. Targeting ligands that may increase specific cancer cell interaction must be carefully attached to present the active groups to the cells[11–13]. In order to develop an efficacious nanoparticle delivery system, it's important to have an understanding of how each component of the nanoparticle system interacts with the drug. Although CDDP is an effective anti-cancer drug it has limited solubility and dose-limiting side effects including: nephrotoxicity, nausea, vomiting and anemia. Thus, there is a need to improve the delivery of CDDP.

CaP offers a naturally biocompatible carrier for delivery of CDDP[14]. A stabilizer molecule is needed to prevent CaP nanoparticle aggregation and to increase injectability of the particulate delivery system[14,15]. We have previously shown that CDDP released from sodium

polyacrylate (D) stabilized CaP nanoparticles ($nCaP^{D}CDDP$) has comparable toxicity to free drug against cancer cells *in vitro*[16]. However, when attached to the $nCaP^{D}$ the CDDP was significantly less toxic than free CDDP *in vitro* and our unpublished animal studies revealed a corresponding lack of *in vivo* anti-tumor efficacy relative to free drug. CDDP attached to CaP microparticles without stabilizer did not lose activity, but were not easily injectable, which led to the conclusion that further work was needed to identify an alternative stabilizer that would not inactivate the drug. The goal of these studies is to develop a stabilized, injectable calcium phosphate nanoparticle system for the delivery of CDDP that releases active drug and can furthermore be targeted to therapy resistant cancer cells. Therapy resistant cells have emerged as important target and in breast cancer those cells have a $CD44^{high}/CD24^{-/low}$ phenotype[17–19]. CD44 is the receptor for hyaluronic acid, which is a widely used non-toxic biomaterial that could be used as a stabilizer of calcium phosphate when modified to contain carboxylate groups, such as carboxymethyl hyaluronic acid (CMHA)[20]. The envisioned biocompatible nanoparticle system may one day impact the longevity of cancer patients by enabling the sustained delivery of higher doses of CDDP directly to the tumor and the subset of therapy resistant cells through intratumoral injections with less toxicity.

Aim #1: Select a stabilizer that achieves a highly drug loaded, stable nanoparticle delivery system. *Hypothesis: If a molecule is a successful stabilizer for a calcium phosphate nanoparticle delivery system for CDDP then CDDP will bind to the stabilized nanoparticles and will be released slowly.* In addition to the previously published stabilizing molecule sodium polyacrylate (Darvan ® 811, D); sodium citrate (CIT)[21] and carboxymethyl hyaluronic acid (CMHA)[20] were also tested. Particle size was assessed with dynamic light scattering (DLS), transmission electron

microscopy (TEM). X-ray diffraction (XRD) determined structure. Inductively coupled plasma optical emission spectrometry (ICP-OES) determined Pt content which corresponds to CDDP. *In vitro* drug release was performed using a modified USP apparatus 4[22].

Aim #2: Examine the anti-cancer activity of CDDP loaded stabilized nanoparticles *in vitro*. *Hypothesis: If the stabilized CaP nanoparticle delivery system does not inactivate CDDP, then the CDDP loaded nanoparticles will have equal or greater* in vitro *cytotoxicity than CDDP alone.* Each stabilized nanoparticle delivery system (nCaP^{x}CDDP, where x = D, CIT or CMHA) made in Aim#1 was analyzed to determine the drug concentration that inhibits proliferation by 50% (IC50) using an MTS assay (Promega CellTiter Aqueous One). nCaP^{x}CDDP and CDDP reacted with stabilizer was compared to CDDP alone to determine if the stabilizer affects the drug activity by itself or as part of the nanoparticle delivery system. Surface Plasmon resonance (SPR) examined the binding of nCaP^{CMHA}CDDP and recombinant human CD44-Fc chimera antibody.

Aim #3: Assess the *in vivo* anti-tumor effect of CDDP loaded nanoparticles after intratumoral delivery. *Hypothesis*: *If the nCaP^{x}CDDP releases active CDDP at locally high concentrations in the tumor environment after intratumoral injections, then nCaP^{x}CDDP treated mice should have reduced tumor growth rate without systemic toxicity as compared to free drug.* Subcutaneous tumors from mouse and human cancer cells were initiated in the flanks of nude mice. Tumor volume and animal weight were measured daily after cell injections. Animals were treated with nCaP^{x}CDDP intratumorally (IT) and, compared to a positive control of CDDP that can only be administered at a lower dose due to systemic toxicity and solubility limits.

1.2 Background

In the United States, approximately 1.7 million new cases of cancer were diagnosed in 2013[2]. Cancer causes one in four disease related deaths in the United States, and an ever aging population is expected to drastically increase the number of cancer-associated deaths over the next 20 years. The rate of cancer incidence has declined in the United States since 1975 yet it was estimated that over 1.6 million new people were diagnosed with cancer in 2013[2]. The National Institutes of Health estimate that the overall cost of cancer was approximately 201.5 billion dollars, in 2008[23]. This dissertation is focused specifically on treatments for head and neck cancer and breast cancer because of the large potential benefit to these patients from localized treatment prior to surgical resection. Tumor reducing treatments could mean normal tissue is spared and chemotherapy side effects are reduced. The incidence, current treatments and outlook for each type of cancer is reviewed.

1.2.1 Head and Neck Cancer

Cancer of the head and neck is the 6th most common cancer worldwide[24]. In 2008, it was estimated that we spent 3.2 billion dollars on head and neck cancer (HNC) treatment in the United States[25]. It is commonly a squamous cell carcinoma found in the oral cavity, nasal cavity, nasal sinuses, oropharynx, hypopharynx, thyroid, lips, or larynx. HNC is typically linked to damage from alcohol and/or carcinogens. Recently, human papillomavirus (HPV) has also been elucidated as a driver for specific types of HNC. It is estimated that 30% of HNCs, specifically those of the oral cavity/pharynx are associated with HPV with a specific genetic profile linked with HPV16-*E6* oncogene expression[26–28]. The complex anatomical locations of HNC are a major consideration during treatment planning for HNC patients. Physicians are tasked with balancing the tumor control/survival and the patients' quality of life and overall functionality,

during and following treatment. There are often major complications with eating, breathing, speaking in addition to disfigurement associated with HNC.

First line therapy is surgical resection but often surgery is very complicated or impossible because tumors are located close to vital anatomy, like the carotid artery[29]. There has been some evidence that neoadjuvant therapy lowers the occurrence of distance metastases, but no benefit in loco-regional control or survival benefit was found[29]. Radiotherapy and chemotherapy are the only options for unresectable tumors, which are often used in combination leading to significant acute and long term side-effects[30]. CDDP is the standard chemotherapy for HNC patients which may be combined with other therapies, yet 50% of patients recur within 2 years following initial treatment[29]. This statistic highlights the necessity for advanced therapies to treat HNC.

An injectable collagen gel carrying CDDP and epinephrine (IntraDose) was entered into several clinical trials for intratumoral therapy against a wide range of solid tumor based cancers. Separate clinical trials were conducted for the treatment of recurrent metastatic breast cancer and head and neck cancer, yet both trials failed due to lack of clinical and patient benefit combined with toxicity[31–35]. There is currently no clinically approved molecular therapy for the treatment of HNC. This is in part due to lack of molecular targets. Generally, those that are currently in clinical trials are known drivers for carcinogenesis being applied to HNC, but are not truly specific to HNC. The few molecular targets for HNC are epidermal growth factor receptor (EGFR), vascular endothelial growth factor and small molecules such as PI3 kinase and mTOR. Inhibitors or monoclonal antibodies have been developed to specifically target these drivers of cancer. More than 35 clinical trials are being conducted specifically for HNC with targeted therapies alone or in combination with chemotherapy at varied disease stages[36,37]. To date, none

of these approaches have stood out above current clinical practice for tumor shrinkage, mean survival time or disease free progression.

1.2.2 Breast Cancer

In the United States, 1 in 36 women will die from breast cancer[38]. The American Cancer Society estimates that 12% of women in the United States will have invasive breast cancer during their lives[2]. Breast cancer risk increases with age and there are specific inheritable mutations that are strongly linked to susceptibility, in the BRCA1 and BRCA2 genes. Treatment options are patient specific, but typically include surgical removal of the mass and often radiation therapy[39]. Many breast cancers over-express estrogen receptor (ER), progesterone receptor (PR) and/or human epidermal growth factor receptor 2 (HER-2). Targeted hormone therapies are approved for patient specific treatment, based on their disease progression and hormone status. It is estimated that 20-25% of women with invasive breast cancer will be classified as triple-negative, which means their tumor lacks expression of ER, PR, and HER-2[40]. Triple negative breast cancers (TNBC) are typically more aggressive and challenging to treat and cannot benefit from directed hormone therapy. This sub-type of breast cancer will be focused on within this dissertation.

Chemotherapy is the first line of defense for TNBC patients, instead of the molecular therapies directed against breast cancers[40]. If the cancer recurs, short-term and overall survival is significantly shorter for those patients than for non-TNBC patients[41]. Recurrence is hypothesized to be due to therapy resistant cells within the tumor[18,42]. Therapy resistant breast cancer cells have a common phenotype of $CD44^{+}/CD24^{low}$ [43–46]. Two studies examining patient samples histologically found a correlation between TNBC, $CD44^{+}/CD24^{low}$ and recurrence[17,19,47,48]. In a

recent multi-center study, TNBC patients were treated with four cycles of CDDP (not commonly used to treat TNBC) and 50% of patients had a good response (22% complete pathologic responses)[49]. This is an important finding for the work performed in Chapter 4 of this dissertation.

In Dr. White's laboratory, at the University of Connecticut Health Center (UCHC), human luminal A breast cancer cells, MCF-7s, were serially cultured into mammospheres for 5 weeks, where each week cells were dissociated and placed into a new mammosphere culture. After 3 weeks, the cells had undergone epithelial to mesenchymal transition (EMT), such that when placed into two-dimensional culture they displayed a mesenchymal, $CD44^{+}/CD24^{-/low}$ phenotype, referred to as luminal to mesenchymal switch (LMS) cells[50]. This protocol was also performed with human luminal breast cancer cells, BT-474s. BT-474 cells have a $CD44^{-/low}/24^{high}$ phenotype[51,52]. After serial mammosphere passages BT-474 cells underwent EMT, referred to as BT-474m cells, resulting in a mesenchymal phenotype including enhanced proliferation rate, up-regulation of vimentin, down-regulation of E-cadherin (unpublished data) and cell surface marker expression of $CD44^{+}/CD24^{-}$. Importantly, these cells were negative for ER, PR and HER-2, making them a representative TNBC cell. This work was performed in Dr. Bruce White's lab at UCHC and will be published elsewhere.

1.2.3 Intratumoral Chemotherapy

Most cancer treatments, especially chemotherapy, kill healthy cells as well as diseased cells, leading to debilitating systemic side effects. Physicians currently use systemic chemotherapy to treat most cancers despite the cancer being in a specific anatomical location[53]. CDDP for example is poorly soluble and causes nephrotoxicity, nausea, anemia and other deleterious side-effects[54]. Intratumoral chemotherapy is the administration of chemotherapy directly into the

primary tumor, allowing for higher doses to be administered while systemic exposure is greatly reduced[55]. Clinicians' interest in intratumoral drug delivery systems began more than 60 years ago, yet advances in this technique have been insufficient to make intratumoral delivery a mainstream practice today[56]. Early work delivering chemotherapy locally showed little benefit over systemic treatment, due to local toxicities and frequent complications[57–59]. The advent of a delivery system able to control the release of drug at a therapeutic concentration within a tumor would alleviate these problems and those due to systemic treatment.

Several drug delivery systems aimed at intratumoral delivery of chemotherapeutic drugs, including CDDP, have been attempted with limited success[32,56,60–64]. IntraDose, a collagen/CDDP/epinephrine gel, had initial pre-clinical success, but ultimately failed to obtain approval for intratumoral treatment of head and neck squamous cell carcinoma from the U.S. Food and Drug Administration (FDA) due to toxicity and a lack of significant clinical benefit[31]. The collagen gel did not control the release of CDDP, leading to the addition of epinephrine (a vasoconstrictor) in an attempt to keep the CDDP within the tumor. The burst release of CDDP from the collagen gel ultimately was not controlled by the epinephrine[32–34]. Particulate bioceramics offer a non-inflammatory, biodegradable carrier for drug, non-viral gene, and protein delivery that may be able to overcome the problems of the previous work including uncontrolled drug release, side-effects due to the drug carrier and accumulation of drug in healthy tissues[65–67]. Calcium phosphate microspheres carrying an anti-angiogenic agent delivered locally to human uterine sarcoma xenografts caused a significant decrease in tumor weight compared to local treatment with the agent alone[68]. Calcium phosphate cements (CPCs) have been studied for local delivery of chemotherapy and concurrent bone healing. CDDP and caffeine delivered from calcium phosphate cement in a rat model of osteosarcoma significantly

reduced tumor size and mean survival of animals due to an extended release time of drug[69]. Delivery of cements and microparticles requires large gauge needles that are not attractive or common for delivery of drugs, therefore a readily injectable suspension would be more attractive. As with most local drug delivery vehicles, it is essential that the release of drug be controlled such release is stably within the therapeutic window to alleviate the necessity of several doses. If this is not achieved the delivery vehicle may not surpass the effectiveness of the drug alone.

1.2.4 Nanoparticles for Cancer Therapy

Attachment of drug to a particulate drug delivery system is a tactic that has long been employed to sustain drug delivery with promising results[70,71]. Human capillaries are approximately 5 um in diameter, thus nanoparticles can freely travel throughout circulation[72]. Nanoparticles are attractive for the treatment of cancer for many reasons. They can be designed to actively or passively target tumors. Passive targeting by nanoparticles relies on the enhanced permeability and retention (EPR) effect, due to leaky tumor vasculature that allows particles to collect within the tumor. Active targeting of nanoparticles involves the incorporation of a ligand, antibody or other specified moiety that will specifically bind cancer cell surface receptors with the goal of cell uptake. Many chemotherapeutics are poorly soluble and have short biological half-lives. Nanoparticles can be loaded with high concentrations of chemotherapeutic drug increasing their solubility and often the drugs' residence time in the body. In recognition of the vast opportunities nanoparticles offer for advances in cancer diagnosis and treatment, the National Cancer Institute (NCI) created the Nanotechnology Characterization Laboratory (NCI-NCL). Researchers can submit applications to NCI-NCL for pre-clinical characterization and toxicity testing of their nanoparticles. To date, FDA approved nanoparticle therapies for the treatment of

cancer is limited, due in part to the complexity of each systems' components and their relative biological effects[6].

Nanoparticles can be synthesized from a wide range of materials including: metals, natural or synthetic polymers, ceramics or proteins. Liposomes were one of the first drug delivery technologies developed. Doxil® (Janssen Products, LLC) is an example of an FDA approved PEGylated-liposomal formulation of doxorubicin. Doxil® is indicated for the treatment of recurrent ovarian cancer and relapsed or refractory multiple myeloma[73]. Polyethylene glycol (PEG) coating of nanoparticles (PEGylation) limits their detection by the immune system, termed stealth nanoparticles[74]. Albumin nanoparticles carrying paclitaxel, Abraxane® (Celgene Corporation), is indicated for the treatment of metastatic breast cancer, advanced non-small cell lung cancer and recently for metastatic pancreatic adenocarcinoma[75].

There has been some success in liposome-based drug delivery systems for cancer therapy but further effort is necessary to make them inert and long-circulating in blood, able to efficiently bind and transfer with targeted sites, and able to sustain release of active components after targeting[5,13,74,76,77]. Clinical trials have been conducted with a liposomal PEGylated CDDP delivery system, SPI-77, for the treatment of non-small cell lung cancer as well as recurrent epithelial ovarian cancer. In both studies patients failed to significantly benefit from the treatment overall in addition to significant concerns regarding high lipid load combined with large deposits of platinum in non-diseases tissues throughout the body[78,79]. Biodegradable polymer-based drug delivery systems often have acidic byproducts, which can produce adverse effects on the body or the drug attached or encapsulated[4,60,71,80]. Naturally occurring biopolymers or synthetic biopolymers such as polypeptides can also be employed as drug carriers, but their

quality, reliability and the high cost of preparation can often prevent their usage[81]. These limitations provide the motivation for continued research in biomaterials for drug delivery.

1.2.5 Polymeric Stabilization of Nanoparticles

Stability is a major concern for nanoparticle formulations. If nanoparticles agglomerate in suspension, they are no longer nanometer in size and will fall out. The most common approach to enhancing nanoparticle stabilization is with the addition of polymers and/or surfactants to the surface of the nanoparticle. PEG is likely the most common polymeric solution to nanoparticle instability, by steric stabilization with the brush-like corona it creates around particles. PEGylation is often performed on liposomal formulations where it serves not only as a colloidal stabilizer but also as a biological stabilizer, allowing the liposomes to avoid opsonization by serum proteins[74,82]. Doxil® is an example of an FDA approved PEGylated liposomal formulation. Calcium phosphate nanoparticles carrying genetic material have also been PEGylated for pH sensitive intracellular delivery of payload[10,83]. Natural polymers such as chitosan have been utilized to stabilize nanoparticles. Calcium phosphate has been effectively stabilized by chitosan for gene transfection and drug delivery[84,85]. Additional methods to stabilize calcium phosphate nanoparticles will be discussed thoroughly in the next section.

1.2.6 Calcium Phosphate Nanoparticles

Significant research has been conducted for the use of CaP as a bone replacement in the form of cement or particles[69,86–88]. Due to its inherent biocompatibility, CaP has been elucidated as an attractive biomaterial for a wide range of applications, such as a vector for gene delivery, probe diagnostic imaging, or adjuvant for vaccinations[84,89–92]. They have a high affinity to proteins, DNA, enzymes and cells giving them great potential as effective delivery vehicles[65,83,89,93]. The

reactive crystal surface of calcium phosphate particles facilitates rapid binding of charged and even neutral molecules to its surface and control of molecule release[67,94]. Nanoparticle formulations of calcium phosphate have been shown to effectively transport several types of molecules across cell membranes[94–96].

Particulate CaP can be synthesized via wet precipitation. Original interests in the controlled synthesis of CaP were to understand and recapitulate the formation of bone and teeth in vertebrates[97]. CaP nanocrystals can be synthesized without stabilizer, but careful control of the precipitation and immediate freeze drying is essential to avoid conversion and agglomeration[66]. These nanocrystals are often sintered or otherwise fused together to create large biomaterial scaffolds, for bone or tooth applications. For drug delivery, Barroug et al. showed poorly crystalline and amorphous calcium phosphate are more reactive than crystalline particles due to more surface defects allowing for greater drug adsorption[15].

Many approaches have been applied to the synthesis of stabilized CaP nanoparticles (nCaP). Stabilization has been achieved by incorporating DNA into the precipitated nCaP, which could then be coated with polymers for enhanced transfection efficiency[89,93,95,98]. nCaP can be stabilized by the addition of sodium citrate due to the interactions of the carboxylate groups of the citrate and the Ca[21,99]. A range of polymers have also been utilized to stabilize nCaP during precipitation including: sodium polyacrylate[16], PEG-*block*-poly(aspartic acid)[10], polyethyleneimine[100], and carboxymethyl cellulose[94,101]. Specific applications of calcium phosphate for delivery of chemotherapeutics have been somewhat limited in comparison to liposomal and polymeric formulations. Recently, Iafisco et al. reported targeted cellular uptake of biomimetic apatite nanocrystals carrying doxorubicin, but their *in vitro* cytotoxicity was not greater than free doxorubicin[102]. The same group has shown that biomimetic hydroxyapatite

nanoparticles can bind and release cationic, anionic and neutral drugs for anti-cancer and simultaneous bone regeneration applications[103]. Work in our lab using sodium polyacrylate to stabilize nCaP for the delivery of CDDP for localized treatment of head and neck cancer will be further explored in the following chapter. CDDP is bound to nCaP utilizing a cationic, aquated species of CDDP. The free Cl ions in physiological environments is a driving force for CDDP release (Figure 1.1 A)[14,15]. Additionally, CaP is known to dissolve in acidic pH, similar to that found in the tumor microenvironment and lysosomes within cells (Figure 1.1 B)[104–107].

1.2.7 Summary

Treatments for cancer patients can be limited due to anatomical location. Surgical resections for HNC can be disfiguring and dangerous, and localized radiation causes major side-effects drastically lowering quality of life for patients[30]. CDDP is an effective chemotherapeutic, but is limited due to low solubility and nephrotoxicity. Localized delivery of a high dose of CDDP to shrink the tumor and minimize side-effects could greatly benefit patients. TNBC patients have limited treatment options, because their cancer presents with none of the commonly targeted hormone receptors in standard BC hormone treatments. Localized treatment with a nanoparticle targeted to $CD44^{+}/CD24^{-/low}$, therapy resistant breast cancer cells is an attractive approach to prevent difficult to treat recurrence. Calcium phosphate nanoparticles are biocompatible and known to bind and release CDDP effectively, but require effective stabilization. Thus this dissertation evaluates stabilizer candidates for: (1) ability to stabilize nCaP, (2) allow for biologically active CDDP to release from the nanoparticles, and (3) effectively deliver a local, high dose of CDDP to tumors *in vivo* to delay tumor growth while causing fewer side-effects than systemic CDDP. We demonstrate that localized delivery of chemotherapy remains a

promising strategy to increase drug effectiveness while decreasing drug side-effects that negatively impact cancer survivors.

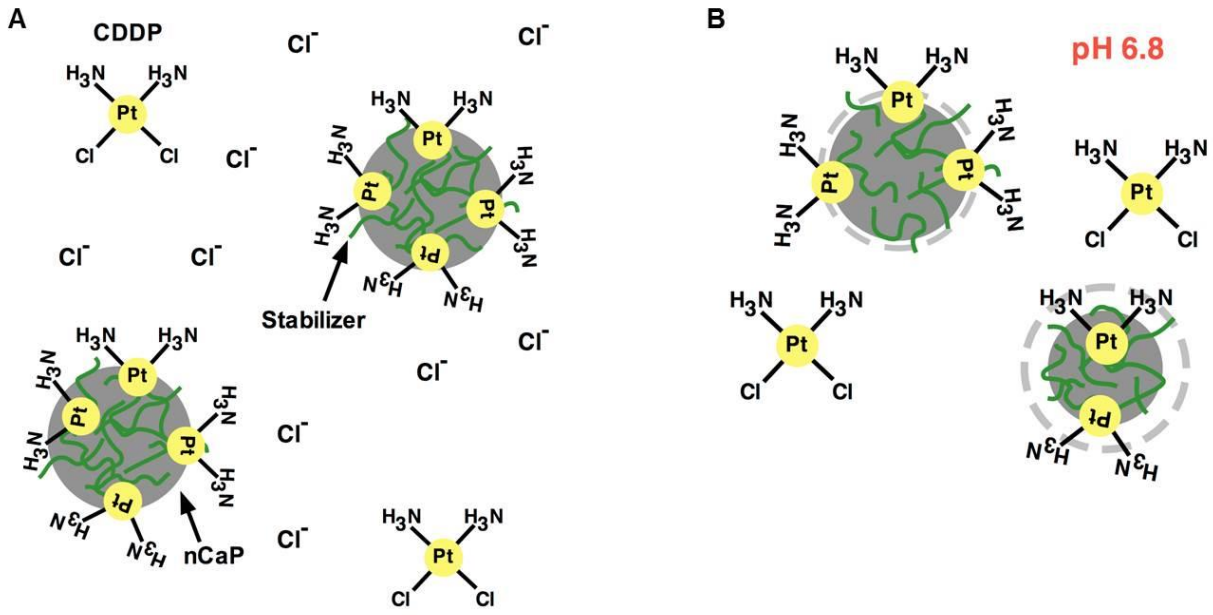

Figure 1.1: Schematic showing the release mechanism for the nCaPxCDDP delivery system. (A) The presence of Cl^- ions is a driving force for CDDP release from nCaP, resulting in re-formation of native CDDP from the bound aquated form of CDDP (B) In acidic pH, like that within tumors or in the lysosome, nCaP will dissolve, releasing active CDDP.

Chapter 2

Sodium Polyacrylate Stabilized Calcium Phosphate Nanoparticles for Delivery of Cisplatin

2.1 Introduction

Calcium phosphate nanoparticles (nCaP) are an attractive vehicle for the delivery of therapeutics due to their biocompatibility, low cost, and ease of manufacture[15,89,91,108,109]. Previous work in our lab showed that sodium polyacrylate (Darvan® 811, D) could effectively stabilize nCaP ($nCaP^D$) , and allow binding cisplatin (CDDP), a commonly used clinical chemotherapeutic to form a drug delivery system for CDDP, $nCaP^DCDDP$[16]. The stabilization of nCaP is achieved by interaction of the free carboxylate groups in each monomer unit of D with the calcium rich surface of calcium phosphate. The research described in this chapter builds upon that promising *in vitro* data published by Cheng & Kuhn, 2007[16]. Working towards a successful clinical drug delivery nanoparticle system, it is essential that parameters of synthesis be controlled and the resulting product be essentially the same from batch to batch[6]. In addition to batch to batch consistency, product stability is essential to define. Essential characteristics of $nCaP^DCDDP$ include particle size, drug loading, and cytotoxicity. We therefore examined these parameters in studies of repeatability & stability, prior to conducting efficacy studies of $nCaP^DCDDP$.

CaP precipitated without stabilizer has been shown to effectively delivery CDDP, but is not readily injectable. Here we made a similar non-stabilized CaP, microCaPCDDP, to examine as a positive control. Both $nCaP^DCDDP$ and microCaPCDDP were tested against three different cell lines: SCCVII, FaDu and A2780cis. The latter two cell types are examples of CDDP resistant human cell lines, HNC and ovarian cancer, respectively. It was hypothesized that the

nanoparticle formulation could overcome CDDP resistance via direct nanoparticle uptake. Yang et al. recently published CDDP core micelles with a PEGylated corona that could overcome CDDP resistance via enhanced cellular uptake, followed by drug release intracellularly[110]. The overall goal for this chapter was to establish a preclinical data set for the treatment of head and neck cancer (HNC) with nCaP^{D}CDDP administered intratumorally (IT) to suppress tumor growth and decrease toxicity associated with CDDP administered systemically. Efficacy against a mouse HNC cell line was examined *in vivo* and compared to CDDP administered systemically (intraperitoneal, IP) or locally (intratumoral, IT).

2.2 Materials and Methods

2.2.1 Materials

$Ca(NO_3)_2 \cdot 4H_2O$ (Sigma C1396), K_2HPO_4 (Sigma S1804), , $Pt(NH_3)Cl_2$ (CDDP, Sigma P4394), and $AgNO_3$ (Silver Nitrate, Sigma S6506) used to prepare the nanoparticles were all purchased from Sigma-Aldrich, (St. Louis, MO). Sodium polyacrylate, Darvan® 811 (D), was supplied by R.T. Vanderbilt (Norwalk, CT). CDDP was prepared at 1 mg/mL in sterile saline (0.9% NaCl), unless otherwise noted. The molecular structure of D is shown in Figure 2.1.

Murine squamous cell carcinoma of the head and neck, SCCVII cells were kindly provided by Dr. C. Johnson at the Roswell Park Cancer Institute. Cells were maintained in RPMI 1640 (Gibco 11875), containing 12% heat-inactivated FBS and 1% penicillin streptomycin. FaDu cells from ATCC and human CDDP resistant ovarian cancer A2780cis cells were used for *intro* cytotoxicity evaluation of the nanoparticles. FaDu cells were maintained in MEM (Gibco 10370) containing 10% heat-inactivated FBS, 1 mM sodium pyruvate (Invitrogen 11360), 2 mM L-glutamine (Invitrogen 25030), 1% penicillin streptomycin. A2780cis cells were

maintained in RPMI 1640 (Gibco 21870) with 10% FBS and 2 mM L-glutamine where every third passage contained 1 μM CDDP to maintain CDDP resistance.

C3H/HeJ mice were purchased from Jackson Laboratory, (Bar Harbor, ME) and used for studies at 6-8 weeks of age.

2.2.2 nCaP^{D}CDDP Production and Optimization

Figure 2.2 is a graphic representation of the nCaP^{D} production procedure. nCaP^{D} was made via precipitation of equimolar and equal volume solutions of $Ca(NO_3)_2$ and K_2HPO_4, where the phosphate solution was manually poured into a stirred calcium solution, followed by the addition of 1.67(v/v)% Darvan®811 (sodium polyacrylate). During studies to optimize the nCaP^{D}CDDP formulation, batches were made using half the concentration of D that is in the standard formulation, these particles are referred to as: nCaP$^{D/2}$CDDP. Additionally, batches were synthesized that contained no stabilizer, creating CaP microcrystals (microCaP). For nCaP$^{D/2}$CDDP and microCaP all procedure steps following precipitation remained the same as normal nCaP^{D}CDDP preparation. Mixing was allowed to continue for one hour. nCaP^{D} was collected via centrifugation, washed with ultrapure H_2O then centrifuged again. Aquated CDDP (Aq CDDP) was made as previously reported[16]. Briefly, 90 mM $AgNO_3$ was reacted with a 1 mg/mL CDDP solution prepped in Ultrapure water at a 2:1 molar ratio. The reaction was allowed to occur for at least 24 hours, after which precipitate was removed with three centrifugation steps followed by 0.2 μM filtration. Binding solution was prepared as a 1:1 solution of 1:1 Aq CDDP at 1 mg/mL to 20 mM potassium phosphate buffer (KPB) pH 6.8. Binding of the Aq CDDP to nCaP^{D} was allowed to occur for ~24 hrs. at 37°C at a concentration of 4 mg nCaP^{D} per 1 mL binding solution. Binding solution was removed via centrifugation and a wash step with 10 mM

KPB, followed by a final centrifugation to concentrate the nCaP^{D}CDDP. nCaP^{D}CDDP was diluted with ultrapure H_2O to form a suspension injectable through a 25G needle. CDDP content was determined by inductively coupled plasma-optical emission spectroscopy (Perkin Elmer® Optima™ 5300 DV, ESIS Inc., Cromwell, CT).

2.2.3 nCaP^{D}CDDP Physical Characterization

Transmission electron microscope (TEM) images were taken using a Hitachi H-7650 TEM (Hitachi High-Technologies Canada, Inc., Toronto). TEM samples were prepared by sonicating the particle suspension and diluting the suspension 26x in 10 mM citrate solution then 10x in 70% ethanol. A 5 uL sample was placed on a formvar carbon coated 300 mesh Cu grid. Sample sat for 1min and then any excess solution was removed using filter paper. Prior to imaging the sample completely dried in air for 5 min. Samples were imaged at 80 kV with the TEM. X-Ray diffraction (XRD) was performed on lyophilized nCaP^{D} using a Bruker AXS D2 Phaser (Cu radiation, λ =1.54184 Å) (Bruker Corp., Germany). Particle size analysis was performed using a 90 Plus Particle Sizer (Brookhaven Instruments, NY). Drug loading (ug CDDP/mg nCaP^{D}) was determined by Pt analysis of the suspension for ug CDDP and drying 3 replicates of 100 uL nCaP^{D} CDDP suspension for ~24 hrs at 37°C to determine the mg nCaP^{D} in 100 uL suspension.

2.2.4 nCaP^{D}CDDP In Vitro *Drug Release Studies*

Two *in vitro* drug release studies were performed. One was performed using a ready to use dialysis device, (Float-A-Lyzer® G2, Spectrum Laboratories Inc., Rancho Dominguez, CA), with a molecular weight cut off of 100 kD. 0.55 mL of nCaP^{D}CDDP suspension (CDDP concentration of 4 mg/mL) was loaded in to the dialysis device and placed in 22 mL of 10 mM PBS. The pH of the PBS was adjusted to 6.8 to mimic an acidic tumor microenvironment.

Beakers were capped, placed on an orbital shaker, and incubated at 37°C. Release samples were drawn at 1h, 6h, 1d, 3d, 5d, 7d, and 14d. At each time point 5 mL of release solution was taken and replaced with 5 mL of fresh PBS. The second release study used a modified USP apparatus 4 with a dialysis sac[22]. 0.4 mL of $nCaP^{D/2}$CDDP suspension (CDDP concentration 5 mg/mL) was placed into the dialysis sac and 40 mL of 50 mM PBS, pH 6.8 was used for release media. Samples were removed in 4 mL volumes at 4, 6, 12 hr, 1, 3, 5, 7 and 9 days. CDDP content in the release solution was determined by inductively coupled plasma-optical emission spectroscopy (Perkin Elmer® Optima™ 5300 DV, ESIS Inc., Cromwell, CT).

2.2.5 Cytotoxicity

Cytotoxicity experiments were conducted using SCCVII cells plated in 96 well plates at 20,000 cells/mL with 50 uL suspension per well. Cells were allowed to proliferate for 24 hours following which drug was added in 50 uL volumes. The following groups were examined: CDDP in saline, Aq CDDP, D alone, $nCaP^{D}$, $nCaP^{D}$CDDP and released drug from $nCaP^{D}$CDDP at 3 days ($nCaP^{D}$CDDP (R)). Each group was serially diluted 1:3 across the plate using PBS. Cells were assayed 48 h after adding drug using in an MTS assay (CellTiter 96® AQ_{ueous} One, G3580, Promega Corp., Madison, WI), where metabolic activity was determined using a Spectramax $Plus^{384}$ Spectrophotometer (Molecular Biosciences, Sunnyvale, CA) at an absorbance of 490nm. Background correction was performed for any CaP treated groups due to background interference. Background plates were handled in the same manner as test plates, but no CellTiter reagent is added prior to reading the absorbance. To determine the IC_{50} (50% inhibitory concentration) a non-linear regression curve fit analysis was performed with at least four replicates per group. All cytotoxicity experiments were repeated at least twice. Statistical significance was determined.

To compare the cytotoxicity of CDDP, nCaP^{D}CDDP, and microCaPCDDP three difference cell lines were examined: SCCVII, FaDu and A2780cis. The latter two cell types are examples of CDDP resistant human cell lines.

2.2.6 Process Repeatability, Product Stability and Stabilizer Optimization

To assess the repeatability of the production of nCaP^{D}CDDP three separate batches were made within one week's time following the procedure as described in section 2.2, using the same batch of Aq CDDP, all other components were prepared fresh. To assess stability, nCaP^{D}CDDP made two (5-11-09) and three years (9-8-08) prior was compared to a batch of nCaP^{D}CDDP made freshly. In an approach to reduce the amount of D added to create particles, batches were made using 0.835% (v/v)% D to produce nCaP$^{D/2}$CDDP which was compared to a standard batch of nCaP^{D}CDDP. For each of these measures drug loading, particle size and IC50 value against SCCVII cells were examined.

Findings from the initial repeatability study, led to modification to the synthesis and Aq CDDP binding procedure. The graphic representation of the changes to the synthesis procedure is in Figure 2.3. Three batches of nCaP^{D} were pooled prior to rinsing with H_2O. After centrifugation, the particles were resuspended in binding solution and split into three tubes for overnight binding. All remaining steps were performed as described previously.

2.2.7 nCaP^{D}CDDP In Vivo *Maximum Tolerable Dose Study*

An initial maximum tolerable dose (MTD) study was performed in 10-12 week old C3H/HeJ female mice. Tumors were initiated intradermally using 7 x 10^4 SCCVII cells in 20 uL at a concentration of 3.5 x 10^6 cells/mL. The MTD was defined for the purposes of this study as the maximum dose that could be administered to a mouse that will result in less than 15% weight

loss. Each mouse received one, intratumoral (IT) injection of the nanoparticle suspension via a 25-gauge needle; (2-6 mice/group) where groups included: 10, 14, 18, and 23 mg/kg nCaP^{D}CDDP. Mouse weight was monitored daily for twelve days, (by day 8 all mice had recovered from the normal initial weight loss seen with CDDP doses in the first few days, or had exceeded 15% weight loss). Mice exceeding 15% weight loss were euthanized.

A second MTD study was conducted in 12 week old female CH3/HeJ mice without tumors. All doses were administered once, subcutaneously. Three animals were in each group. Groups were as follows: 9 mg/kg CDDP, 9, 18, 23 and 27 mg/kg nCaP^{D}CDDP.

2.2.8 nCaP^{D}CDDP in vivo *anti-tumor efficacy and toxicity studies*

C3H/HeJ mice were inoculated with 5x10^{5} SCCVII cells in 20 uL of 2.5x10^{6} cells/mL PBS intradermally in the right rear flank via a 25-gauge needle. A total of 42 female, 8 week old, C3H/HeJ mice were included in the study, (6 mice/group, 7 groups). Tumors were measured daily using digital calipers to calculate the tumor volume as follows: $V = W^2 * L * 0.4$, where W = width, L = length, and V = volume.

When tumor volume reached 100 ± 20 mm^{3} animals were enrolled into treatment groups as follows: 20 µL of saline (IT), 10 µL of nCaP^{D} (IT), 6.5 mg/kg CDDP (IT), 6.5 mg/kg CDDP (IP), 6.5 mg/kg nCaP^{D}CDDP (IT), or 12 mg/kg nCaP^{D}CDDP (IT). Systemic toxicity was evaluated by weight change and overall grooming/appearance. Tumor volume and mouse weight were monitored daily. Mice were euthanized due to significant weight loss (> 15%), a tumor length measurement greater than 20 mm, or completion of the study (day 30).

The efficacy study was repeated with modifications due to fast growing necrotic tumors in the first study. 12 week old C3H/HeJ mice were injected subcutaneously with 4x10^{4} SCCVII

cells in 50 uL of a 80% BD Matrigel (Franklin Lakes, NJ) and 20% cells + base media. 32 mice were entered into treatment groups when their tumor volume reached 160 ± 10 mm^3 with 6 mice/group. The groups were as follows: 50 uL Saline (IT), 10 mg/kg CDDP (IP), 2.2 mg/kg (50 uL) CDDP (IT) and 11 mg/kg $nCaP^{D}$CDDP (IT). The volume of 50 uL was an estimate based on clinician collaborator suggestion to administer only what would be feasible to administer to a solid human tumor. This is considered to be 20% of the total tumor volume[111,112]. Here that would have been a volume of 30 uL, but the dose of CDDP that could be administered in a 30 uL volume was very low. We therefore used 50 uL which is approximately 31% of the tumor volume at time of treatment. All animal experimental procedures were approved by the Animal Care and Use Committee of the University of Connecticut Health Center, (Farmington, CT).

2.2.9 In Vitro *Cytotoxicity Assessment of Darvan, due to Toxicity Shown* In Vivo

Due to unforeseen weight loss to animals administered 11 mg/kg $nCaP^{D}$CDDP (IT) compared to 10 mg/kg CDDP IP, *in vitro* cytotoxicity testing was employed. We examined the toxicity of D alone against SCCVII cells. The D was prepared at a concentration of 65 mg/mL. This concentration was picked based on thermogravimetric analysis of $nCaP^{D,}$ which revealed $nCaP^{D}$ is approximately 27% D by weight. We then based our calculations on the average mg $nCaP^{D}$ in the top concentration of $nCaP^{D}$CDDP: used in the top concentration of cytotoxicity tests relative to CDDP. Additionally, SCCVII (murine HNC), FaDu (human CDDP resistant HNC) and A2780cis (human ovarian CDDP resistant cancer) cells were used to examine the cytotoxicity of $nCaP^{D}$CDDP compared to CDDP, Aq CDDP and microCaPCDDP.

2.2.10 Statistical Analysis

Statistical analysis was performed using an unpaired t-test for comparison of two batches. When comparing three or more batches a one-way ANOVA was used with either a Tukey (when comparing all groups to one another) or Dunnet (when comparing test groups to a control group) post-test. A P-value of less than 0.05 was considered statistically significant. Data is presented as a mean value with its standard deviation indicated (mean $\pm$ SD).

2.3 Results

2.3.1 Physical Characterization of nCaP^{D}CDDP

Transmission electron microscopy (TEM) (Figure. 2.4 A and B) and particle size analysis via dynamic light scattering showed that nCaP^{D}CDDP in suspension form small aggregates with an average size of 150 ± 40 nm. Average drug loading of the suspension is 75 $\pm$ 10 µg CDDP/mg nCaP^{D}. XRD of lyophilized nCaP^{D} shows a poorly crystalline hydroxyapatite (HA), Figure 2.5[113].

2.3.2 nCaP^{D}CDDP In Vitro *Release Studies*

The release profile of the nCaP^{D}CDDP using a Float-a-Lyzer® device in PBS, pH 6.8, at 37° C can be seen in Figure 2.6 A. In comparison, *in vitro* release of CDDP from nCaP$^{D/2}$CDDP was performed using a United States Pharmacopeia (USP) apparatus 4 modified with a dialysis adapter (Figure 2.6 B). nCaP^{D}CDDP and nCaP$^{D/2}$CDDP show continuous *in vitro* release. nCaP^{D}CDDP released 47% of the total CDDP bound after 12 days in the Float-A-Lyzer® system. A burst release was exhibited in the first 3 days, with slower, continuous release out to day 12. After 9 days in the modified USP apparatus 4 nCaP$^{D/2}$CDDP released 76% of the total CDDP bound. Again there was a burst release over the first 3 days, followed by a tapering of release over the remainder of the experiment.

2.3.3 Cytotoxicity

Figure 2.7 A, shows a non-linear regression curve fit analysis for a CDDP cytotoxicity experiment, with four replicates. Figure 2.7 B shows an example of background correction when examining nCaP^{D}CDDP. The blue line represents the original data measured from the test plate including cells, nCaP^{D}CDDP treatment and CellTiter 96® AQueous One reagent after 4 hours of incubation. The green line is the background plate that includes cells and nCaP^{D}CDDP treatment. These absorbance values were then subtracted from the original data to result in the pink line which represents the corrected data. The corrected curve is what is used to calculate the IC50. The carrier alone, nCaP^{D}, did not show any significant toxicity at a concentration of 20 ug/mL that matches its average concentration in nCaP^{D}CDDP at the IC50 relative to CDDP (Figure 2.8).

The *in vitro* cytotoxicity of nCaP^{D}CDDP and the released CDDP from nCaP^{D}CDDP (nCaP^{D}CDDP) were compared to CDDP and Aq CDDP against SCCVII cells using an MTS assay. The respective curves are plotted in Figure 2.9 A and the calculated IC50 values are plotted in Figure 2.9 B. CDDP released from nCaP^{D}CDDP has the same cytotoxicity as CDDP alone and Aq-CDDP. nCaP^{D}CDDP was significantly less cytotoxic than CDDP ($P < 0.0001$).

2.3.3 Process Repeatability, Product Stability and Stabilizer Optimization

The relative stability of batches of nCaP^{D}CDDP was examined. The particle size of batches stored for 2 or 3 years was significantly larger (152 & 158 nm, respectively) than that made freshly (125 nm)($P < 0.0001$) (Figure 2.10 A). The drug loading also varied with one batch having significantly lower drug loading (63 ug CDDP/ mg nCaP^{D}) than the freshly made control (87 ug CDDP/ mg nCaP^{D}) ($P < 0.05$) (Figure 2.10 B). Lastly, the IC50 value of the batch stored

for 3 years (3.3 ug/mL) was significantly higher than the fresh batch (2.8 ug/mL) ($P < 0.0001$) (Figure 2.10 C).

$nCaP^{D/2}$CDDP synthesized using half the concentration of D compared to $nCaP^{D}$CDDP created significantly smaller nanoparticles, 120 nm vs 125 nm ($P = 0.0213$) (Figure 2.11 A), with a significantly higher drug loading 105 vs 87 ug CDDP/ mg $nCaP^{D}$ ($P = 0.0056$) (Figure 2.11 B). There was no statistical difference between the IC50 values against SCCVII cells 2.8 vs 3 ug/mL for D/2 (Figure 2.11 C).

The batch to batch repeatability was examined by comparing three separately synthesized batches using particle size, drug loading, yield and IC50 values against SCCVII cells. Batches were labeled: $nCaP^{D}$CDDP 1, $nCaP^{D}$CDDP 2 and $nCaP^{D}$CDDP 3 and all results are listed in this order. The yield varied from batch to batch, 0.8, 0.9, vs 1.2 g (Figure 2.12 D and E), no statistics could be performed. Interestingly, the yield did not follow the same trend after Aq CDDP binding: 1.1, 1.5, vs 1.4 g. No significant differences were found between the three batches in particle size 168, 202, vs 161 (Figure 2.12 A). The drug loading varied significantly from batch to batch 66, 124, vs 81 ug CDDP/ mg $nCaP^{D}$ ($P < 0.0001$) (Figure 2.12 B). The IC50 of batch 2 at 1.5 ug/mL significantly varied from batches 1 and 3, at 1.2 ug/mL ($P < 0.001$) (Figure 2.12 C).

To address issues with batch to batch repeatability, modifications were made to the nanoparticle synthesis procedure at shown in Figure 2.3, resulting batches are labeled $nCaP^{D}$CDDP A, $nCaP^{D}$CDDP B and $nCaP^{D}$CDDP C. These modifications led to a more uniform $nCaP^{D}$ and $nCaP^{D}$CDDP. Although the particle size of batch C was significantly

smaller than A and B (P = 0.0077) (Figure 2.13 A), the drug loading of all three batches was uniform. Their resulting IC50 values against SCCVII cells were also uniform (Figure 2.13 C).

2.3.4 nCaP^{D}CDDP In Vivo *Maximum Tolerable Dose Study*

A maximum tolerable dose (MTD) study was performed in C3H/HeJ mice with tumors. The MTD is defined as the maximum dose that can be administered to a mouse that will result in less than 15% weight loss and is a measure of systemic toxicity of the tested materials. The dose of 14 mg/kg nCaP^{D}CDDP IP is the maximum tolerable dose that can be administered to a C3H/HeJ mouse without experiencing significant weight loss (> 15%). The average weight loss following a single treatment of 10, 14, 18 and 23 mg/kg nCaP^{D}CDDP IT dose are shown in Figure 2.14 A-D, respectively. The 18 and 23 mg/kg dose groups each had one mouse whose weight loss dipped below the acceptable 15%, therefore these doses are not tolerable.

A second MTD study was performed in CH3/HeJ mice this time without tumors. Animals were administered treatment subcutaneously, once with three animals per group. In this study 9 mg/kg CDDP (Figure 2.15 E) was compared 9, 18, 23 and 27 mg/kg nCaP^{D}CDDP (Figure 2.15 A-D). Both of the 9 mg/kg treatments were well tolerated. One of the mice receiving CDDP experienced10% weight loss, but was able to recover. The animals treated with 9 mg/kg nCaP^{D}CDDP lost a maximum of 5% of the weight at the time of treatment. One of the animals in the 18 mg/kg group lost more than 15% of her weight and therefore that dose and the higher doses of 23 and 27 mg/kg were not well tolerated. These higher doses were therefore not considered for animal efficacy studies. A dose of 12 mg/kg was chosen for the first efficacy study.

2.3.5 nCaP^{D}CDDP In Vivo *Anti-Tumor Efficacy and Toxicity Studies*

The *in vivo* anti-tumor efficacy of the nCaP^{D}CDDP was evaluated using SCCVII tumors in CH3/HeJ mice. When tumors reached 100 ± 20 mm^3 animals were enrolled into a treatment group (6 mice/ group) Tumors were treated once with either CDDP intraperitoneally (IP) at 6.5 mg/kg or intratumorally (IT) with saline (20 uL), CDDP (6.5 mg/kg), nCaP^{D} (10 uL) or nCaP^{D}CDDP (6.5 or 12 mg/kg). The change in tumor volume and mouse weight was evaluated for 20 days post treatment, (Figure 2.16 A - F). 6.5 mg/kg CDDP IT resulted in delayed tumor growth with one tumor completely going away and two not growing beyond their volume at treatment (Figure 2.16 D). The IT dose of CDDP was significantly more effective at delaying tumor growth than the same dose delivered IP (Figure 2.17). As expected, saline IT and nCaP^{D} IT (no CDDP) had no effect preventing tumor growth. A one-way ANOVA was performed comparing average tumor volume per group for each day. On day 6 following treatment 12 mg/kg nCaP^{D}CDDP, 6.5 mg/kg CDDP IP & IT were significantly more effective at delaying tumor growth than the vehicle control (saline) ($P < 0.05$) (Figure 2.18 A). Additionally, at day 6 it was determined that 6.5 mg/kg CDDP IT was significantly more effective than the same dose of nCaP^{D}CDDP IT ($P < 0.05$). No animals in this study lost more than 10% of their weight at treatment. Maximum weight loss was compared across groups, relative to their respective maximum weight loss day post-treatment (Figure 2.18 A). Here it was found that nCaP^{D}CDDP at 12 mg/kg IT caused significantly more weight loss than nCaP^{D} IT ($P < 0.05$) (Figure 2.18 B).

The *in vivo* anti-tumor efficacy of the nCaP^{D}CDDP was repeated using SCCVII tumors in CH3/HeJ mice. In an attempt to slow the growth of the tumors, animals were administered fewer cells, 4 x 10^4 in a Matrigel basement membrane, subcutaneously. Animals were enrolled into treatment groups when their tumors reached 160 ± 10 mm^3 in size. There were 6 animals per group. Groups were: CDDP IP (10 mg/kg), Saline IT (50 uL), CDDP IT (50 uL, 2.2 mg/kg)

and nCaP^{D}CDDP IT (11 mg/kg). Here CDDP IP at 10 mg/kg was the most effective at delaying tumor growth (Figure 2.19). A one-way ANOVA was performed comparing the average tumor volume per group each day. At day 6, CDDP IP was significantly more effective at delaying tumor growth than Saline and nCaP^{D}CDDP at 11 mg/kg ($P < 0.05$) Figure 2.20 A. Again the maximum observed weight loss per group was compared relative to the day it occurred on (Figure 2.20 A). Importantly, we determined that nCaP^{D}CDDP at 11 mg/kg caused significantly greater weight loss than CDDP IT (2.2 mg/kg) and Saline IT ($P < 0.05$), with two animal dropping below 15% weight loss (Figure 2.20 B). Survival was also plotted for this study (Figure 2.21). CDDP IP at 10 mg/kg allowed for the longest survival times at 15 days post-treatment. Most animals were euthanized due to tumor volume exceeding nearing 2 cm in diameter and/or due to necrosis.

2.3.6 In Vitro *Cytotoxicity Assessment of Darvan, due to Toxicity Shown* In Vivo

The purpose of local intratumoral administration of chemotherapy, i.e. IT, is to lessen systemic toxicity experienced by the animal or patient. Here the *in vivo* efficacy studies revealed unforeseen toxicity from nCaP^{D}CDDP administered IT. This is cause for concern about the formulation or a component within the formulation. We therefore examined the *in vitro* cytotoxicity of D (Figure 2.22 A). We found that doses of D found in nCaP^{D}CDDP are cytotoxic. The IC50 value of D was 455 ug/mL and the concentration of D estimated to be in nCaP^{D}CDDP in concentrations typically utilized for cytotoxicity studies is 564 ug/mL. We therefore believe animals experienced weight loss due to the D in the nCaP^{D}CDDP in addition to the CDDP, though in cytotoxicity studies nCaP^{D}CDDP is not more effective than CDDP alone.

To further examine the biological effects of D in nCaP^{D}CDDP, we compared the cytotoxicity of nCaP^{D}CDDP to CDDP, Aq CDDP and microCaPCDDP to SCCVII (murine HNC), FaDu (human CDDP resistant HNC) and A2780cis (human ovarian CDDP resistant cancer) cells (Figure 2.22 C-D). The same trend was found for all three cell types, where nCaP^{D}CDDP was significantly less cytotoxic than CDDP alone ($P < 0.0001$). For A2780cis cells microCaPCDDP was significantly more cytotoxic than CDDP ($P < 0.0001$).

2.4 Discussion

The research described in this chapter was an effort to validate the synthesis and resulting properties of nCaP^{D}CDDP, along with assessing it's efficacy in a murine HNC model. The long-term goal of clinical usage of nCaP^{D}CDDP for the treatment of HNC cannot be realized if the synthesis of nCaP^{D}CDDP cannot be repeated with comparable batch to batch results. As the development of nanoparticle systems progress, it is essential to take into consideration the scale-up of production from the bench top to clinical and eventually commercial scale. The FDA has issued Guidance for Industry: Liposomal Drug Products and created a nanotechnology task force in an effort to stay ahead of the advancing technology. Within the document they highlight the need for control of product manufacture to ensure a repeatable product during scale-up, as seemingly small processing parameters can drastically change the resulting product[114]. In this study, we employ a bottom-up approach to form nCaP^{D}CDDP, made by precipitation of calcium, phosphate, and sodium polyacrylate (D), which was then reacted with CDDP. We found that from batch to batch nCaP^{D} differs in yield and particle size because of lack of control over the precipitation with manual addition of components. The variability in particle size likely contributes to the variability in drug loading. We were able to minimize the variability by a

minor modification to the nCaP^{D} protocol. Creation of a combined large batch of nCaP^{D} allowed for uniform nanoparticles, which resulted in uniform drug loading.

In vitro release testing of controlled release parenteral dosage forms such as the locally administered nanoparticle suspension studied here are essential for quality control, product development, and in-vitro-in-vivo-correlation (IVIVC). In comparison to solid oral dosage forms, extended or controlled release parenterals have complex physicochemical properties and are varied in their components and resulting release characteristics. Due to these factors, there is currently no standard compendial method to examine *in vitro* release from controlled release parenterals, where many exist for oral dosage forms[115]. The Federation International Pharmaceutique (FIP) / American Association of Pharmaceutical Scientists (AAPS) report on *in vitro* release testing of novel dosage forms specifies that release testing methods used to screen formulations may not be feasible to use for quality control, but should be reevaluated towards use of a compendial apparatus[116]. The release testing methods used for liposomes and nanoparticle suspensions can be generally categorized into: (1) sample and separate[16,117], (2) dialysis sac[84,118,119], or (3) continuous flow[22].

Herein, we utilized two types of *in vitro* release testing. First we used the dialysis sac method with a Float-a-Lyzer® device which is a commercially available "Ready-to-Use Dialysis Device." nCaP^{D}CDDP suspension was loaded into the sac and submerged into release medium agitated via an orbital shaker, covered in a temperature controlled chamber. Only 45% of bound CDDP released from nCaP^{D}CDDP using the Float-a-Lyzer® device. This method is quite commonly used for initial screening of drug release from nanoparticle formulations, but has several drawbacks. Due to their high surface area and small particle size, nanoparticles can release drug rapidly. When using a dialysis based method it is assumed that there is not a

significant resistance in diffusion of drug across the dialysis membrane. Zambito, Pedreschi and Di Colo showed that diclofenac released near completely from chitosan nanoparticles within an hour into the medium within the dialysis sac, but the dialysis membrane limited diffusion into the receiving medium[120]. Diclofenac has a similar molecular weight to CDDP used here, 296 versus 300 g/mol, respectively. This study used a significantly smaller molecular weight cut off than we used in our study, which may have less of an effect on diffusion, 12 kDa versus 100 kDa. Additionally, high variation can be found in this method for reasons including: limited agitation within the dialysis tubes and high density of nanoparticles in the small volume of the dialysis tube, slowing diffusion[121].

For these reasons, we sought a more accurate and repeatable method to perform *in vitro* release testing. Bhardwaj and Burgess developed a novel dialysis adapter to modify the United States Pharmacopoeia (USP) apparatus 4 for *in vitro* release testing of colloids[22]. Where they showed the modified USP 4 apparatus could discriminate between different liposomal formulations where dialysis sac methods could not, likely due to sufficient agitation within the sample cell. Also of importance, sample replicates had low variation. Here we found the modified USP apparatus 4 allowed for 78% of CDDP bound to nCaP$^{D/2}$CDDP to release. A majority of the CDDP was released in the first 72 hours, with 59% of drug releasing in this time. Importantly, we determined the CDDP released from nCaP^{D}CDDP was as cytotoxic as CDDP against SCCVII cells, meaning active CDDP is released from the formulation.

CaP is inherently biocompatible, as it is a major constituent of bones and teeth[109,122]. When synthesized via wet precipitation, CaP will form microcrystals. These microcrystals effectively bind and release CDDP[14], but cannot be easily injected using a 25G needle. Additionally, microparticles are too large to pass through the circulatory system[70,123]. Here the

addition of sodium polyacrylate halts the precipitation process leading to nanoparticles 150 nm in diameter on average. A polyacrylate formed the arms of a star shaped polymeric nanoconjugate to deliver CDDP, which was shown through *in vitro* cytotoxicity testing of the conjugate to be significantly less cytotoxic than CDDP alone against several types of cancer cells[124]. Here similar results were found with nCaP^{D}CDDP, but the lessened cytotoxicity was not as pronounced and we know the released CDDP is effective. This lessened cytotoxicity we believe is due to the short time frame of the cytotoxicity test, where free drug can readily diffuse into cells and nanoparticles would require drug to release or cellular uptake to cause cell death. Additionally, it has been shown that positively charged particles are more readily taken up by cells[95] and nCaP^{D}CDDP is negatively charged thus limiting cellular uptake.

The goal of intratumoral delivery of chemotherapy is to localize a higher dose of drug at the tumor site while causing less systemic toxicity, for enhanced tumor reduction. That is the focus of our delivery mechanism. Many other nanoparticle formulations are administered systemically and hypothesized to enhance drug delivery based on the EPR effect[76]. This method has proven effective for some formulations resulting in approval by the FDA. Doxil® is an FDA approved liposomal formulation of doxorubicin. Doxil is readily used clinically to treat recurrent ovarian and relapsed multiple myeloma[73]. STEALTH® liposomal CDDP (SPI-77), using the same liposomal formulation as found in Doxil, was quickly entered into several clinical trials in patients with advanced cancers, finding no clinical efficacy because drug could not release from the liposome *in vivo*[78,79,125–127]. These findings highlight the significant problem of insufficient characterization of nanoparticle system components and their interactions with carried drug both physico-chemically and biologically prior to clinical efficacy testing. Importantly, the nanoparticle materials should not incur long-term deleterious effects on the patient. Patients

treated with SPI-77 incurred a significant increase in cholesterol (lipid) levels. Similarly, Doxil® is not recommended for patients with a history of heart disease due to lipid load associated with treatment.

The toxicity experienced by animals treated with 11 mg/kg nCaP^{D}CDDP was not expected. Though not significantly, the toxicity surpassed that of 10 mg/kg systemic CDDP. The overall goal of intratumoral delivery of CDDP via nCaP^{D}CDDP was to diminish systemic toxicity experienced. This prompted cytotoxicity testing of D alone, which showed that at concentrations found in nCaP^{D}CDDP, D is cytotoxic itself. This explains the toxicity experience by the animals in the efficacy study.

Another noteworthy point of discussion is that SCCVII tumors are extremely aggressive. Within 10 days following vehicle treatment animals needed to be euthanized due to excessive tumor growth as per the Animal Care Committee guidelines at UCHC. This was found in other labs as well[63,128]. Even with CDDP at the MTD tumors grew frenetically causing loss of animals in the treatment group after as little as 10 days. *In vitro* SCCVII cells are considered a CDDP sensitive cell line, yet *in vivo* their aggressive phenotype overcomes any CDDP sensitivity. For future studies evaluating new therapeutics a less aggressive model would be better to use to limit large tumor burden and extend animal survival in negative control groups.

2.5 Conclusions

This study showed nCaP^{D}CDDP can be made with batch to batch repeatability and retains particle size and biological activity after 3 years of storage. The CDDP released from nCaP^{D}CDDP is as biologically active as freshly prepared CDDP, *in vitro*. *In vivo* nCaP^{D}CDDP was ineffective at delaying tumor growth in comparison to a lower dose of CDDP administered

IT. IT delivery of CDDP was repeatedly effective at delaying tumor growth of the very aggressive SCCVII tumors. This finding may have clinical relevance and will be studied further. From these studies it was determined that D is an effective stabilizer of CaP, but negatively impacts biological activity of CDDP and is toxic. For these reasons, other stabilizers will be researched for the nCaPxCDDP delivery system.

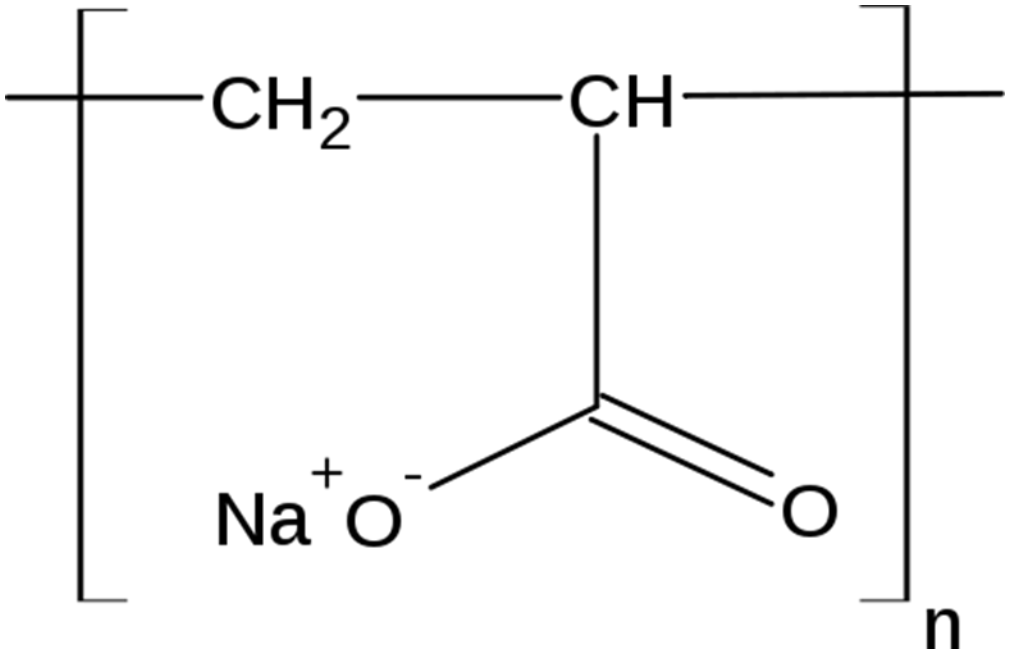

Figure 2.1 Molecular structure of sodium polyacrylate (Darvan® 811, D).

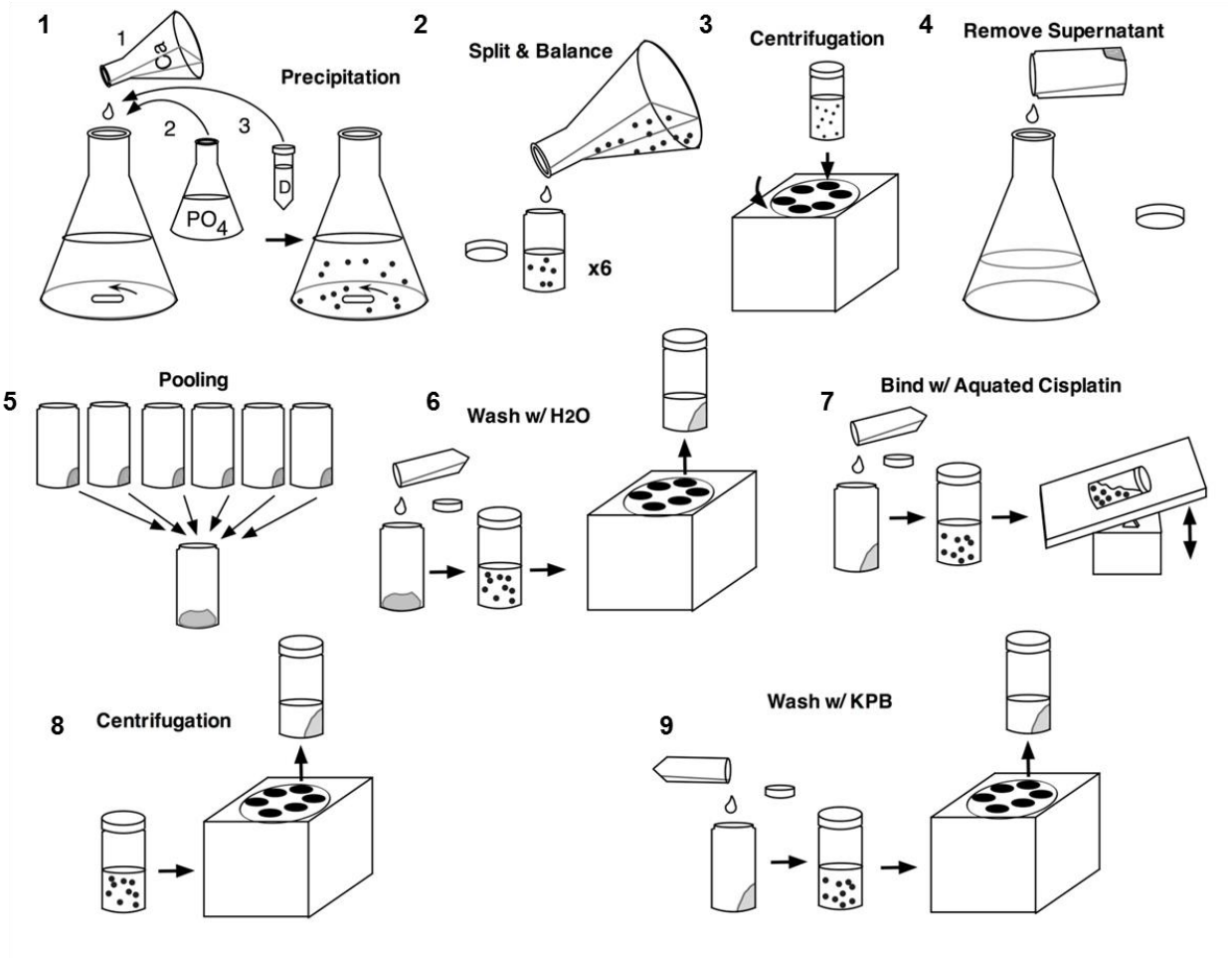

Figure 2.2 Graphic representation of nCaPxCDDP synthesis. Steps follow from left to right. After the final wash with KPB, particles are resuspended in sterile, deionized water.

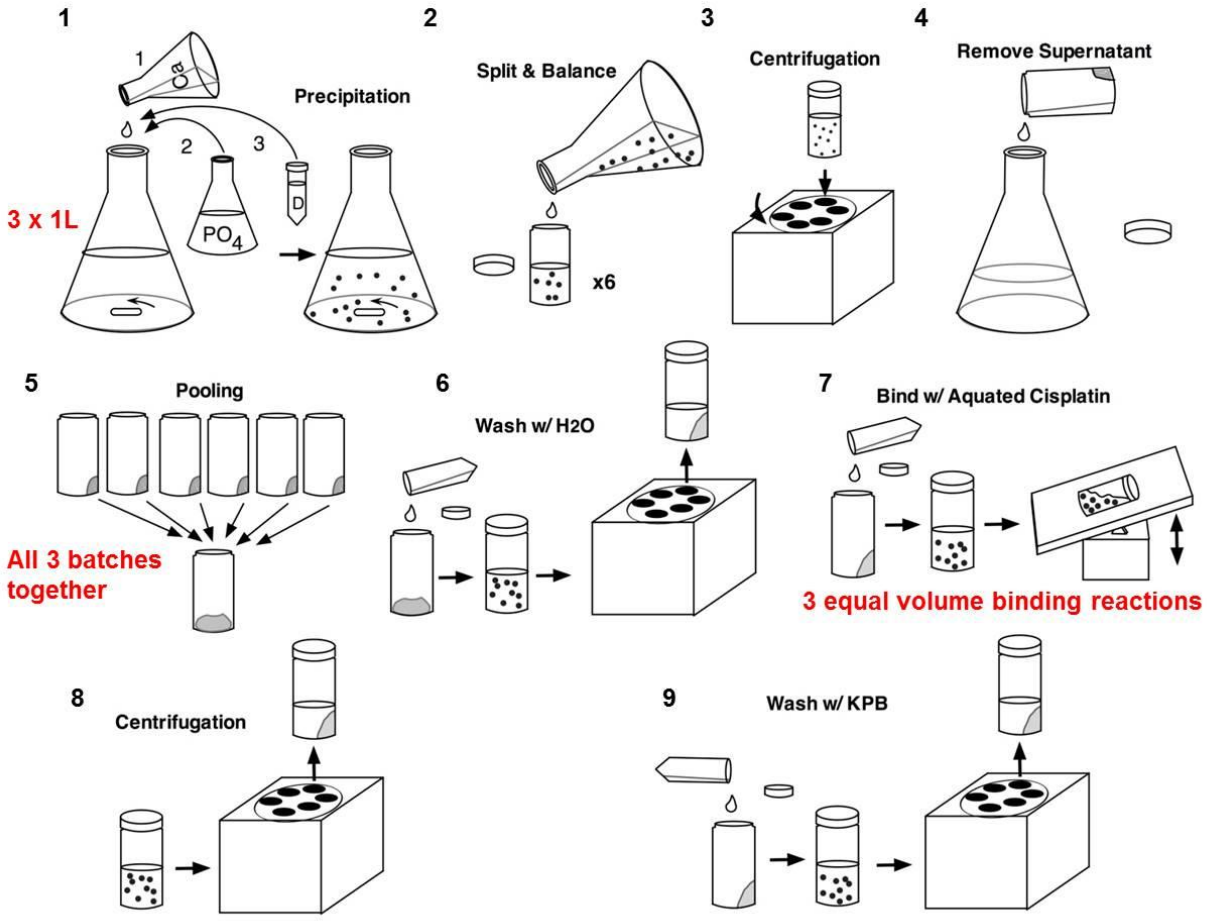

Figure 2.3 The nanoparticle synthesis method represented in Figure 2.2 resulted in large batch to batch variability of particle size and drug loading. The nCaP^{D}CDDP synthesis procedure was modified to achieve a more uniform nCaP^{D}, prior to CDDP binding. This is a graphic representation of the modifications to the nCaPxCDDP synthesis steps. Three 1 L batches were made and pooled prior to washing. The pooled nCaP^{D} was washed, resuspended in CDDP binding solution and split into three tubes for overnight binding.

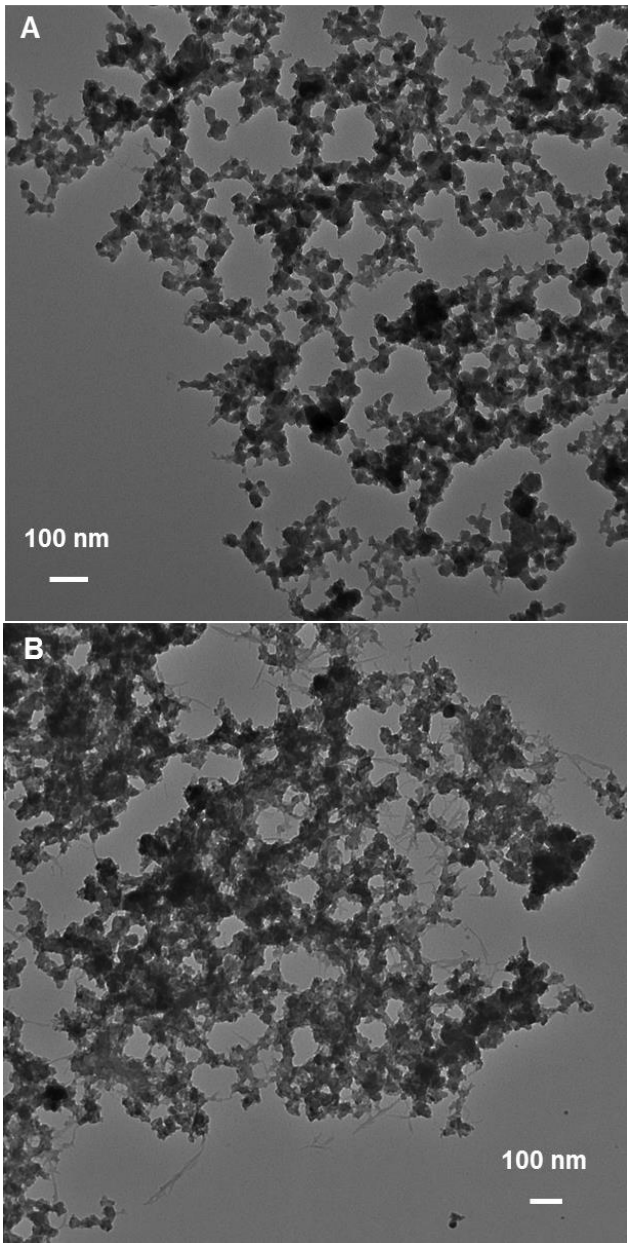

Figure 2.4 TEM images (A) nCaP^{D} deposited directly on the grid, and (B) nCaP^{D}CDDP directly deposited on the grid, showing 20-30 nm particles agglomerated into larger clusters of particles 120-180 nm in diameter.

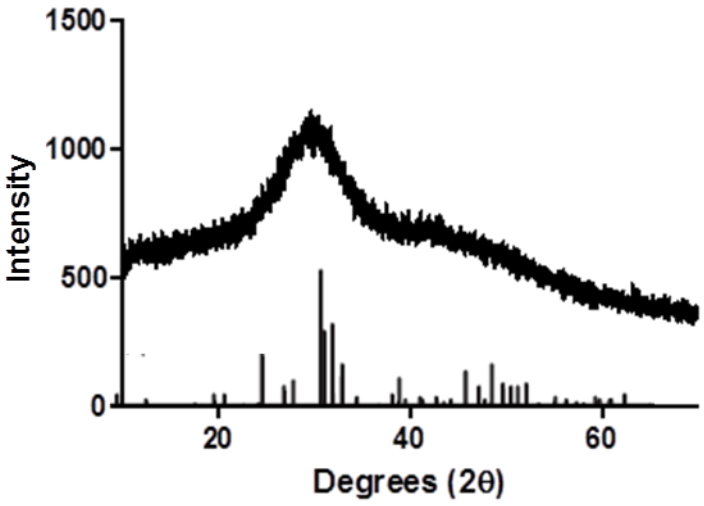

Figure 2.5 X-ray diffraction spectra (Cu radiation, λ =1.54184 Å) of lyophilized $nCaP^D$ (top solid line) compared to hydroxyapatite standard (JCPDS, #09-0432) (bars). The match between the broad peaks of the $nCaP^D$ with the standard indicates it is poorly crystalline hydroxyapatite.

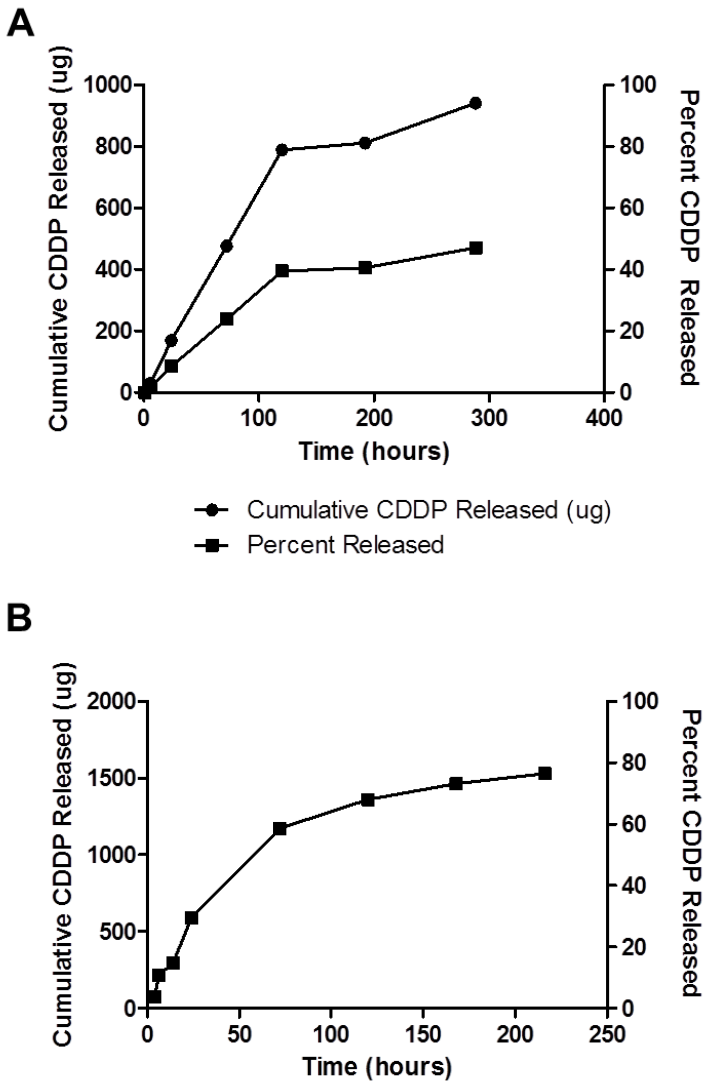

Figure 2.6 *In vitro* release testing shows initial burst release over first 24 hours that tapers as release continues. Cumulative CDDP released is plotted using the left y-axis, percent CDDP released using right y-axis. (A) Released CDDP from nCaP^{D}CDDP using a Float-a-Lyzer device with Mw cutoff of 100 kDa released into PBS, pH 6.8 to mimic acidic tumor microenvironment. (B) Released CDDP from nCaP$^{D/2}$CDDP using a USP apparatus 4 modified with a dialysis adapter, Mw cutoff of 100 kDa released into PBS, pH 6.8.

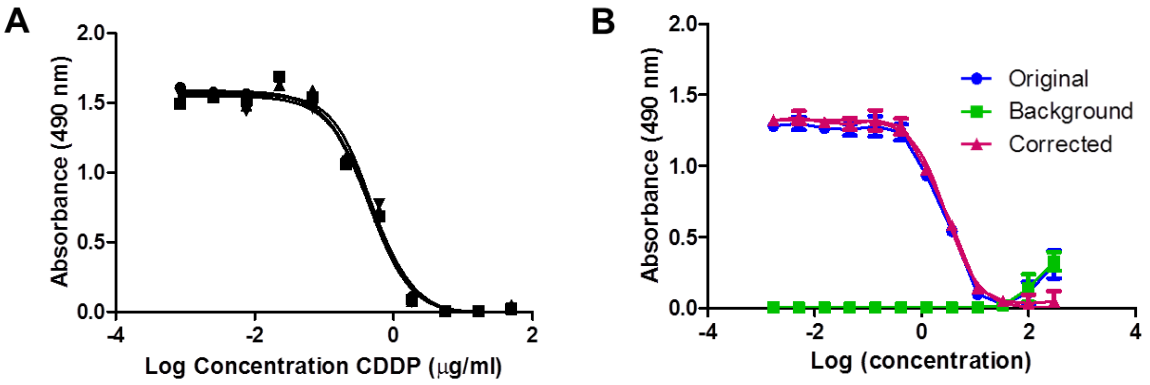

Figure 2.7 Cytotoxicity testing analysis using an MTS assay against SCCVII cells. (A) Demonstration of typical four parameter logistic curve fit for CDDP data. (B) The highest concentrations of nCaP^{D}CDDP in the assay interfere with absorbance readings at 490 nm. To correct for this, cells treated with the same concentration of nCaP^{D}CDDP over the same time period are read on the plate reader without the addition of CellTiter 96® AQueous One reagent, labeled as Background. These average background absorbance readings are subtracted from the Original, to find the Corrected curve. The Corrected curve is used for IC50 determination.

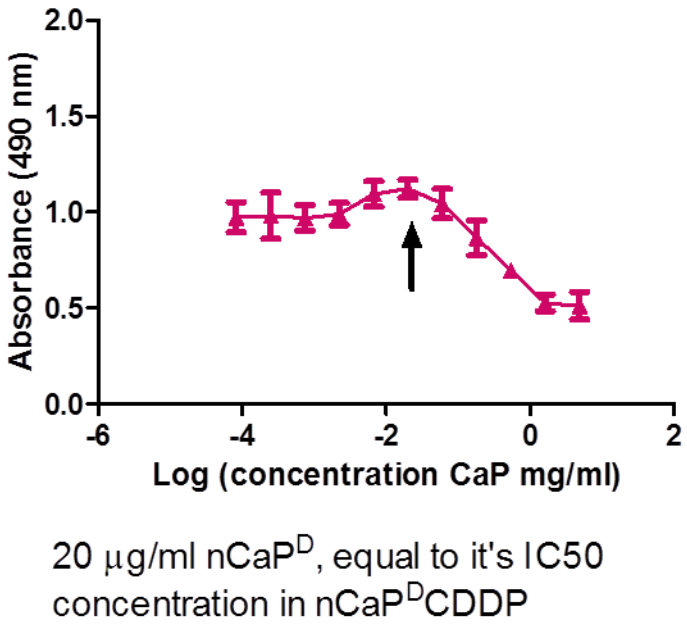

Figure 2.8 Assessment of $nCaP^D$ cytotoxicity measured at 490 nm from MTS assay against SCCVII cells. Arrow shows the concentration of $nCaP^D$ in $nCaP^D$CDDP at its IC50 value relative to CDDP. $nCaP^D$ is not cytotoxic atIC50 value of $nCaP^D$CDDP.

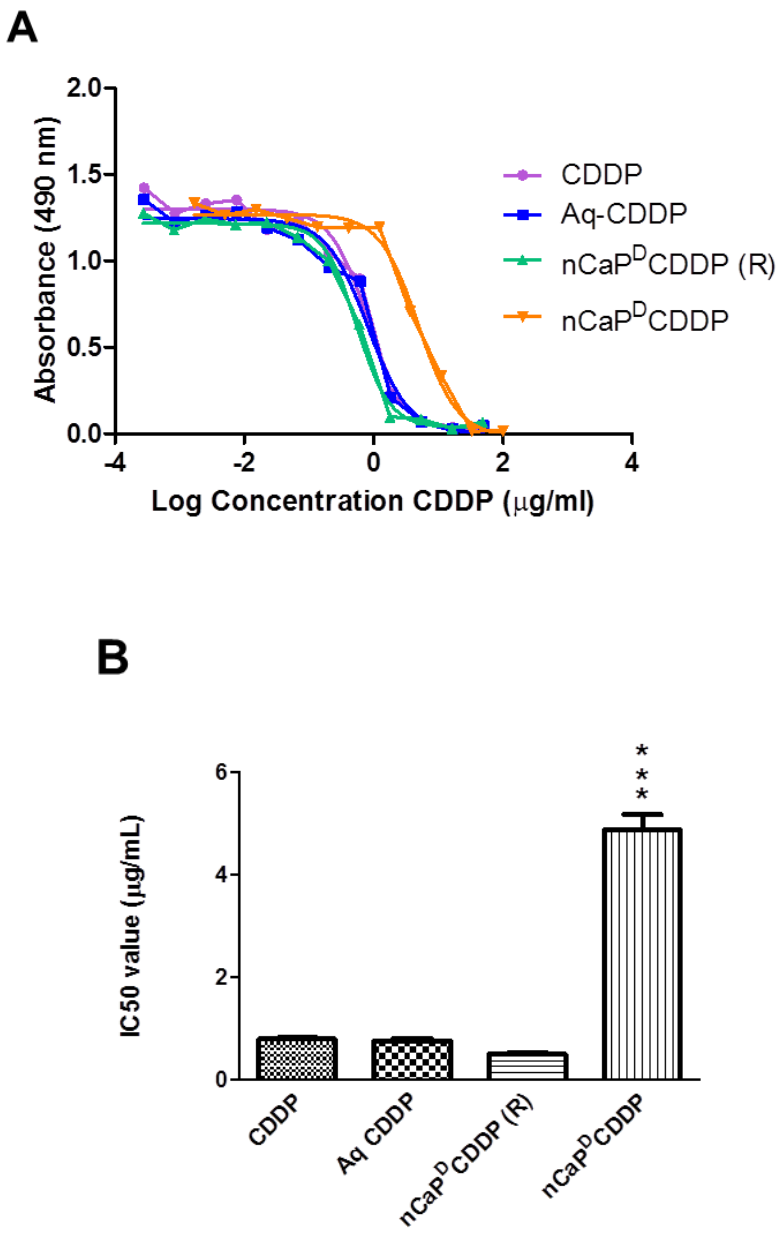

Figure 2.9 (A) Cytotoxicity curves of CDDP, Aq CDDP, nCaP^{D}CDDP (R) and nCaP^{D}CDDP. (B) Calculated IC50 values from cytotoxicity curves in A, where data represents 4 replicates. This data demonstrates that CDDP released from nCaP^{D}CDDP is as cytotoxic as CDDP and Aq CDDP. nCaP^{D}CDDP is significantly less cytotoxic than CDDP, Aq CDDP and released CDDP ($P < 0.0001$).

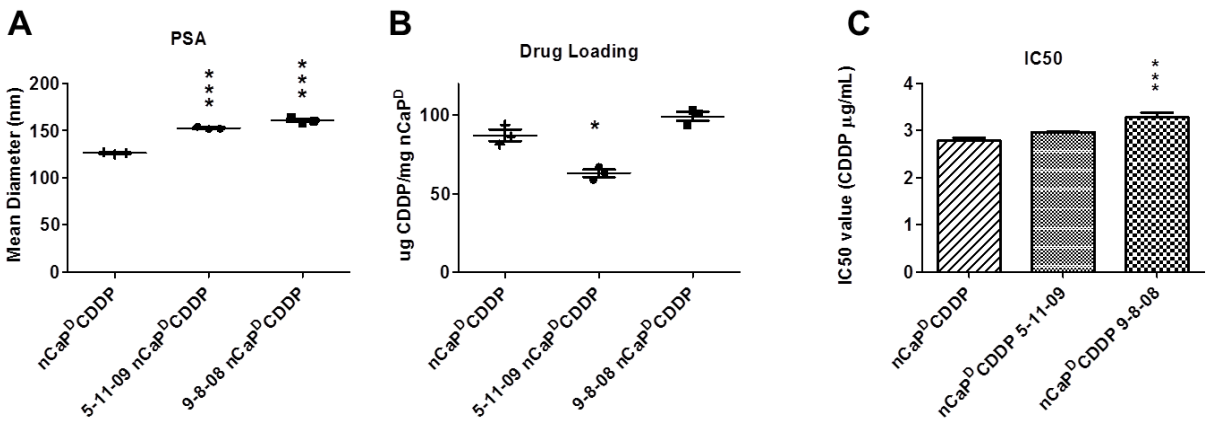

Figure 2.10 Stability studies. Freshly prepared nCaP^{D}CDDP was compared to batches that had been stored for 2 (nCaP^{D}CDDP 5-11-09) and 3 years (nCaP^{D}CDDP 9-8-08). Particle size, drug loading and IC50 values against SCCVII cells of nCaP^{D}CDDP were found to vary significantly with time stored. (A) Average particle size of stored batches was significantly larger than freshly made batch of nCaP^{D}CDDP, ~22% larger ($P < 0.0001$). (B) Drug loading varied significantly from a freshly made batch of nCaP^{D}CDDP for one of the two stored batches tested by ~25% ($P < 0.05$). (C) IC50 value of batch stored for three years was significantly less cytotoxic than freshly made batch ($P < 0.0001$).

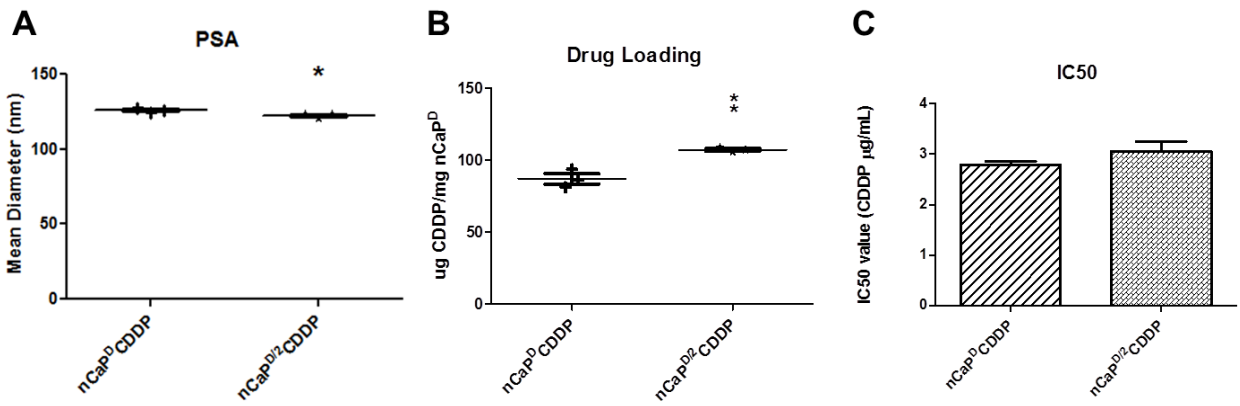

Figure 2.11 Effects of reducing D stabilizer concentration by half. To determine if less D could be utilized to stabilize nCaP, half the concentration was examined. (A) Average particle size of nCaP$^{D/2}$CDDP is significantly smaller than nCaP^{D}CDDP ($P = 0.0213$). (B) Drug loading of nCaP$^{D/2}$CDDP is significantly greater than nCaP^{D}CDDP ($P = 0.0056$). (C) IC50 value of nCaP$^{D/2}$CDDP was not significantly different from nCaP^{D}CDDP against SCCVII cells.

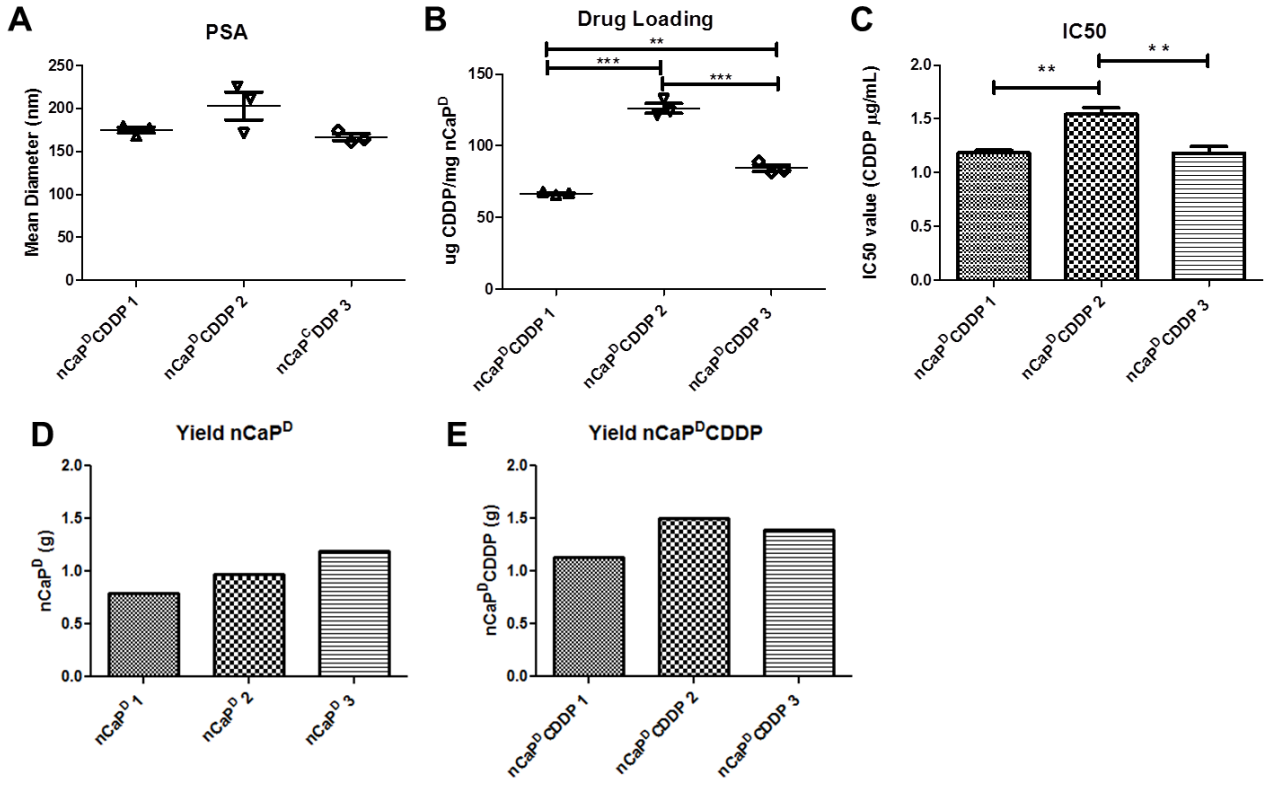

Figure 2.12 Batch to-batch variability assessment. Three separate batches of nCaP^{D}CDDP were made using exactly the same method. Although particle size was not significantly different from batch to batch, drug loading and IC50 values were. (A) Average particle size of three batches of nCaP^{D}CDDP. (B) Each batch had significantly different drug loading than the next ($P < 0.0001$). (C) IC50 value of batch two is significantly higher than the other two batches against SCCVII cells ($P < 0.001$). (D) Yield varied from batch to batch, before and (E) after CDDP binding.

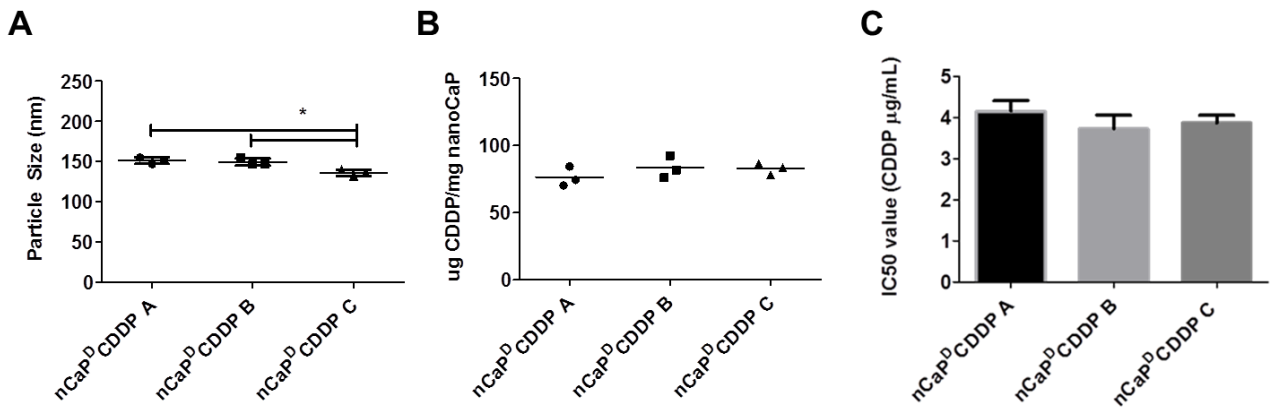

Figure 2.13 Following minor modifications to the nCaP^{D}CDDP outlined in Figure 2.3 synthesis variation in drug loading and IC50 values were mitigated. (A) Average particle size of three batches of nCaP^{D}CDDP made using modified method. Batch C was significantly smaller than the others, but it was only 3% smaller, which is typically acceptable deviation. (B) Differences in drug loading from batch to batch were mitigated with minor modifications to the synthesis and binding procedure. (C) Differences in IC50 value against SCCVII cells from batch to batch was also mitigated.

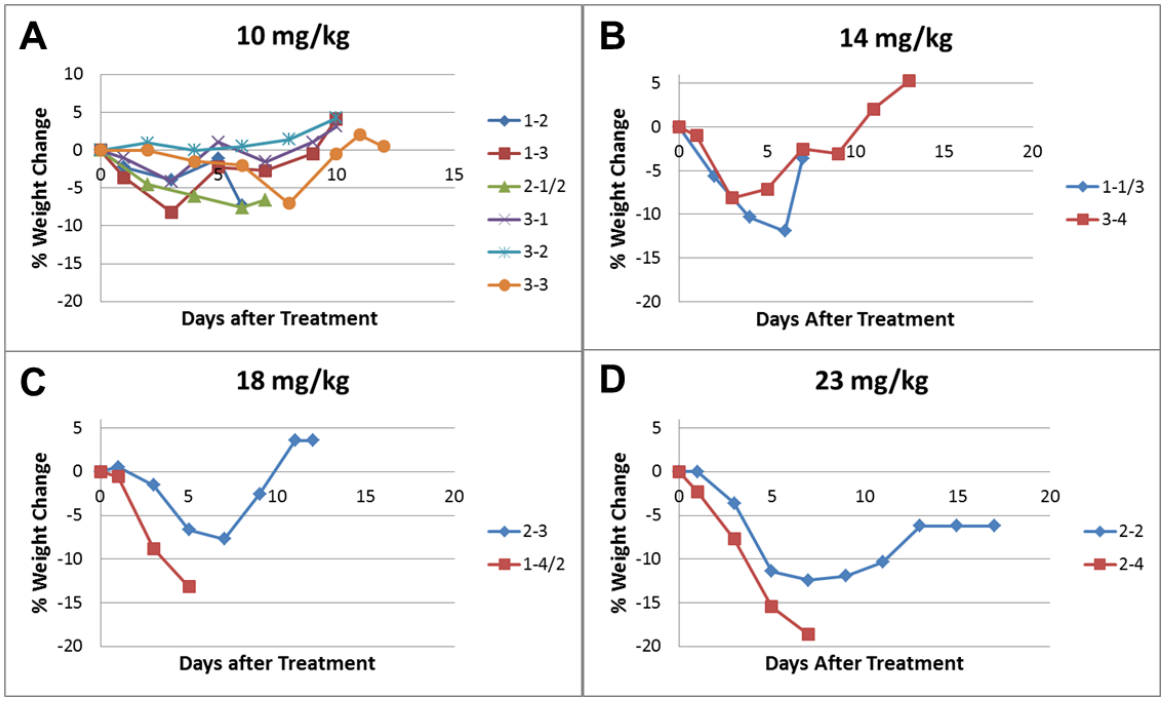

Figure 2.14 Maximum tolerable dose of nCaP^{D}CDDP was conducted on CH3/HeJ mice bearing SCCVII tumors. nCaP^{D}CDDP was administered once intratumorally. Weight loss was monitored every other day following treatment and shown for each animal. The legend indicates the animal number. (A) The 10 mg/kg dose was well tolerated. (B) The 14 mg/kg dose caused weight loss down to 13%, but the animals recovered. (C) The 18 mg/kg dose caused one animal to drop to 13% weight loss and was euthanized due to weight loss and tumor necrosis. (D) The 23 mg/kg dose caused one animal to drop below the 15% weight loss threshold.

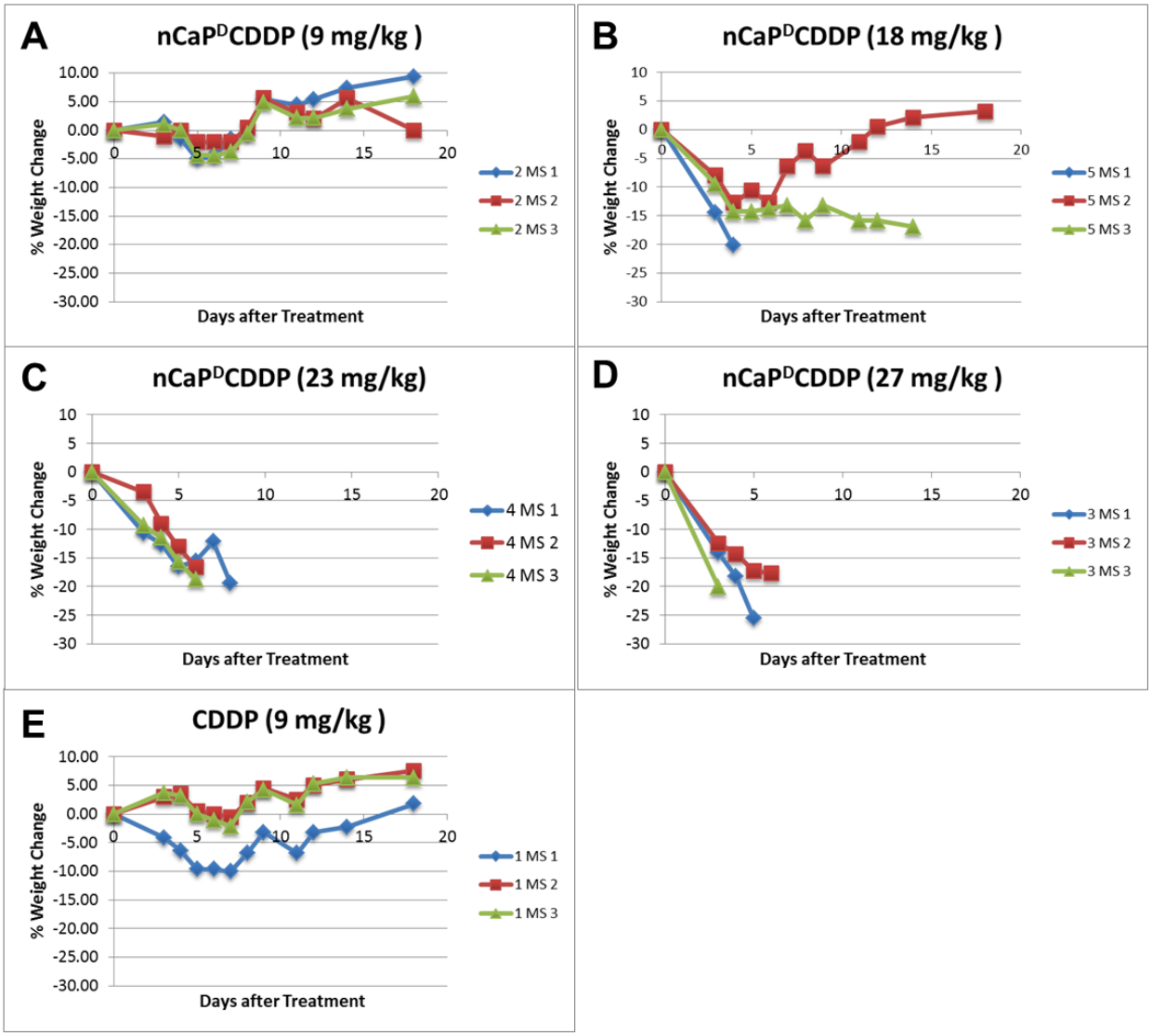

Figure 2.15 A maximum tolerable dose study for the nCaP^{D}CDDP was conducted on CH3/HeJ mice and compared to the free drug without nanoparticles. Drug was administered once subcutaneously. Weight loss was monitored every other day following treatment (A) The 9 mg/kg dose nCaP^{D}CDDP was well tolerated. (B) The 18 mg/kg dose nCaP^{D}CDDP caused weight loss beyond 15%. (C) The 23 mg/kg dose nCaP^{D}CDDP caused all animals to drop below the 15% weight loss threshold. (D) The 27 mg/kg dose nCaP^{D}CDDP caused all animals to drop below the 15% weight loss threshold. (E) The 9 mg/kg CDDP was well tolerated.

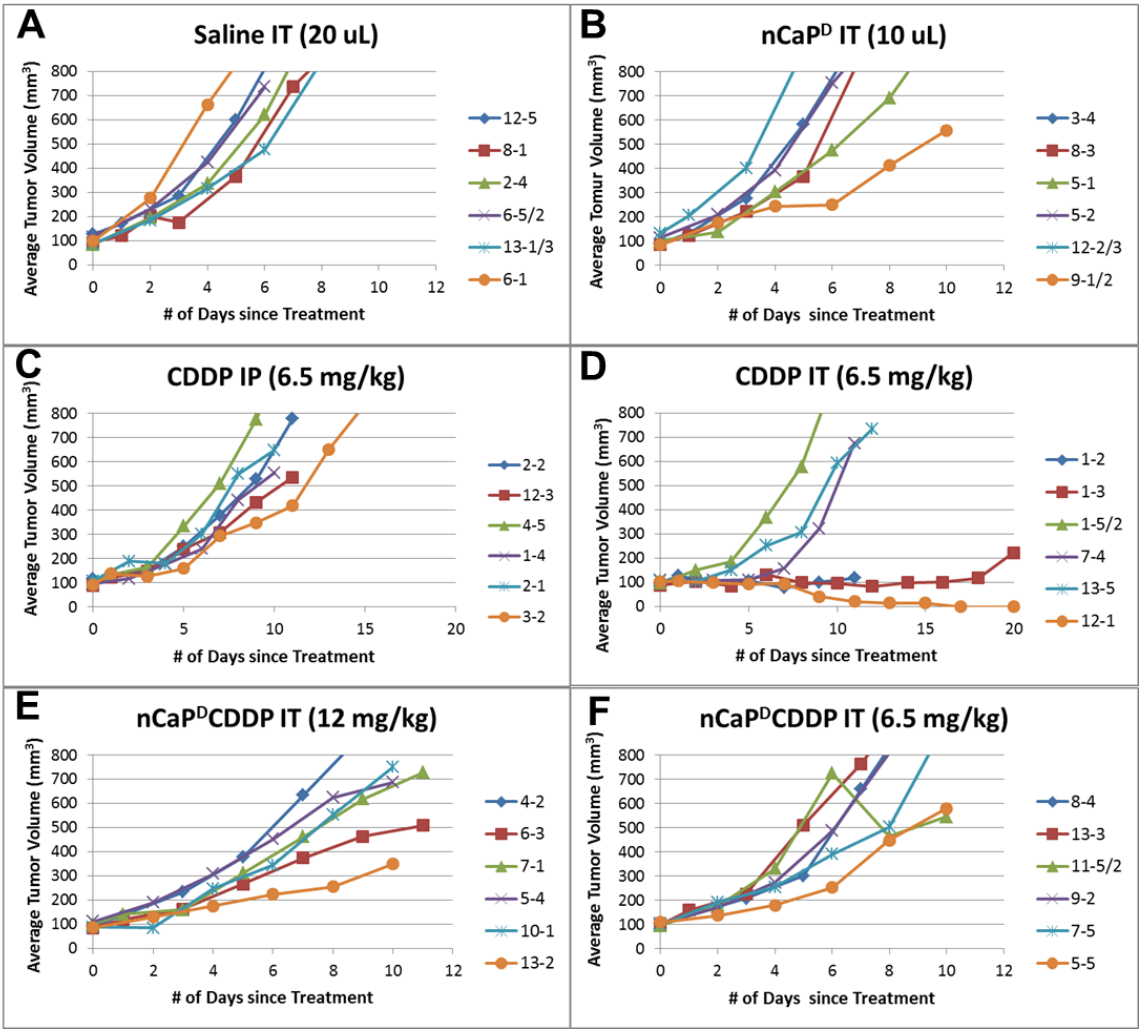

Figure 2.16 Efficacy study of nCaP^{D}CDDP was conducted on CH3/HeJ mice bearing SCCVII tumors. Animals were treated once when their tumor volume reached 120 ± 20 mm^3. Each graph shows individual tumor volume (mm^3) vs days post treatment for each animal in the group. The legend indicates the animal number. (A) Negative control, saline IT, did not delay any tumor growth. (B) Negative control, nanoparticles without drug IT, no significant tumor growth delay was seen. (C) Positive control, 6.5 mg/kg CDDP IP, was also not effective. (D) Positive control, 6.5 mg/kg CDDP IT, to which response was split between near complete response and nearly no response. (E & F) nCaP^{D}CDDP IT at two different doses (6.5 and 12 mg/kg). Neither significantly delayed tumor growth

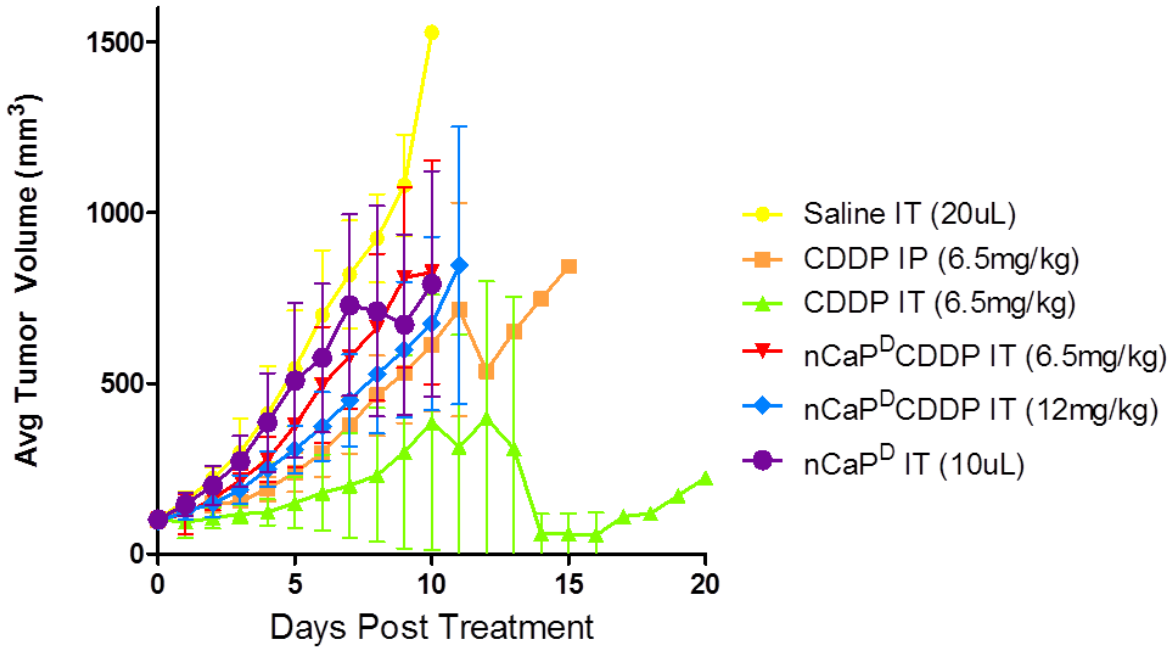

Figure 2.17 Efficacy study of nCaP^{D}CDDP was conducted on CH3/HeJ mice bearing SCCVII tumors. Animals were treated once when their tumor volume reached 120 ± 20 mm^3 and compared to 9 mg/kg CDDP. Tumor volume, grooming and weight loss were monitored every other day following treatment. The graph shows average tumor volume (mm^3) for each treatment group versus days post treatment. The negative control Saline IT (20 uL) had no effect on tumor growth. nCaP^{D} (10 uL) had no effect on tumor growth. Free drug at 6.5 mg/kg CDDP intraperitoneally delayed tumor growth. 6.5 mg/kg CDDP caused tumors to stop growing or disappear in 50% of animals treated. 12 mg/kg nCaP^{D}CDDP did not significantly delay tumor growth. 6.5 mg/kg nCaP^{D}CDDP did not significantly delay tumor growth.

A

% Weight Change Average						
	Saline IT	nanoCaP IT (10ul)	nanoCaP/CDDP IT (6.5mg/kg)	nanoCaP/CDDP IT (12mg/kg)	CDDP IT (6.5mg/kg)	CDDP IP (6.5mg/kg)
Average	2.6	3.2	-2.3	-4	-2	-2.1
StDev	2.3	3.2	3.3	5.5	3.2	3.1
Day	4	3	4	5	6	5

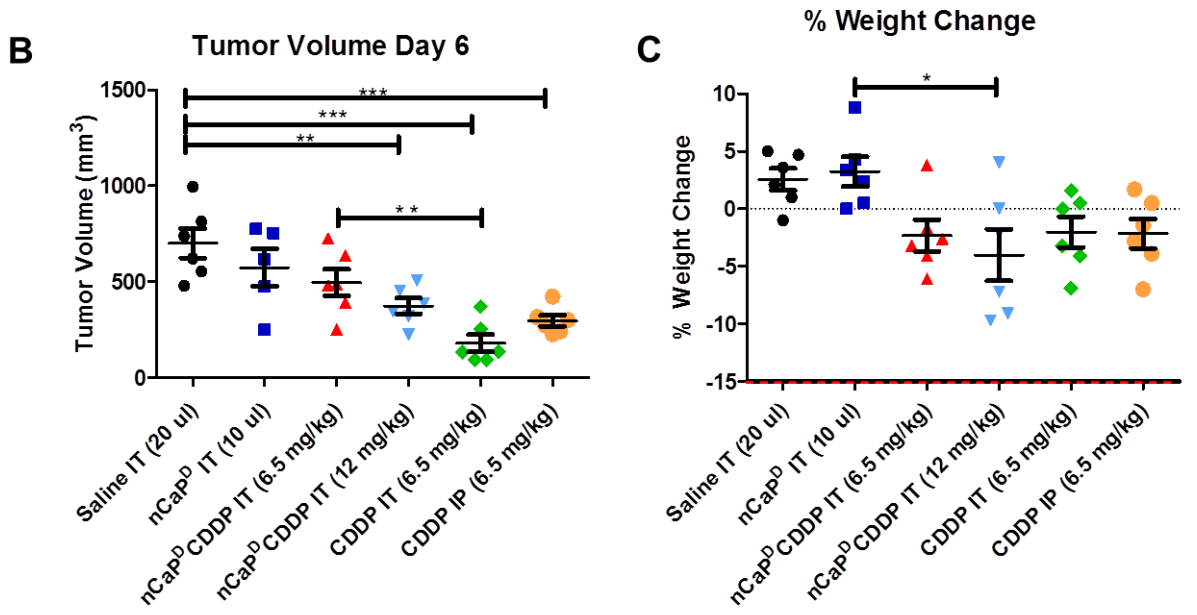

Figure 2.18 Efficacy and toxicity study of nCaP^{D}CDDP was conducted on CH3/HeJ mice bearing SCCVII tumors. Animals were treated once when their tumor volume reached 120 ± 20 mm^{3}. Tumor volume, grooming and weight loss were monitored every other day following treatment. The average weight loss was determined for each group on each day following treatment. From that, the maximum weight loss for each treatment group was determined. (A) The table shows for each treatment group the maximum percent weight loss, the standard deviation and the day following treatment the weight loss occurred on. (B) At day 6 following treatment CDDP IT at 6.5 mg/kg was the most effective treatment for the delay of tumor growth ($P < 0.05$). 6.5 mg/kg nCaP^{D}CDDP was significantly less effective at delaying tumor growth than CDDP IT at 6.5 mg/kg. (C) Is a graphical representation of tabulated values in A. 12 mg/kg nCaP^{D}CDDP caused the most significant weight loss overall.

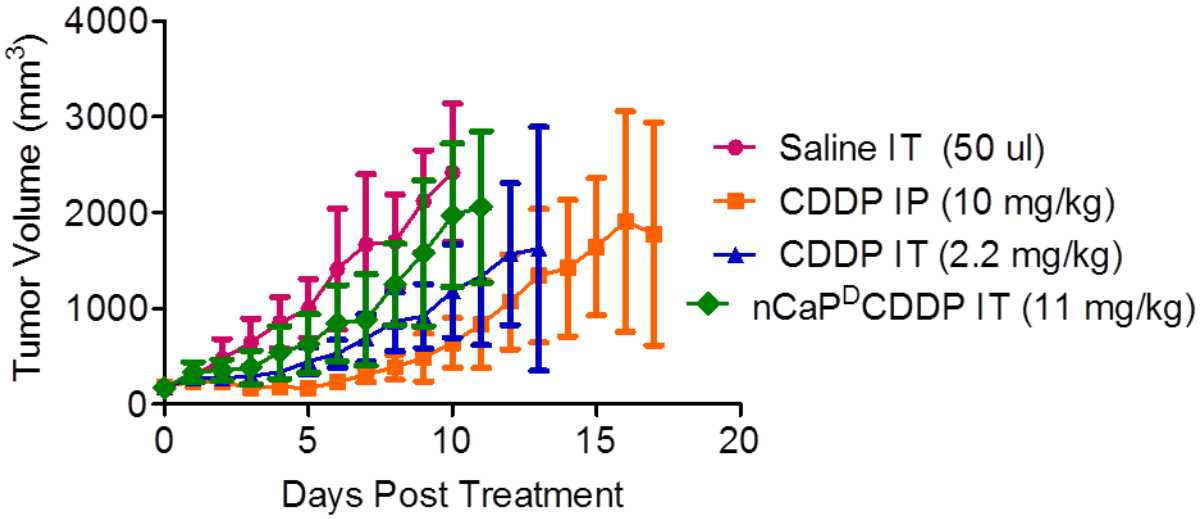

Figure 2.19 A repeated efficacy study of nCaP^{D}CDDP was conducted on CH3/HeJ mice bearing SCCVII tumors. Animals were treated once when their tumor volume reached 160 ± 10 mm^3 and compared to 10 mg/kg CDDP IP. Tumor volume, grooming and weight loss were monitored every other day following treatment. The graph shows average tumor volume (mm^3) versus days post treatment (6 animals/group). The negative control Saline IT (50 uL) had no effect on tumor growth. IP CDDP (10 mg/kg) delayed tumor growth, but ultimately was not effective at stopping growth of SCCVII tumors.

A

% Weight Change Average				
	Saline IT	CDDP IP (10mg/kg, MTD)	CDDP IT (2.2mg/kg, MTV)	NanoCaP-D/CDDP (11mg/kg)
Average	-2.16	-6.32	-1.43	-10.17
StDev	2.8	1.72	2.57	5.97
Day	2	6	3	5

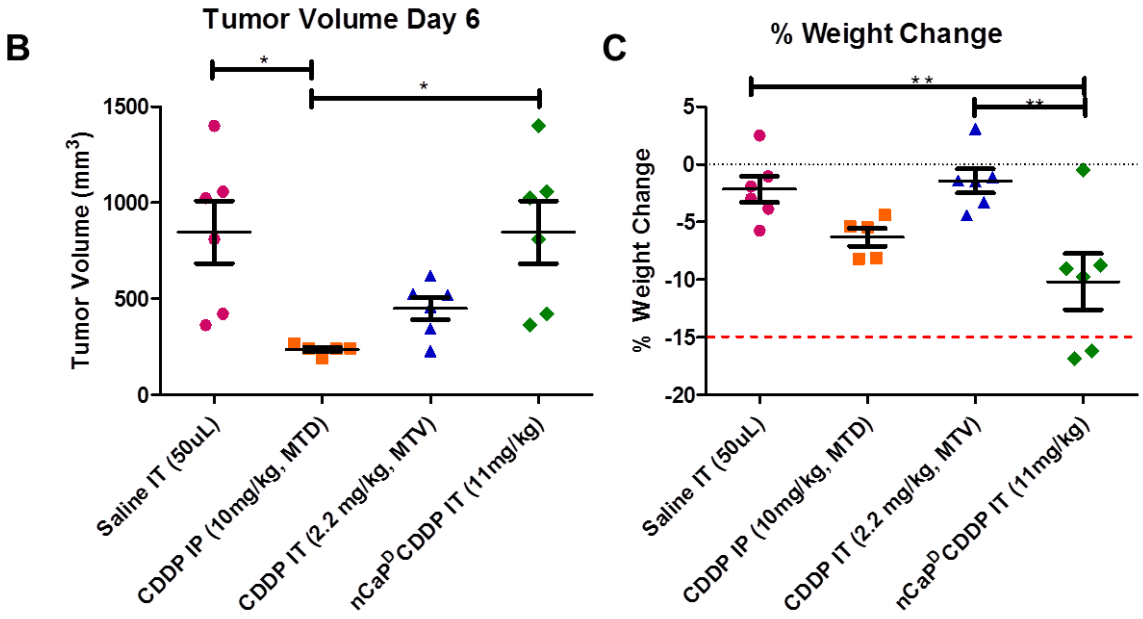

Figure 2.20 Repeated efficacy and toxicity study of nCaP^{D}CDDP was conducted on CH3/HeJ mice bearing SCCVII tumors. Animals were treated once when their tumor volume reached 160 ± 10 mm^{3} and compared to 10 mg/kg CDDP IP. Tumor volume, grooming and weight loss were monitored every other day following treatment. The average weight loss was determined for each group on each day following treatment. From that, the maximum weight loss for each treatment group was determined. (A) The table shows for each treatment group the maximum percent weight loss, the standard deviation and the day following treatment the weight loss occurred on. (B) CDDP IP at 10 mg/kg was the most effective treatment for the delay of tumor growth ($P < 0.05$). A dose of 11 mg/kg nCaP^{D}CDDP was significantly less effective at delaying tumor growth than CDDP IP at 10 mg/kg. (C) Graphical representation of A. The 11 mg/kg nCaP^{D}CDDP IT caused the most significant weight loss overall.

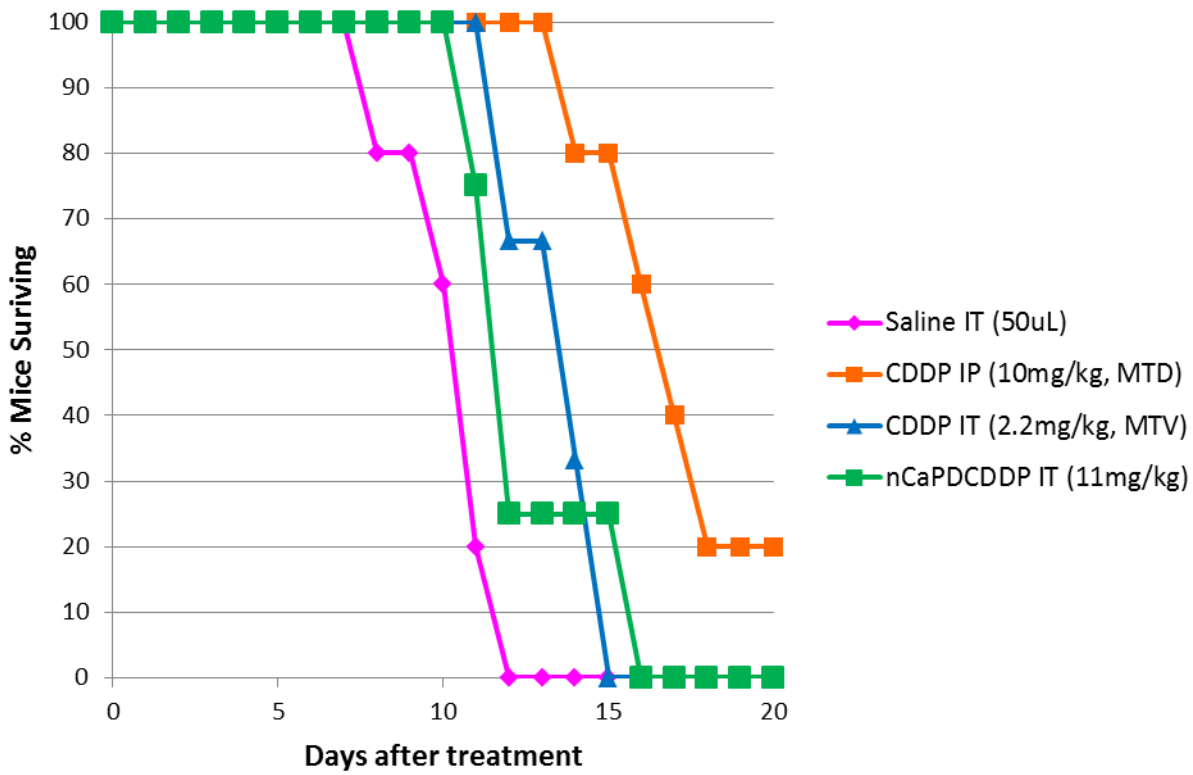

Figure 2.21 Survival curve for the repeated murine HNC animal model efficacy study shown in Figure 2.19. Survival was defined as > 15% weight loss, tumor diameter > 2 mm, or inability to groom. CDDP IP at 10 mg/kg was the most effective at prolonging survival of the mice.

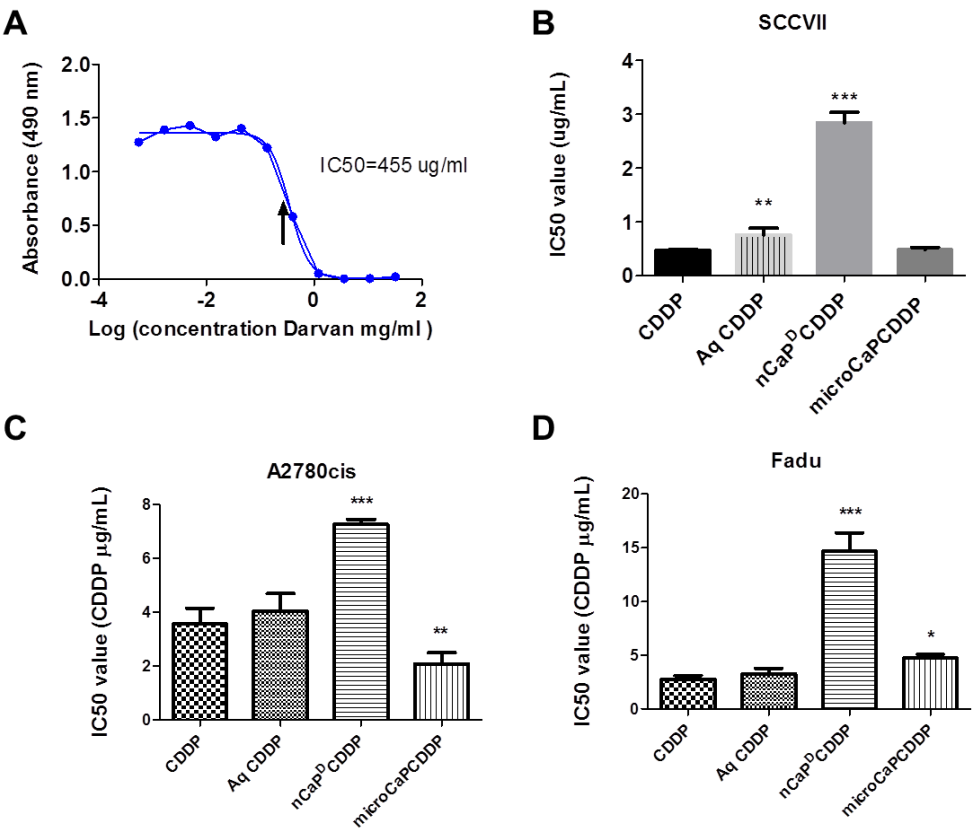

Figure 2.22 Darvan ® 811 is cytotoxic at concentrations found in nCaP^{D}CDDP and inhibits CDDP cytotoxicity. (A) Cytotoxicity curve of D against SCCVII cells. The arrow indicates D concentration in nCaPDCDDP at top concentration used for IC50 determination (564 ug/mL). IC50 values from cytotoxicity curves of CDDP, Aq CDDP, nCaP^{D}CDDP and microCaPCDDP against: (B) SCCVII (C) A2780cis and (D) FaDu cells.

Chapter 3

Sodium Citrate Stabilized Calcium Phosphate Nanoparticles for the Delivery of Cisplatin

3.1 Introduction

Head and neck cancer (HNC) patients suffer from many serious side-effects due to treatments including severe mucositis and complications with eating and talking[29]. If the tumor is in close proximity to vital anatomy, like the carotid artery, surgery is very dangerous and often impossible. For patients with these non-resectable tumors chemo-radiation is the standard of care, but the 5 year relative survival rate for is only 35%[129]. There is a desperate need for better localized treatments for HNC patients.

Calcium phosphate is an attractive inorganic material for drug delivery because it is biocompatible, resorbable and relatively inexpensive to manufacture[65,66,130,131]. Calcium phosphate is an effective carrier for drugs and genetic material, that is readily made via precipitation, dissolves in acidic conditions, does not incite an immune response and is non-toxic[15,67,89,96,109,132]. Precipitation of calcium phosphate will result in aggregated microcrystals unless a stabilizer is added to halt crystal growth and limit aggregation[100]. In Chapter 2, we showed sodium polyacrylate (Darvan ® 811) is cytotoxic *in vitro* and caused toxicity to animals as measured by weight loss when administered as a local injection of nCaP^{D}CDDP This chapter describes the use of sodium citrate to stabilize calcium phosphate for the delivery of CDDP. Sodium citrate is a known stabilizer of calcium phosphate and is on the Generally Regarded as Safe (GRAS) list from the Food and Drug Administration[21,133,134]. The molecular structure of sodium citrate is shown in Figure 3.1. Sodium citrate stabilized calcium phosphate nanoparticles

carrying CDDP (nCaP^{CIT}CDDP) were physically characterized, tested for *in vitro* cytotoxicity and examined for *in vivo* intratumoral anti-tumor efficacy against a mouse model of human head and neck cancer.

3.2 Materials and Methods

3.2.1 Materials

The $CaCl_2$ (Sigma C4901), K_2HPO_4 (Sigma S1804), $C_6H_5Na_3O_7$ $2H_2O$ (Sodium Citrate, Sigma P3786), $Pt(NH_3)Cl_2$ (CDDP, Sigma P4394), and $AgNO_3$ (Silver Nitrate, Sigma S6506) used to prepare the nanoparticles were all purchased from Sigma-Aldrich, (St. Louis, MO). Aq-CDDP was prepared as described previously [1]. BD Matrigel™ for cell injections was purchased from BD Biosciences, (San Jose, CA).

Murine squamous cell carcinoma of the head and neck, SCCVII, human hypopharyngeal carcinoma, FaDu cells from ATCC and human CDDP resistant ovarian cancer A2780cis cells were used for *intro* cytotoxicity evaluation of the nanoparticles. FaDu cells were used for *in vivo* anti-tumor efficacy. SCCVII cells were maintained as previously mentioned. FaDu cells were maintained in MEM (Gibco 10370) containing 10% heat-inactivated FBS, 1 mM sodium pyruvate (Invitrogen 11360), 2 mM L-glutamine (Invitrogen 25030), 1% penicillin streptomycin.

The C3H/HeJ and Nu/J female mice were purchased from Jackson Laboratory, (Bar Harbor, ME) and used for studies at 6-8 weeks of age.

3.2.2 nCaP^{CIT}CDDP Production and Physical Characterization

nCaP^{CIT}CDDP synthesis was based on a previously reported method for nCaPCDDP[16]. To make the nCaP^{CIT} equal volumes of 30 mM $CaCl_2$ and 30 mM K_2HPO_4 + 20 mM citrate were mixed by

adding the phosphate/citrate solution to the calcium and allowed to precipitate for 10 minutes with stirring. Nanoparticles were collected via centrifugation (12000 rpm for 45 min) and washed once with MilliQ ® water. The particles were then allowed to adsorb Aq-CDDP for 20 hours. The concentration of the CDDP was determined by inductively coupled plasma-optical emission spectroscopy (Perkin Elmer® Optima™ 5300 DV, ESIS Inc., Cromwell, CT). Following binding, the particles were collected via centrifugation, rinsed twice with MilliQ ® water to remove unbound Aq-CDDP and diluted 2x with 20 mM citrate solution to make a suspension that was injectable through a 25 gauge needle. All solutions/liquids during the synthesis process were sterile-filtered with a 0.2 μm filter. The $nCaP^{CIT}$CDDP suspension was stored at room temperature and shielded from light.

Aq-CDDP content within the nanoparticles was determined by inductively coupled plasma-optical emission spectroscopy (Perkin Elmer® Optima™ 5300 DV, ESIS Inc., Cromwell, CT) on samples of known volume dissolved in 1N of HCl. Particle size analysis (PSA) was performed via dynamic light scattering technique using a 90 Plus Particle Sizer (Brookhaven Instruments, NY). Samples were prepared by sonicating the particle suspension and diluting the suspension 12x in MilliQ ® water. The morphology and size of the particles were observed by using a Hitachi H-7650 transmission electron microscope (TEM). TEM samples were prepared by sonicating the particle suspension and diluting the suspension 26x in 10 mM citrate solution then 10x in 70% ethanol. A 5 uL sample was placed on a formvar carbon coated 300 mesh Cu grid. Sample sat for 1min and then any excess solution was removed using filter paper. Prior to imaging the sample completely dried in air for 5 min. Samples were imaged at 80 kV with the TEM. X-ray diffraction (XRD) was used to determine changes in crystallinity with addition of citrate stabilizer and to compare dry vs wet $nCaP^{CIT}$. Samples of lyophilized calcium

phosphate without citrate (microCaP), lyophilized nCaP^{CIT} and wet nCaP^{CIT} were analyzed using a Bruker D2 Phaser.

3.2.3 nCaP^{CIT}CDDP In Vitro *Drug Release Studies*

In vitro drug release studies were performed using ready to use dialysis devices, (Float-A-Lyzer® G2, Spectrum Laboratories Inc., Rancho Dominguez, CA), with a molecular weight cut off of 100 kD. 0.55 mL of particle suspension was loaded in to the dialysis device and placed in 22 mL of 10 mM PBS. The pH of the PBS was adjusted to 6.8 to mimic an acidic tumor microenvironment. The samples were capped, placed on an orbital shaker, and incubated at 37°C. Release samples were drawn at 1h, 6h, 1d, 3d, 5d, 7d, and 14d. At each time point 5 mL of release solution was taken and replaced with 5 mL of fresh PBS. CDDP content in the release solution was determined by inductively coupled plasma-optical emission spectroscopy (Perkin Elmer® Optima™ 5300 DV, ESIS Inc., Cromwell, CT).

3.2.4 Cytotoxicity

Cytotoxicity experiments were conducted using FaDu and SCCVII cells plated in 96 well plates at 60,000 and 20,000 cells/mL, respectively with 50 uL suspension per well. Cells were allowed to proliferate for 24 hours following which drug was added in 50 uL volumes. The following groups were examined with top concentration tested in parentheses: Citrate (10 mM), nCaP^{CIT} (to match nCaP^{CIT} in nCaP^{CIT}CDDP), (CDDP in saline (405 ug/mL), aquated CDDP (466 ug/mL), 20 mM citrate reacted with to Aq CDDP (Aq CDDP-CIT) (458 ug/mL), nCaP^{CIT}CDDP (500 ug/mL), and nCaP^{CIT}CDDP release 3d (R) (119 ug/mL). Each group was serially diluted 1:3 across the plate using PBS. Cells were assayed 48 h after drug addition using in an MTS assay (CellTiter 96® AQ_{ueous} One, G3580, Promega Corp., Madison, WI), where metabolic

activity was determined using a Spectramax Plus^{384} Spectrophotometer (Molecular Biosciences, Sunnyvale, CA) at an absorbance of 490nm. To determine the IC_{50} (50% inhibitory concentration) a non-linear regression curve fit analysis was performed with at least four replicates per group.

3.2.5 nCaP^{CIT}CDDP In Vivo *Maximum Tolerable Dose Study*

A maximum tolerable dose (MTD) study was performed in 6 month old C3H/HeJ female mice without tumors (1-4 mice/group) as follows. The MTD was defined for the purposes of this study as the maximum dose that could be administered to a mouse that will result in less than 15% weight loss. Each mouse received one, intraperitoneal (IP) injection of the nanoparticle suspension via a 25-gauge needle; groups included: 10, 20, 30, and 40 uL injections of nCaP^{CIT}CDDP at a CDDP concentration of 16.7 mg/mL. These volumes result in average doses of 7.4 mg/kg, 13.3 mg/kg, 20.8 mg/kg, and 24.5 mg/kg respectively, based on individual mouse weight and CDDP concentration of the nanoparticle suspension. Mouse weight was monitored daily for eight days, (by day 8 all mice had recovered from the normal initial weight loss seen with CDDP doses in the first few days, or had exceeded 15% weight loss). Mice exceeding 15% weight loss were euthanized.

3.2.6 FaDu Tumor Take Rate in Nu/J Mice

To assess the growth parameters of FaDu tumor initiated in Nu/J mice two tumor take rate studies were performed. This was performed to ensure that tumors will growth at a steady pace, without growing too fast causing necrosis or too slow such that they regress on their own. The first study used a BD Matrigel™ to cells in base media ratio of 80:20. Four mice were used per groups and the groups were: 8 x 10^5 cells in a 200 uL volume injection or 2 x 10^5 cells in a 100

uL injection, in the right rear flank via a 25-gauge needle. Animals were monitored every other day for 15 days following inoculation.

The second tumor take rate study was conducted again using a 80:20 ratio of Matrigel : cell suspension. Here groups were: 5 x 10^6 cells in 200 uL injection (5 animals) and 2 x 10^6 cells in 200 uL injection (3 animals), in the right rear flank via a 25-gauge needle. Animals were monitored every other day for 15 days following inoculation.

3.2.7 nCaP^{CIT}CDDP In Vivo *Anti-Tumor Efficacy and Toxicity Studies*

Two efficacy and toxicity studies were performed using FaDu cells in Nu/J mice. The first study included 33 mice inoculated with 2x10^6 FaDu cells in 100µL of a 70 : 30 ratio of BD Matrigel™ : cell-media in the right rear flank via a 25-gauge needle. A total of 33 female, 8 week old, Nu/J mice were included in the study, (4-6 mice/group, 6 groups). Tumors were measured daily using digital calipers to calculate the tumor volume as follows: $V = (W)^2 * L * 0.4$. Tumors were treated once with: 10 mg/kg CDDP IP, 30 µL of saline IT, 20 µL of nCaP^{CIT} IT(without CDDP), 1.4 mg/kg CDDP IT, 13.7 mg/kg nCaP^{CIT}CDDP IT or 20.7 mg/kg nCaP^{CIT}CDDP IT, when tumor volume reached 120 ± 20 mm^3.

In the repeat efficacy and toxicity study Nu/J mice were inoculated with 2x10^6 FaDu cells in 100µL of a 60 : 40 ratio of BD Matrigel™ : cell-media in the right rear flank via a 25-gauge needle. A total of 28 female, 5 week old, Nu/J mice were included in the study, (7 mice/group, 4 groups). Tumors were measured daily using digital calipers to calculate the tumor volume as follows: $V = (W)^2 * L * 0.4$, where W = width, L = length, and V = volume.

Tumors were treated once, intratumorally (IT), with either 30 µL of saline, 30 µL of $nCaP^{CIT}$ (without CDDP), 1.4 mg/kg CDDP in saline (CDDP IT), or 10 mg/kg $nCaP^{CIT}$CDDP, when tumor volume reached 140 ± 14 mm^3.

For both studies systemic toxicity was evaluated by weight change and overall grooming/appearance. Tumor volume and mouse weight were monitored at least every other day. Mice were euthanized due to significant weight loss (> 15%), a tumor length measurement greater than 20 mm, or completion of the study (day 30). All animal experimental procedures were approved by the Animal Care and Use Committee of the University of Connecticut Health Center, (Farmington, CT).

3.2.8 Statistical Analysis

Statistical analysis was performed using an unpaired t-test or Tukey one-way ANOVA, as indicated in the methods. A P-value of less than 0.05 was considered statistically significant. Data is presented as a mean value with its standard deviation indicated (mean $\pm$ SD).

3.3 Results

3.3.1 Physical Characterization of $nCaP^{CIT}$CDDP

A diagram of the $nCaP^{CIT}$CDDP composition is shown in Figure 3.2. Positively charged Aq CDDP electrostatically binds to negatively charged $nCaP^{CIT}$ to make $nCaP^{CIT}$CDDP. Release of Aq CDDP is achieved when $nCaP^{CIT}$CDDP is placed in *in vitro* or *in vivo* conditions in the presence of chloride ions which cause the re-formation of native CDDP. Transmission electron microscopy (TEM) (Figure 3.3 A) and particle size analysis via dynamic light scattering (Figure 3.3 B) showed that $nCaP^{CIT}$CDDP in suspension form small aggregates with an average size of

180.6 ± 19.5 nm. Average drug loading of the suspension is 158.7 ± 11.6 µg CDDP/mg $nCaP^{CIT}$. These results, in addition with polydispersity, are summarized in Table 3.1. XRD comparing $nCaP^{CIT}$ as a wet suspension, $nCaP^{CIT}$ lyophilized and microCaP showed $nCaP^{CIT}$CDDP is poorly crystalline with the major peak occurring at 30º corresponding well with hydroxyapatite (HA) while microCaP was more crystalline in nature resembling brushite and poorly crystalline HA (Figure 3.4) [113,135]. The comparison of microCaP with both wet and dry $nCaP^{CIT}$ clearly demonstrate that crystal growth of CaP was halted by the addition of citrate, creating nanoparticles with no long order crystal structure.

3.3.2 $nCaP^{CIT}$CDDP In Vitro *Release Studies*

The release profile of the $nCaP^{CIT}$CDDP in PBS, pH 6.8, at 37° C can be seen in Figure 3.5. $nCaP^{CIT}$CDDP has continuous *in vitro* release. A burst release of CDDP was exhibited in the first 24 h, with slower, continuous release out to day 14. Total percent CDDP release after 14 days is 27% based on total CDDP bound.

3.3.3 Cytotoxicity

FaDu cells were used to determine the cytotoxicity of $nCaP^{CIT}$CDDP, $nCaP^{CIT}$CDDP, citrate, Aq CDDP-CIT, CDDP and Aq CDDP. Non-linear regression curve fit analysis of each of these treatments is shown in Figure 3.6 A-F. $nCaP^{CIT}$ is not cytotoxic as all concentrations tested had comparably high absorbance readings (Figure 3.6 D). Citrate alone caused some toxicity at a top dose of 10 mM (Figure 3.6 C). The *in vitro* cytotoxicity of $nCaP^{CIT}$CDDP and the released CDDP from $nCaP^{CIT}$CDDP were determined with FaDu and SCCVII cells using an MTS assay. The 50% inhibitory concentrations (IC_{50}) are plotted in Figure 3.7. CDDP released from

nCaP^{CIT}CDDP has the same cytotoxicity as CDDP alone and Aq-CDDP. Sodium-citrate when reacted with Aq CDDP inhibits the cytotoxicity of Aq CDDP.

3.3.4 FaDu Tumor Take Rate in Nu/J Mice

Two tumor take rate studies were conducted in Nu/J mice. The first study used either 2 x 10^5 or 8 x 10^5 cells per injection, both of which were determined to be insufficient for regular tumor growth (Figure 3.8 A. Tumors did not grow steadily and growth tapered after 10 days. The second tumor take rate study used 2 x 10^6 or 5 x 10^6 FaDu cells per injection (Figure 3.8 B). The early shrinking of tumor volume is due to degradation of Matrigel. Once the Matrigel degrades tumor growth continues.

3.3.5 nCaP^{CIT}CDDP In Vivo *Maximum Tolerable Dose Study*

A maximum tolerable dose (MTD) study was performed in C3H/HeJ mice without tumors, (Figure 3.9). The MTD is defined as the maximum dose that can be administered to a mouse that will result in less than 15% weight loss and is a measure of systemic toxicity of the tested materials. The maximum tolerable dose that can be administered to a C3H/HeJ mouse without experiencing significant weight loss (> 15%) is 13 mg/kg nCaP^{CIT}CDDP IP. The conjugation of CDDP to nCaP^{CIT} allows for an increase in MTD compared to CDDP IP (MTD 10 mg/kg). The results shown in Fig. 13.9 show the average weight loss for the 13.3 and 24.5 mg/kg nCaP^{CIT}CDDP IP dose, in addition to the average weight loss of a 9 mg/kg CDDP IP dose performed in C3H/HeJ, female, 6 month old mice, but from a previous study.

3.3.6 nCaP^{CIT}CDDP In Vivo *Anti-Tumor Efficacy and Toxicity Studies*

The *in vivo* anti-tumor efficacy of the nCaP^{CIT}CDDP was evaluated using FaDu human hypopharyngeal carcinoma tumors in Nu/J. Nu/J mice were injected with 2x10^6 Fadu cells in 100 µL of 70% Matrigel™ 30% cells and media subcutaneously. Tumors were treated once with: 10 mg/kg CDDP IP, 30 µL of saline IT, 20 µL of nCaP^{CIT} IT(without CDDP), 1.4 mg/kg CDDP IT, 13.7 mg/kg nCaP^{CIT}CDDP IT or 20.7 mg/kg nCaP^{CIT}CDDP IT, when tumor volume reached 120 ± 20 mm^3. The change in tumor volume and mouse weight was evaluated for 15 days post treatment (Figure 3.10 A and B). Due to large standard deviations statistical differences were not detected between the treatment groups. The average tumor volume for animals treated with 1.4 mg/kg CDDP IT was the lowest, with 10 mg/kg CDDP IP and 13.7 mg/kg nCaP^{CIT}CDDP.

For the repeat efficacy and toxicity study , 5 week old, Nu/J mice (Jackson Laboratories) were injected subcutaneously with 2x10^6 Fadu cells in 100 µL of 60% Matrigel™ 40% cells and media. Tumors were treated intratumorally (IT) with varying doses of: saline, CDDP in saline, or nCaP^{CIT}CDDP, once when tumor volume reached 140±14 mm^3. The change in tumor volume and mouse weight was evaluated for 30 days post treatment. 10 mg/kg nCaP^{CIT}CDDP IT resulted in delayed tumor growth (Figure 3.11 A). As expected, saline IT and nCaP^{CIT} IT (no CDDP) had no effect preventing tumor growth. 10 mg/kg nCaP^{CIT}CDDP and CDDP were significantly more effective at slowing tumor growth than saline or nCaP^{CIT} (Tukey one-way ANOVA). 1.4 mg/kg CDDP IT was significantly most effective in inhibiting tumor growth. For each treatment group, average mouse weight loss was not significant (> 15%), (data not shown). Toxicity of the nCaP^{CIT}CDDP was also evaluated via survival (Figure 3.11 B). During the anti-tumor efficacy study mice were euthanized due to weight loss greater than 15%, tumor necrosis, or having a

tumor width measurement of 20 mm or greater. Mice treated with 1.4 mg/kg CDDP IT observed 100% survival at day 30. Mice treated with 10 mg/kg nCaP^{CIT}CDDP IT resulted in 57% survival at day 30. Both saline IT and nCaP^{CIT} IT observed 0% survival by day 30.

3.4 Discussion

These results show that sodium citrate is an effective stabilizer for calcium phosphate nanoparticles carrying CDDP enabling the delivery of a higher dose of CDDP compared to free CDDP administration with comparable toxicity to the treated animals. The *in vitro* drug release profile for nCaP^{CIT}CDDP shows a maximum release of 27% of CDDP loaded onto the nanoparticles is released over the 14 day time period studied. It was expected that nCaP^{CIT}CDDP would be more effective at treating the tumors locally than a lower dose of free CDDP, however this was not found in this xenograft model of head and neck cancer. Ultimately no treatment successfully shrank tumors to their size at treatment nor caused remission, but the 1.4 mg/kg dose of CDDP administered IT resulted in significantly smaller tumors than controls or nCaP^{CIT}CDDP at 10 mg/kg. This may be due to FaDu cells being moderately CDDP resistant[136,137] combined with the larger tumor volume range at the start of treatment (up to 154 mm^3). We examined the biological activity of the CDDP released from nCaP^{CIT}CDDP in a cytotoxicity assay, finding no statistically significant differences between CDDP released from nCaP^{CIT}CDDP, CDDP and Aquated CDDP.

The *in vitro* release study conducted here was performed using a commercially available, "ready-to-use" dialysis sac device. This is one of several general methods of studying drug release that are performed for nanoparticles, including: sample and separate, dialysis sac and flow through methods[116]. This method was utilized as a screening method to determine if

biologically active drug released from the formulation and if so, approximately how much. To mimic intratumoral conditions we utilized a release medium with pH 6.8[138]. This step is insufficient for development of an in-vitro-in-vivo-correlation (IVIVC), as IVIVC for parenteral controlled release systems is challenging based on the *in vivo* site of administration[139,140], here intratumoral. Sink conditions were utilized for our studies and within a dense tumor, there is limited fluid available and likely sink conditions are not present. At a workshop of the American Association of Pharmaceutical Scientists (AAPS), Food and Drug Administration (FDA) and United States Pharmacopoeia (USP) it was stated that a drug release of 80% is desirable from controlled release parenterals for both safety and the production of an economical dosage form[115]. Here we were unable to achieve 80% release from nCaP^{CIT}CDDP, this may be due to lack of sufficient agitation within the dialysis device and high nanoparticle content within the sac limiting release within and diffusion out of the sac into the release medium[120]. An additional method we could have employed to overcome some of these pitfalls would be to perform reverse dialysis, where the nanoparticles would be suspended within the release medium in the large vessel and samples removed from within the dialysis sac. This method would alleviate the challenge posed by nanoparticles being too concentrated within the dialysis sac[121]. Further development of this formulation would require a more accurate and reproducible method of drug release testing. A newly developed method, in Dr. Burgess' lab at the University of Connecticut, incorporated a dialysis adapter into the flow through sample cell of a USP apparatus 4[22]. They were able to discriminate between small variations in liposomal formulations and maintained minimal variability between replicates. Additionally, this would be a step towards use of a compendial apparatus for *in vitro* release testing, which is more analogous to what is performed for oral dosage forms[141].

The anti-tumor efficacy of the 1.4 mg/kg CDDP administered IT has not been previously published to our knowledge. This low IT dose of CDDP had not been reported to be sufficient for delayed tumor growth. The lowest reported dose for CDDP administered IT in a murine model is 5 mg/kg, which showed minimal tumor growth delays on the order of 3-5 days[61,142,143]. We confirmed this finding by repeating the animal study with the same results. Additionally, FaDu cells are considered a relatively CDDP resistant HNC cell line, with a published IC50 of 6 μM (1.8 μg/mL) [137], and in our lab we found they were even more resistant with an average IC50 of 13.3 μM (4 μg/mL). This is therefore an excellent model for comparison to HNC patients because it is estimated that 50% of patients with locally advanced HNC will recur with chemotherapy resistant cancer[29]. Intratumoral CDDP for the local treatment of HNC may be a viable alternative for non-resectable tumors, or partially resectable tumors. This further supports the need to develop an effective local delivery system for CDDP that allows for prolonged delivery of high local concentrations of biologically active CDDP.

In our lab and others, one of the primary complications to the development of an effective delivery system is sufficient release of active drug that can penetrate through the tumor mass once released. Many different approaches to local therapy for HNC patients have been researched. Poly-Ɛ-caprolactone blended with poly(DL-lactide-co-Ɛ-caprolactone) sheets loaded with CDDP were examined in a model of murine HNC where partial surgical resection was combined with radiotherapy which found the polymer sheet with CDDP and radiotherapy significantly reduced tumor burden, but the polymer sheet with CDDP alone was not effective [144]. These findings correlate well with many reports of CDDP as a radiosensitizer[61,63,145–147]. An injectable polymer, poly (sebacic acid-co-ricinoleic acid ester anhydride), for intratumoral delivery of CDDP was examined in a model of murine bladder cancer, where the polymer alone

inhibited tumor growth compared to untreated mice[143]. The authors speculated the delayed tumor growth from polymer alone was due to physical injury to the tumor. We examined nCaP^{CIT} alone IT, but did not cause any delay in tumor growth. We believe this is due to the superior biocompatibility of CaP as a drug carrier, compared to polymers that often have acidic degradation by-products.

Nanoparticles for the local delivery of chemotherapy to a tumor have also been researched. Li et al., examined block copolymer methoxy poly(ethylene glycol)-polycaprolactone CDDP nanoparticles against a murine model of liver cancer finding when delivered IT, the particles were no more effective than CDDP IT at equivalent doses [142]. Albumin microparticles carrying chemotherapeutic drug mitoxantrone were examined for IT efficacy against murine breast cancer where the microspheres were not able to increase the MTD for the carried drug nor were they more effective than free drug alone at increasing animal survival[148]. One of the major advantages of a successful IT delivery system is the ability to deliver a higher dose of drug directly at the site of the tumor. Theoretically the local delivery offers a therapeutic advantage by limiting systemic drug clearance and drug exposure to healthy tissues thereby decreasing systemic toxicity[57]. Here we found that local delivery of very low doses, 14% of a standard systemic dose of 10 mg/kg for a mouse, of free CDDP was able to significantly delay tumor growth. This is likely due to the ability of CDDP to more freely diffuse throughout the dense tumor tissue, versus the nanoparticles which are too large to move through the interstitial collagen barrier in solid tumors[82]. Achieving evenly distributed drug using a nanoparticle delivery system is an ongoing challenge for cancer treatment.

3.5 Conclusion

In this study we were able to deliver higher doses of CDDP with nCaP^{CIT}CDDP IT compared to systemic CDDP, with comparable toxicity. nCaP^{CIT}CDDP caused a significant delay in tumor growth compared to nCaP^{CIT} and saline controls, but was surpassed by free CDDP administered IT. Although the anti-tumor efficacy of CDDP IT at 1.4 mg/kg is unexpected relative to the literature, it is very clinically relevant and therefore important to explore further.

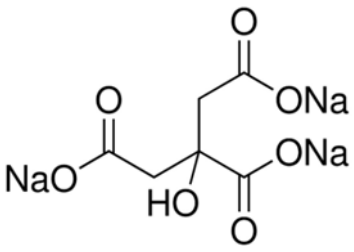

Figure 3.1 Molecular structure of sodium citrate.

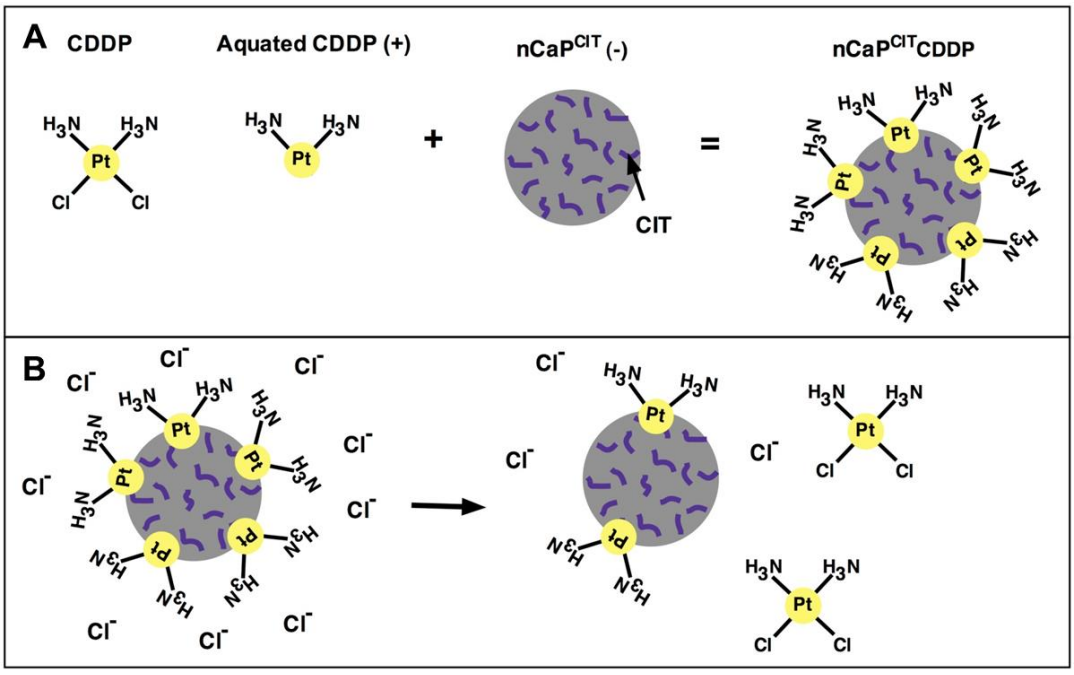

Figure 3.2 Schematic representation of aquated CDDP binding and release from nCaP^{CIT}CDDP. (A) From left to right, CDDP can be made into aquated CDDP, via a reaction with $AgNO_3$. AgCl precipitate is removed via centrifugation and filtration, leaving a net positively charged aquated CDDP. nCaP^{CIT} is negatively charged to bind the positively charge aquated CDDP, resulting in nCaP^{CIT}CDDP. (B) In a chloride rich environment, like within the body, a driving chloride ions act as a driving force for the release of aquated CDDP to reform native CDDP.

Table 3.1 Addition of sodium citrate to calcium phosphate precipitation results in nano-sized particles.

Particle Size (nm)	Polydispersity	Zeta Potential (mV)	Drug Loading (μg CDDP/mg $nCaP^{CIT}$)
180.6 ± 19.5	0.16 ± 0.03	-31.6 ± 4	158.7 ± 11.6

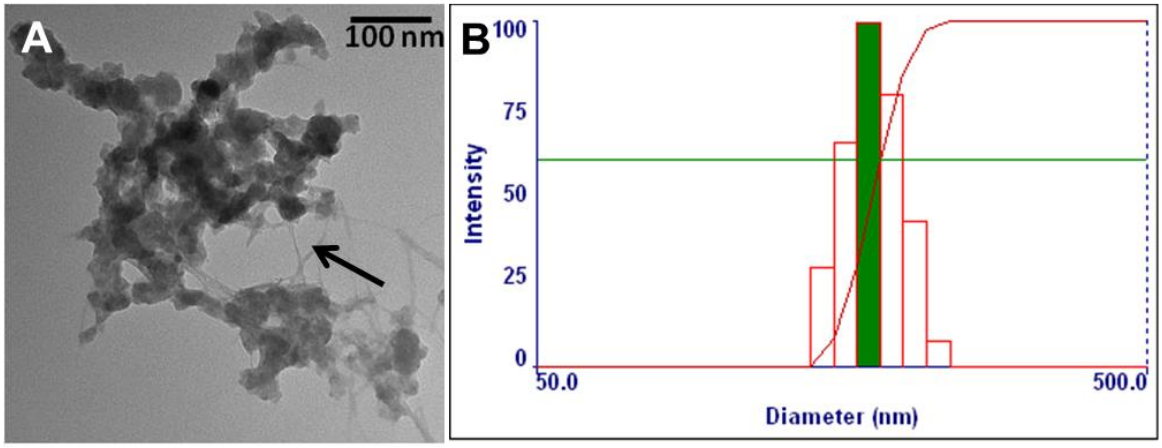

Figure 3.3 Characterization of the nanoparticles. (A) TEM image of $nCaP^{CIT}$CDDP, scale bar is 100 nm. Arrow indicates spindle-like citrate molecules. Image shows 20-50 nm particles agglomerated into larger clusters of particles 120-180 nm in diameter (B) Particle size distribution of $nCaP^{CIT}$CDDP, bar represents average particle size of 178 nm.

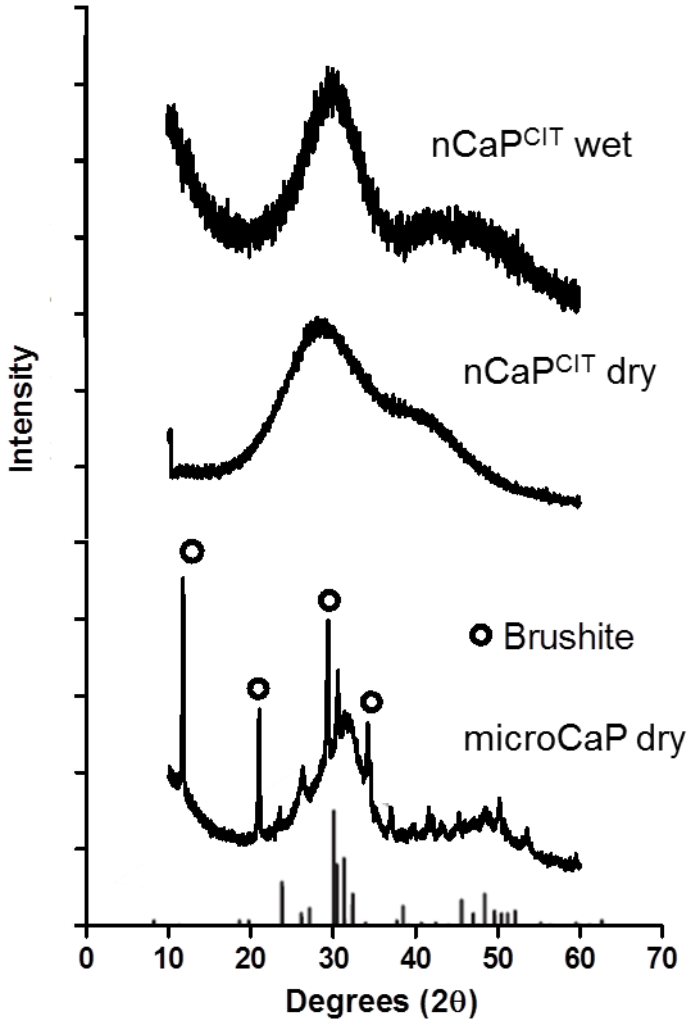

Figure 3.4 XRD of $nCaP^{CIT}$ suspension ($nCaP^{CIT}$ wet), lyophilized $nCaP^{CIT}$ ($nCaP^{CIT}$ dry) and lyophilized CaP without citrate stabilizer added during precipitation (microCaP dry) shown from top to bottom (Cu radiation, λ =1.54184 Å). The circles demonstrate major peaks of Brushite within microCaP. This demonstrates that citrate halted the long order crystal growth when present during precipitation, compared to the crystalline peaks observed in microCaP that has no stabilizer present. For comparison hydroxyapatite standard (JCPDS, #09-0432) (bars) is shown.

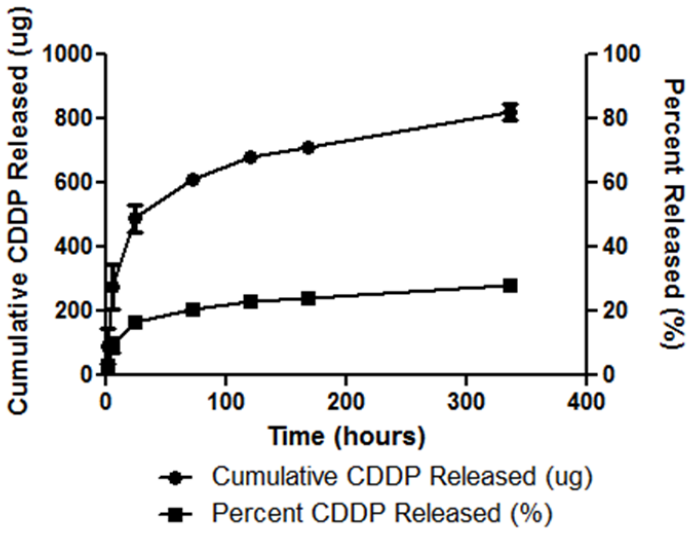

Figure 3.5 nCaP^{CIT}CDDP provides sustained delivery of CDDP *in vitro*. Average percent CDDP release after 14 days is 27% based on total CDDP available for release. Release studies were performed using Float-a-Lyzers ® in PBS, pH 6.8, at 37° C, molecular weight cutoff = 100 kDa.

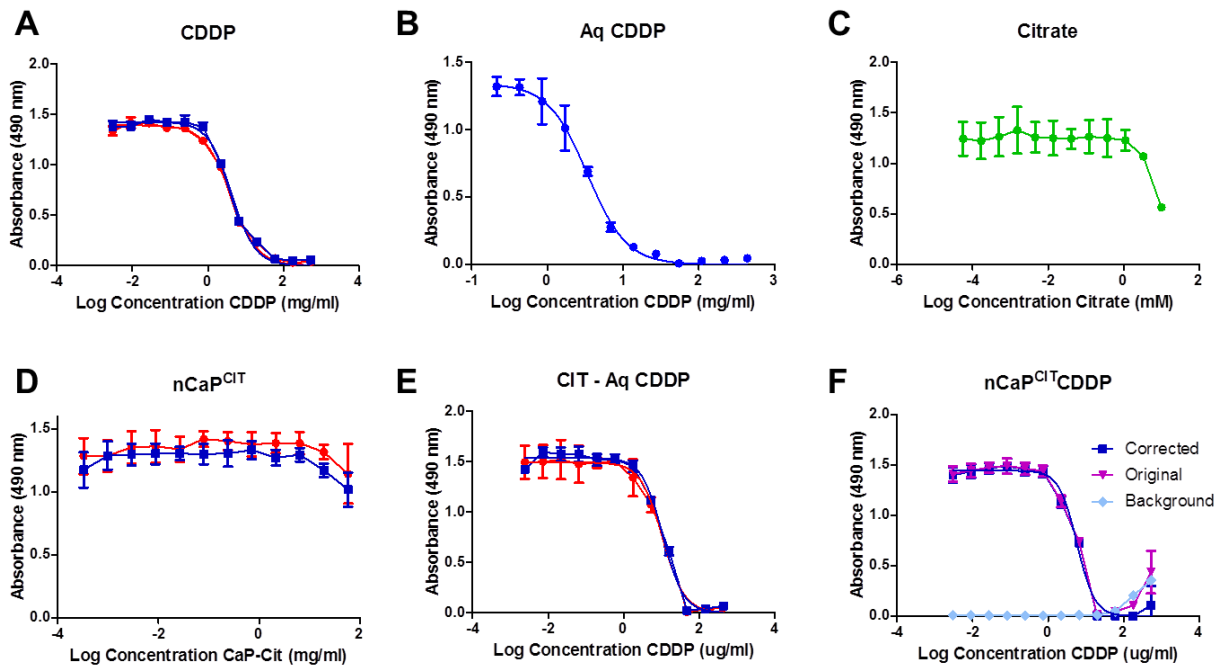

Figure 3.6 FaDu, human head and neck cancer cells were used to examine the *in vitro* cytotoxicity of: (A) CDDP (blue and red colors show replicates), (B) Aq CDDP, (C) Citrate, (D) nCaP^{CIT}, (E) Aq CDDP – CIT, and (F) nCaP^{CIT}CDDP. The highest concentrations of nCaP^{CIT}CDDP in the assay interfere with absorbance readings at 490 nm. To correct for this, cells treated with the same concentration of nCaP^{CIT}CDDP over the same time period are read on the plate reader without the addition of CellTiter 96® AQueous One reagent, labeled as Background. These average background absorbance readings are subtracted from the Original, to find the Corrected curve. The Corrected curve is used for IC50 determination.

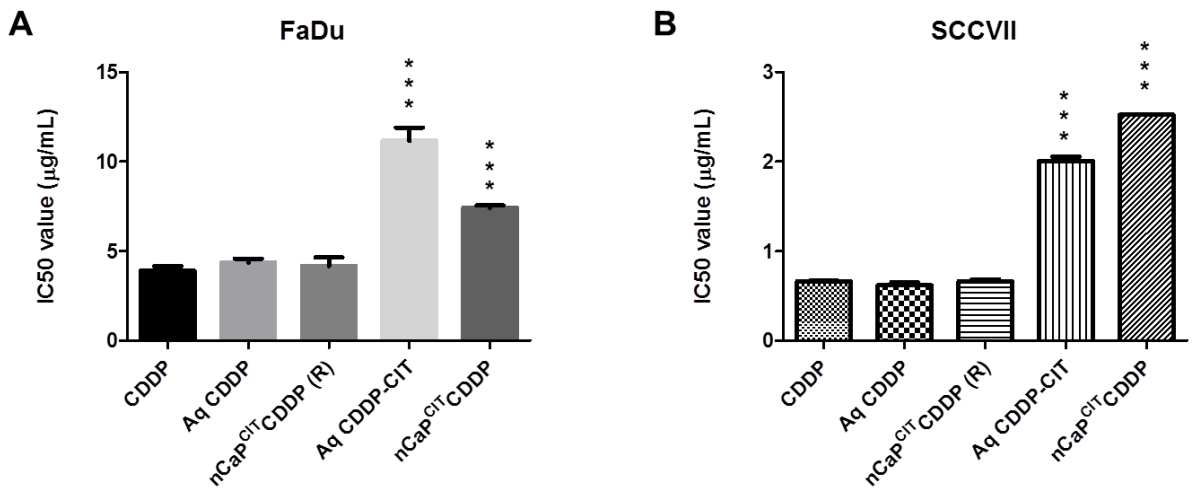

Figure 3.7 Cytotoxicity test of nCaP^{CIT}CDDP against (A) FaDu (human HNC) and (B) SCCVII (mouse HNC) cells in an MTS assay to determine the IC50 value of each treatment. These studies show that CDDP released from nCaP^{CIT}CDDP (nCaP^{CIT}CDDP (R)) has the same cytotoxicity as free CDDP, for both cell types. Reacting sodium-citrate with Aq CDDP significantly decreases the cytotoxicity of Aq CDDP, for both cell types ($P < 0.05$). nCaP^{CIT}CDDP was significantly less cytotoxic than CDDP for both cell types ($P < 0.05$).

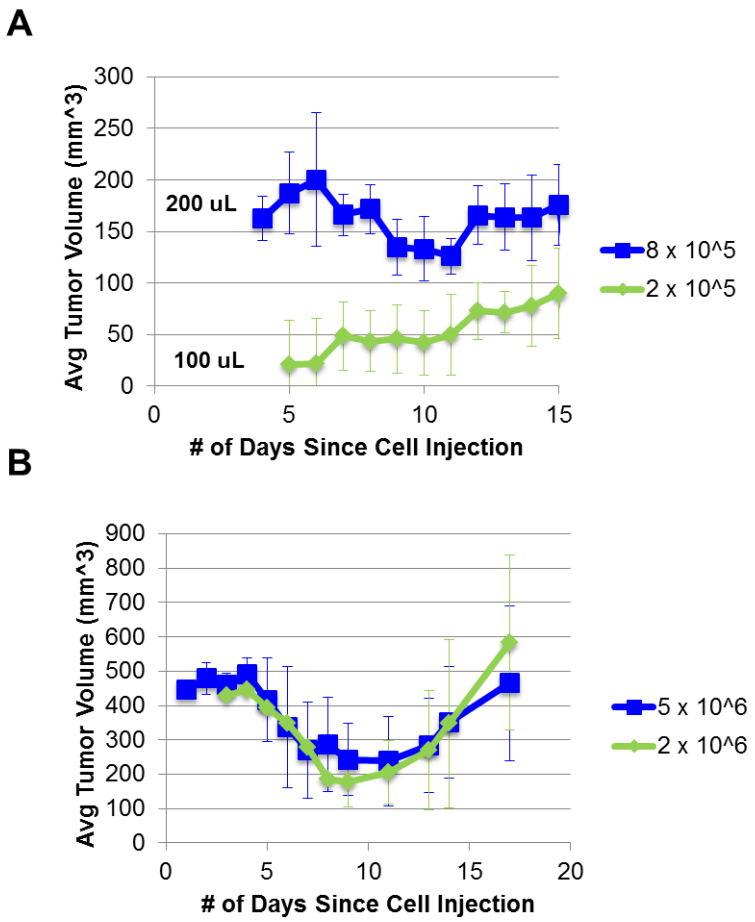

Figure 3.8 Tumor take rate studies performed in Nu/J mice using FaDu cells at two different concentrations injected in right rear flank of animals. Plots show average tumor volume per group (mm^3) vs number of days since injection of cells, error bars show standard deviation. A cell number of 2 x 10^6 was deemed sufficient to initiate tumors, and 2 x 10^5 or 8 x10^5 cell number injections grew too slow. (A) Cell number and injection volume were as follows: 8 x 10^5 in 200 uL or 2 x 10^5 FaDu cells in 100 uL volume using Matrigel (4 animals/group). (B) Cell number injected per 200 uL volume: 5 x 10^6 or 2 x 10^6 FaDu cells in Matrigel (5 and 3 animals/group, respectively).

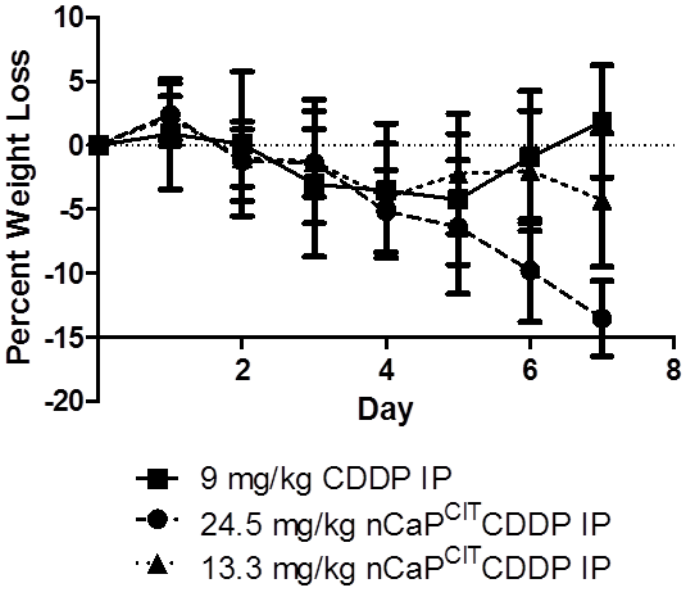

Figure 3.9 Weight loss over time with intraperitoneal injections in CH3/HeJ mice. A dose 13 mg/kg nCaP^{CIT}CDDP IP is the maximum tolerable dose (MTD) that can be administered IP without experiencing significant weight loss (> 15%). Delivering CDDP using nCaP^{CIT} allows for an increase in MTD 13 mg/kg compared to CDDP IP (MTD 10 mg/kg). A dose of 24.5 mg/kg nCaP^{CIT}CDDP IP caused significant weight loss and therefore cannot be used for treatments.

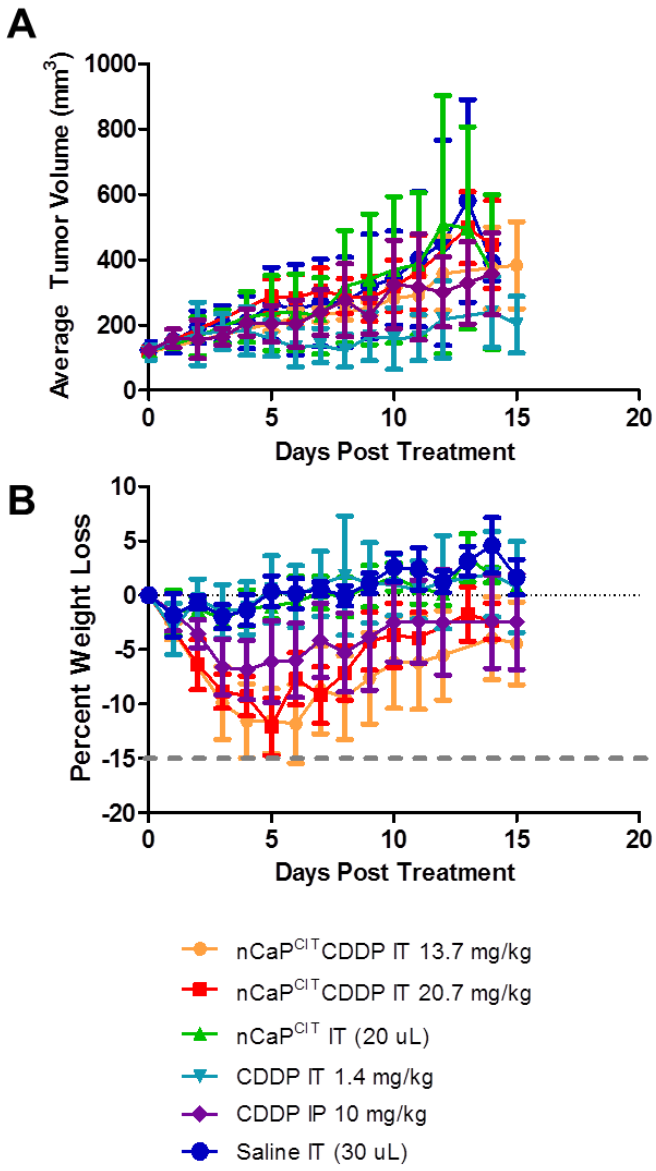

Figure 3.10 Nu/J mice were injected with $2x10^6$ Fadu cells in 100 µL using Matrigel, subcutaneously. Tumors were treated with varying doses of: saline, CDDP, $nCaP^{CIT}$ or $nCaP^{CIT}$CDDP when tumor volume reached 120±20 mm^3. No significant differences in tumor volume were found between groups (A) Average tumor volume (mm^3) per group vs. days post treatment. (B) Average percent weight loss for each treatment group.

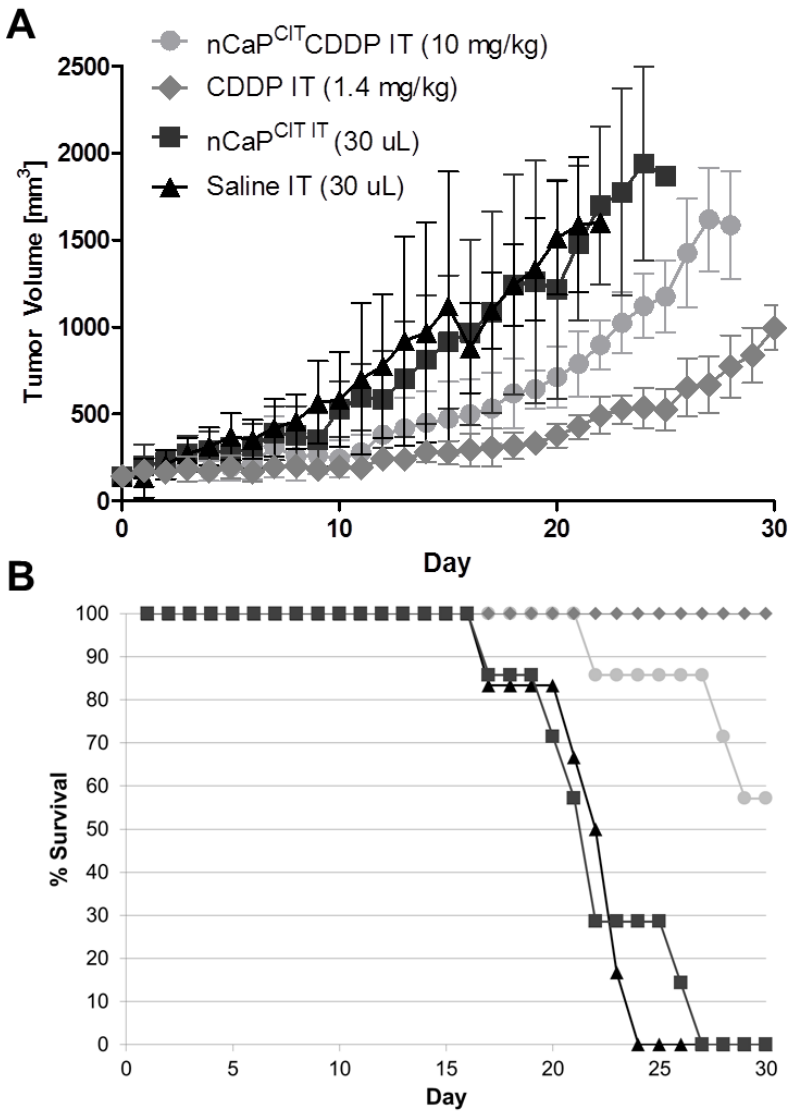

Figure 3.11 A repeat efficacy testing of nCaP^{CIT}CDDP in a mouse model of human HNC was conducted. Nu/J mice injected with 2x10^6 Fadu cells in 100 µL using Matrigel, subcutaneously. Tumors were treated once tumor volume reached 140 ± 14 mm^3. In this study a lower dose of 10 mg/mg nCaP^{CIT}CDDP was administered intratumorally. (A) Graph shows average tumor volume (mm^3) per group versus days following treatment. A 10 mg/kg dose of nCaP^{CIT}CDDP resulted in delayed tumor growth. There were significant differences between Saline and 10 mg/kg nCaP^{CIT}CDDP, Saline and CDDP IT, and 10 mg/kg nCaP^{CIT}CDDP and CDDP ($P < 0.05$). (B) Survival curve showing percent surviving animals versus days following treatment. Survival

was defined as > 15% weight loss, tumor diameter > 2 mm, or inability to groom. CDDP IT allowed for 100% survival to day 30 following treatment. The 10 mg/kg dose of nCaP^{CIT}CDDP allowed for 57% survival to day 30. NOTE: The legend applies to both graphs.

Chapter 4

Carboxymethyl Hyaluronic Acid Stabilized Calcium Phosphate Nanoparticles for Delivery of Cisplatin

4.1 Introduction

Triple negative breast cancer (TNBC) patients have limited treatment options because their cancer does not present with hormone receptors that are effectively targeted for treatment in breast cancer[149]. These patients could greatly benefit from a localized treatment that can reduce the tumor prior to surgical resection, with the goal of lessening chances for recurrence. In this study calcium phosphate nanoparticles (nCaP) were synthesized with carboxymethyl hyaluronic acid (CMHA) to determine if CMHA could simultaneously stabilize nCaP and target cancer cells. CMHA is hyaluronic acid (HA) that has been modified to contain extra carboxylate groups which are known to interact with Ca and P ions in the during precipitation of CaP[134] (Figure 4.1). Hyaluronic acid (HA) is a major component of the extracellular matrix, a glycosaminoglycan[150] and CD44 is a transmembrane molecule that is a major binding and homing receptor for HA. Therapy resistant breast cancer cells have a common phenotype of $CD44^{+}/CD24^{low}$. The presence of these cells in patients with triple negative breast cancer (TNBC) is a poor prognostic indicator and linked with recurrence[48]. Therefore the goal of this study was to determine if $nCaP^{CMHA}$CDDP could effectively target and kill TNBC cells with the $CD44^{+}/CD24^{low}$phenotype.

Calcium phosphate is an excellent biomaterial because it is biocompatible, resorbable and non-immunogenic[94,99,108]. In Chapters 2 and 3, we found that both sodium polyacrylate (Darvan ® 811) and sodium citrate effectively stabilize nCaP, but have inhibitory effects on the biological

activity of cisplatin (CDDP). Here we introduced carboxymethyl hyaluronic acid (CMHA) during the precipitation process of CaP, creating $nCaP^{CMHA}$, with the goal of achieving both nCaP stabilization and biological targeting of CD44. CDDP is an effective anti-cancer drug, but has dose limiting nephrotoxicity. This study was the first to use carboxymethyl-HA (CMHA) to stabilize nCaP and simultaneously target CD44 expressing cells while carrying CDDP, $nCaP^{CMHA}$CDDP. $nCaP^{D}$CDDP was used as a negative control for evaluating the targeting capacity of $nCaP^{CMHA}$CDDP. $nCaP^{CMHA}$CDDP was physically characterized using: transmission electron microscopy (TEM), X-Ray diffraction, particle size analysis and *in vitro* drug release studies. The ability of CMHA and $nCaP^{CMHA}$CDDP to bind CD44 was examined using surface plasmon resonance. Cytotoxicity of $nCaP^{CMHA}$CDDP and the impact of CMHA on Aq CDDP were examined *in vitro* against both CD44- and CD44+ cell types. Lastly, an anti-tumor efficacy study was performed on a model of human therapy resistant TNBC with BT-474m cells.

4.2 Materials and methods

4.2.1 Materials

Calcium lactate pentahydrate (Sigma C8356), K_2HPO_4 (Sigma S1804), $Pt(NH_3)Cl_2$ (CDDP, Sigma P4394), and $AgNO_3$ (Silver Nitrate, Sigma S6506) used to prepare the nanoparticles were all purchased from Sigma-Aldrich, (St. Louis, MO). Darvan® 811 was purchased from R.T. Vanderbilt Holding Company, Inc. (Norwalk, CT). CMHA and HA for these studies was graciously supplied by Dr. Glenn Prestwich at the University of Utah. Aq-CDDP was prepared as described previously [1]. BD Matrigel™ for cell injections was purchased from BD Biosciences, (San Jose, CA).

Mouse fibroblast cells, NIH-3T3, were purchased from ATCC. They were maintained in DMEM high glucose (Gibco 11995) with 10% Fetal Calf Serum and 1% penicillin streptomycin. LMS, BT-474 and BT-474m cells were kindly provided by Dr. Bruce White at the University of Connecticut Health Center. BT-474 cells were maintained in DMEM/F12 (Gibco 11330) with 10% FBS, 1% p/s and 1% insulin. LMS and BT-474m cells were maintained in DMEM/F12 (Gibco 11330) with 10% FBS, 1% p/s.

J:Nu female mice were purchased from Jackson Laboratory, (Bar Harbor, ME) and used for studies at 6-8 weeks of age. Female athymic nude mice, 6-8 weeks of age, were obtained from Charles River Laboratories International, Inc. (Wilmington, MA).

4.2.2 nCaP^{CMHA}CDDP Production and Physical Characterization

nCaP^{CMHA}CDDP synthesis was based on a previously reported method for nCaPCDDP[16]. To make nCaP^{CMHA}, 30 mM Calcium lactate was added to the reaction vessel and mixing initiated. To which an equal volume of 30 mM K_2HPO_4 was added, immediately followed by 2% (w/v) CMHA (34 kDa) in water at 20% of the total volume of precipitation. Mixing continued for 10 minutes. Nanoparticles were collected via centrifugation (12000 rpm for 45 min) and washed once with MilliQ ® water. The particles were then allowed to adsorb Aq CDDP for 20 hours. The nanoparticle s were protected from light on a heated rocker (LAB-LINE® thermorocker, Barnstead Thermolyne, Dubuque, IA) maintained at 37ºC. Following binding, the particles were collected via centrifugation, rinsed with 10 mM KPB to remove unbound Aq CDDP and diluted to approximately 175 mg nCaP^{CMHA}CDDP / mL MilliQ water to make a suspension that was injectable through a 25 gauge needle. All solutions/liquids during the synthesis process were sterile-filtered with a 0.2 μm filter. The nCaP^{CMHA}CDDP suspension was stored at room

temperature and shielded from light. nCaP^{D}CDDP was made as previously described except Calcium Lactate pentahydrate was used instead of $Ca(NO_3)_2 \cdot 4H_2O$), to match the calcium used in nCaP^{CMHA}CDDP.

The concentration of CDDP was determined by inductively coupled plasma-optical emission spectroscopy (ICP-OES) (Perkin Elmer® Optima™ 5300 DV, ESIS Inc., Cromwell, CT) on nCAPCDDP samples of known volume dissolved in 1N HCl. Particle size analysis (PSA) was performed via dynamic light scattering using a 90 Plus Particle Sizer (Brookhaven Instruments, NY). Samples were prepared by sonicating the particle suspension and diluting the suspension 12x in MilliQ ® water. The morphology and size of the particles were observed by using a Hitachi H-7650 transmission electron microscope (TEM). TEM samples were prepared by sonicating the particle suspension and diluting the suspension 26x in MilliQ water then 10x in 70% ethanol. A 5 uL sample was placed on a formvar carbon coated 300 mesh Cu grid. Sample sat for 1min and then any excess solution was removed using filter paper. Prior to imaging the sample completely dried in air for 5 min. Samples were imaged at 80 kV with the TEM. X-ray diffraction (XRD) was used to determine changes in crystallinity with addition of stabilizer and to compare dry vs wet nCaP. Samples of lyophilized calcium phosphate without stabilizer (microCaP), lyophilized nCaP^{CMHA} or nCaP^{D} and wet nCaP^{CMHA} and nCaP^{D} were analyzed using a Bruker D2 Phaser.

4.2.3 nCaP^{CMHA}CDDP and nCaP^{D}CDDP In Vitro *Drug Release*

In vitro drug release studies were performed using a USP apparatus 4 (Sotax CE, Sotax, Horsham, PA) modified with a dialysis adapter with a molecular weight cut off of 100 kD. A sample of 0.4 mL of particle suspension was loaded into the dialysis adapter with 100 uL release

medium. Release medium was 10 mM PBS pH 7.4 with 0.1% sodium azide. A flow rate of 8 mL/min was used for the study with the cell temperature maintained at 37ºC. Release samples were drawn at 1h, 3h, 5h, 7 hr, 12 hr, 1d, 2d, 3d, 4d, 5d, 6d, 7d and 10d. At each time point 5 mL of release solution was taken and replaced with 5 mL of fresh PBS. CDDP content in the release solution was determined by ICP-OES. Media replacement during the release study was considered in the calculation of cumulative release.

Another type of release study was conducted to obtain CDDP released from $nCaP^{CMHA}$CDDP (drug loading 139 ug CDDP/ mg $nCaP^{CMHA}$) and $nCaP^{D}$CDDP (drug loading 216 ug CDDP/ mg $nCaP^{D}$) specifically for use in cytotoxicity studies. In these release studies 100 uL of the nCaPxCDDP suspensions were loaded into triplicate Eppendorf tubes with 1.2 mL sterile 0.9% saline. Samples were sonicated then placed on a heated rocker at 37ºC for 3 days, where mixing was conducted by tumbling the tube contents. The samples were centrifuged 14000 rpm in an Eppendorf Micro Centrifuge with a 5415 C rotor (Hamburg, Germany). The entire supernatant was collected and filtered using a 0.2 µm filter. The three samples of nCaPxCDDP supernatant were pooled and CDDP content was measured by ICP-OES.

4.2.4 Surface Plasmon Resonance

Interaction of $nCaP^{CMHA}$CDDP, CMHA (~34 kDa) and HA (60 kDa) with CD44 were studied with surface plasmon resonance, BioRad ProteOn™ XPR36 with a GLC ProteOn™ sensor chip (BioRad, Hercules, CA). Recombinant human CD44-Fc chimera (~170 kDa) (R&D Systems, Minneapolis, MN) was immobilized on the sensor chip using amine coupling chemistry ProteOn Amine Coupling Kit. Briefly, the sensor chip surface was activated with 1:1 mixture of sulfo-N-hydroxysuccinimide (sulfo-NHS) and ethyl-3(3-dimethylamino)propyl carbodiimide (EDC) for 7

min. CD44-Fc was dissolved in 10mM acetate buffer pH 4 to a concentration of 5 ug/mL and flown over the activated surface for 14 min. The remaining reactive groups were blocked with 1M ethanolamine HCl pH 8.5. A blank flow channel (FC) was prepared by EDC/NHS activation without the CD44 receptor. Throughout all the SPR measurements PBS pH 7.4 supplemented with 0.005% Tween 20 was used as the running buffer. Samples were diluted with running buffer. CMHA and HA were diluted to concentrations of 1 uM and 5 uM. . nCaPxCDDP samples were diluted to a concentration of 350 ug/ml, which was found to be a good compromise between sufficient binding response and bulk refractive index shift. The samples were injected over the sensor chip surface coated with human CD44-Fc at 100 uL/min for 150 s. The dissociation in the running buffer took place for another 600 s. Between the measurement cycles the sensor chip surface was regenerated with 10mM glycine HCl pH 2.0 at a flow rate of 200 uL/min. The responses on the blank flow cell were subtracted from the CD44-Fc coated flow cell.

4.2.5 Flow Cytometry

LMS, BT-474 and BT-474m cells were analyzed for CD44 and CD24 expression using flow cytometry. NIH-373 cells were analyzed for CD44 expression alone. Cells were washed once with phosphate-buffered saline (PBS) and then harvested with 0.05% trypsin/0.025% EDTA. Detached cells were washed with PBS that is supplemented with 0.2% (w/v) bovine serum albumin (BSA) (wash buffer), and resuspended in the wash buffer (10^6 cells/100 uL). Combinations of fluorochrome-conjugated monoclonal antibodies obtained from BioLegend® (San Diego, CA) reactive against human and mouse CD44 (Alexa Fluor® 647) and BD Pharmingen™ (San Jose, CA) CD24 (PE-Cy7) or their respective isotype controls were added to the cell suspension at concentrations recommended by the manufacturer and incubated at 4°C in

the dark for 30 to 40 min. The labeled cells were washed in the wash buffer, then analyzed on a MACSQuant® Analyzer, MACS Miltenyi Biotec (Auburn, CA).

4.2.6 Cellular Uptake Studies

$nCaP^{CMHA\text{-}AF488}$ was made via the method described in 4.2.2, with minor modifications. Briefly, Alexa Fluor® 488 labeled CMHA was incorporated into the CMHA solution at 6% the total volume of CMHA used in the precipitation. Otherwise all reaction steps to create $nCaP^{CMHA}$ were performed the same. BT-474m cells were seeded at a density of 1×10^5 cells in an 8-well glass bottom plate and allowed to adhere for 24 hours. After which $nCaP^{CMHA\text{-}AF488}$ was added at the following concentrations: 200 ug/mL, 1 mg/mL, or 2 mg/mL in 500 uL complete media. After 2, 8, and 18 h post-incubation, the glass slide chambers were washed 2x with PBS to remove any loose nanoparticles, and the cells were fixed 4% paraformaldehyde in PBS for 15 min. The fixed cells were washed with PBS 3x to remove the excess paraformaldehyde, and then dried for 3 h. The fixed cells were stained and mounted with Prolong® Gold anti-fade mounting media containing the nuclear stain 4′,6-diamidino-2-phenylindole (DAPI) (Thermo Fisher Scientific, Waltham, MA). Microscopic analysis was performed using a Nikon A1R Spectral Confocal Microscope. Conditions of the confocal microscopic analysis were a Z-stack thickness of 11 um, individual stack thickness of 0.35 um and an oil immersed 40x objective.

4.2.7 Cytotoxicity

Cytotoxicity experiments were conducted using NIH-3T3, LMS, BT-474 and BT-474m cells plated in 96 well plates. at 4×10^4, 5×10^4, 6×10^4, and 2×10^5 cells/mL, respectively with 50 uL suspension per well. NIH-3T3 and BT-474 cells were negative control cell types relative to CD44 expression, as both cell types have CD44 negative or low expression. LMS and BT-474m

cells were experimental cells for CD44 targeted cytotoxicity. These cell types allow for the determination of cytotoxicity of $nCaP^{CMHA}CDDP$ relative to CD44 expression to elucidate if CMHA enhances cell uptake and consequently cytotoxicity. Cells were allowed to proliferate for 24 hours following which drug was added in 50 uL volumes. The following groups were examined: CDDP, Aq-CDDP, CMHA reacted with Aq CDDP (Aq CDDP – CMHA), D reacted with Aq CDDP (Aq CDDP – D), CDDP released from $nCaP^{CMHA}CDDP$, CDDP released from $nCaP^{D}CDDP$, $nCaP^{CMHA}CDDP$, $nCaP^{D}CDDP$, $nCaP^{CMHA}$, $nCaP^{D}$, CMHA and D. Each group was serially diluted 1:3 across the plate using PBS. Cells were assayed 48 h after drug addition using in an MTS assay (CellTiter 96® AQ_{ueous} One, G3580, Promega Corp., Madison, WI), where metabolic activity was determined using a Spectramax $Plus^{384}$ Spectrophotometer (Molecular Biosciences, Sunnyvale, CA) at an absorbance of 490nm. To determine the IC50 (50% inhibitory concentration) a non-linear regression curve fit analysis was performed with at least four replicates per group per concentration. All experiments shown were repeated at least twice and often thrice.

4.2.8 BT-474m Tumor Take Rate

To assess the growth parameters of BT-474m tumors a tumor take rate study was performed. This was performed to ensure that tumors will growth at a steady pace, without growing too fast causing necrosis or too slow such that they regress on their own. We utilized a BD Matrigel™ to cells in base media ratio of 60:40. Four mice were used per group. The tumor take rate study was conducted using 8, 6-8 week old, athymic nude mice. 5×10^5 cells in a 100 uL volume were injected subcutaneously, based on the cell number utilized for a comparable transformed breast cancer cell type[50]. Animals were monitored at least every other day for normal grooming and appearance. Tumors were measured beginning at day 7 following inoculation. At this time, the

Matrigel has degraded from the initial 100 uL injection, allowing for a true cell-based tumor volume measurement.

4.2.9 nCaP^{CMHA}CDDP In Vivo *Maximum Tolerable Dose Determination*

Two J:Nu mice carrying BT-474m tumors were injected once intratumorally with 10 mg/kg nCaP^{CMHA}CDDP (80-90 uL per injection). A second study was conducted using athymic nude mice, where a 7 mg/kg dose of nCaP^{CMHA}CDDP (60-70 uL) was administered once intratumorally. For both studies animals were monitored daily for weight loss and grooming.

4.2.10 nCaP^{CMHA}CDDP In Vivo *Anti-Tumor Efficacy and Toxicity Study*

An efficacy and toxicity study was performed using BT-474m cells in J:Nu mice. The study included 24, 6 week old mice inoculated with $5x10^5$ BT-474m cells in 100µL of a 60 : 40 ratio of BD Matrigel™ : cells in base media in the right rear flank via a 25-gauge needle. Tumors were measured daily 7 days following inoculation using digital calipers to calculate the tumor volume as follows: $V = (W)^2 * L * 0.4$

Tumors were treated once with: 2.8 mg/kg (60 uL) CDDP NT (8 mice), 60 uL of saline NT (4 mice), 60 µL of nCaP^{CMHA} NT (4 mice), 7 mg/kg nCaP^{CMHA}CDDP NT (8 mice), when tumor volume reached 100 ± 10 mm^3.

Systemic toxicity was evaluated by weight change and overall grooming/appearance. Tumor volume and mouse weight were monitored at least every other day. Mice were euthanized due to significant weight loss (> 15%), a tumor length measurement greater than 20 mm, or completion of the study (day 30). All animal experimental procedures were approved by the

Animal Care and Use Committee of the University of Connecticut Health Center, (Farmington, CT).

4.2.11 Statistical Analysis

Statistical analysis was performed using an unpaired t-test (comparing two groups) or Tukey one-way ANOVA (comparing three or more test groups to a control group), as indicated in the methods. A P-value of less than 0.05 was considered statistically significant. Data is presented as a mean value with its standard deviation indicated (mean $\pm$ SD).

4.3 Results

4.3.1 Physical Characterization of nCaP^{CMHA}CDDP

A side by side comparison of nCaP^{CMHA}CDDP and nCaP^{D}CDDP is shown in Table 4.1. Nanoparticle yield is of great importance for scale up[123]. Precipitation of nCaP^{CMHA} results in a 7x the yield of nCaP^{D}. The average CDDP concentration in suspension is higher for nCaP^{D}CDDP, as is the drug loading. nCaP^{CMHA}CDDP are statistically larger than nCaP^{D}CDDP, but their polydispersities are comparable. Transmission electron microscopy (TEM) (Figure 4.2) showed that nCaP^{CMHA}CDDP and nCaP^{D}CDDP in suspension form small aggregates that correlate well with their measured particle size using DLS, 204 ± 13 nm and 149 ± 7 nm, respectively. Zeta potentials of nCaP^{CMHA}CDDP and nCaP^{D}CDDP were -43±4 mV and -35±5 mV, respectively. A zeta potential of ± 30 mV has enhanced stability as the surface change aids in preventing aggregation[74]. XRD comparing the nCaPs as a wet suspension, nCaP lyophilized and microCaP showed that both nCaPs are poorly crystalline with the major peak occurring at 30º corresponding well with hydroxyapatite (HA) while microCaP was more crystalline in nature resembling brushite and poorly crystalline HA (Figure 4.3) [113,135].

4.3.2 nCaP^{CMHA}CDDP In Vitro *Release*

The *in vitro* release of the nCaP^{CMHA}CDDP and nCaP^{D}CDDP in PBS, pH 7.4, at 37° C over time can be seen in Figure 4.4. Both formulations exhibit continuous *in vitro* release. A burst release of CDDP was exhibited in the first 2 days, with slower, continuous release out to day 10. At day 2, nCaP^{CMHA}CDDP released 74% of the total CDDP available while nCaP^{D}CDDP released 45%. At the 7 day completion of the release study nCaP^{CMHA}CDDP released 86% of bound CDDP and nCaP^{D}CDDP released 74.5%. Drug was released significantly faster and more completely from nCaP^{CMHA}CDDP than from nCaP^{D}CDDP.

In the three day release study conducted to obtain a concentrated supernatant to assess if active drug was released via cytotoxicity testing, nCaP^{CMHA}CDDP released 89% of the total CDDP loaded. nCaP^{D}CDDP released only 34% of the total CDDP available for release. Both supernatants containing released drug were stored and used for direct comparison to the same batch of intact nCaP^{CMHA}CDDP and nCaP^{D}CDDP in cytotoxicity studies.

4.3.3 Surface Plasmon Resonance

To assess the interaction and binding of CMHA and nCaP^{CMHA}CDDP to CD44, SPR was performed. Human CD44 chimera was immobilized on the sensor chip to determine the binding of HA, CMHA, nCaP^{CMHA}CDDP. To correct for bulk shift due to size of the nanoparticles, nCaP^{D}CDDP was examined as a control. As expected the HA most effectively bound CD44 with CMHA nearing the binding affinity of HA but not matching it (Figure 4.5). nCaP^{CMHA}CDDP also binds CD44, but this binding is lower than free CMHA or HA. Importantly, this binding is specific as it overcomes any bulk interactions observed with nCaP^{D}CDDP.

4.3.4 Flow Cytometry

Flow cytometry analysis of NIH-3T3 cells revealed that they minimally express CD44, at 8.94% of the population after isotype control subtraction (Figure 4.6). We did not examine these cells for CD24, as they are mouse fibroblasts and their expression of CD24 is not important for this study. LMS cells which are transformed human mammary cancer cells, were analyzed for CD24 and CD44 expression, finding they stained 97.3% positive for CD44 and negative for CD24 (Figure 4.7 C). Importantly, this phenotype is associated with the breast CSC phenotype[52]. BT-474 stained 1.71% positive for both CD44 and CD24, but the majority of cells stained positively for CD24 alone, 98.3% (Figure 4.8 C) BT-474m cells stained 99.7% positive for CD44 and negative for CD24, comparable to profile of the LMS cells, $CD44^{+}/CD24^{-/low}$.

4.3.5 Cellular Uptake Studies

In this cell uptake experiment, BT-474m cells were used as they have high CD44 expression. Cells were administered varying doses of $nCaP^{CMHA\text{-}AF488}$ at 200 ug/mL, 1 mg/mL, or 2 mg/mL. Cells were imaged at 2, 8, and 18 h of incubation following washing to remove any free nanoparticles. No significant uptake was found for the 200 ug/mL or 1 mg/mL concentrations at any time tested (images not shown). At the 2 mg/mL dose, significant cellular uptake was found at 18 hours post treatment. These results are shown in Figure 4.9 A-D. Z-stack images were obtained, confirming the $nCaP^{CMHA\text{-}AF488}$ was within the cell with nuclei counterstained with DAPI.

4.3.6 Cytotoxicity Evaluation of $nCaP^{CMHA}$CDDP and $nCaP^{D}$CDDP

NIH-3T3 ($CD44^{low}$) and LMS ($CD44^{+}/CD24^{-}$) cells were used to study the cytotoxicity of: CDDP, Aq-CDDP, CMHA reacted with Aq CDDP (Aq CDDP – CMHA), D reacted with Aq

CDDP (Aq CDDP – D), CDDP released from nCaP^{CMHA}CDDP (nCaP^{CMHA}CDDP (R)), CDDP released from nCaP^{D}CDDP (nCaP^{D}CDDP (R)), nCaP^{CMHA}CDDP, nCaP^{D}CDDP, CMHA and D. CMHA is not cytotoxic (Figure 4.9 A). Darvan alone caused some toxicity at a top dose of 1 mg/mL (Figure 4.9 B). Non-linear regression curve fit analysis was performed for each of these treatments and the resulting IC50 values are shown in Figure 4.9 C. Both CDDP released from nCaP^{CMHA}CDDP and nCaP^{D}CDDP have comparable cytotoxicity to CDDP alone. D reacted with Aq CDDP inhibits the cytotoxicity of Aq CDDP, this interaction also inhibits the cytotoxicity of nCaP^{D}CDDP ($P < 0.05$).

LMS cells were analyzed against the same groups as the NIH-3T3 cells. CMHA has no cytotoxicity to LMS cells (Figure 4.10 A). D has some cytotoxicity at the top dose administered, 1 mg/mL (Figure 4.10 B). The calculated IC50 values are shown in Figure 4.10 C. CDDP released from nCaP^{CMHA}CDDP has comparable cytotoxicity to CDDP. Both nanoparticle formulations were significantly less cytotoxic than CDDP ($P < 0.05$).

BT-474 ($CD44^{-/low}/CD24^{+}$) and BT-474m ($CD44^{+}/CD24^{-/low}$) cells were examined in cytotoxicity tests against: CDDP, Aq-CDDP, CMHA reacted with Aq CDDP (Aq CDDP – CMHA), D reacted with Aq CDDP (Aq CDDP – D), nCaP^{CMHA}CDDP and nCaP^{D}CDDP. The calculated IC50 values for each group with BT-474 cells are shown in Figure 4.11 A. Overall, a similar trend was found against BT-474 cells as those previously tested with one important exception; nCaP^{CMHA}CDDP was significantly more cytotoxic than CDDP against BT-474 cells($P < 0.05$). Against BT-474m cells the calculated IC50 values are shown in Figure 4.11 B. Importantly, nCaP^{CMHA}CDDP was as cytotoxic as free CDDP. nCaP^{D}CDDP and D reacted with Aq CDDP were significantly less cytotoxic than CDDP ($P < 0.05$).

Upon a routine mycoplasma test, it was determined that our BT-474 and BT-474m cells were positive for mycoplasma (MycoAlert™ Mycoplasma Detection Kit, Lonza Group Ltd., Basel, Switzerland). Mycoplasma is a very common cell culture contamination that affects laboratories worldwide. It is estimated that ATCC, National Cancer Institute and the FDA have an average mycoplasma contamination rate in cell culture of 13.5%[151]. This rate is expected to be higher at academic institutions, due to a lack of testing for mycoplasma and reliance of antibiotics. In cell culture a mycoplasma can outnumber the cells by 1000:1, competing for nutrients causing changes in cell growth and protein production[152]. Due to this, a commercial mycoplasma removal kit was purchased and used on the BT-474 and BT-474m cells (MycoZap™ Elimination Reagent, Lonza). After treatment both cell types tested negative for mycoplasma and thus all of the studies were repeated using mycoplasma free cells.

Flow cytometry was repeated on the BT-474m cells after mycoplasma removal to ensure their expression of CD44 remained high. The $CD44^{+}/CD24^{-/low}$ phenotype remained after mycoplasma removal, Figure 4.12 C. BT-474 cells normally have a $CD44^{-/low}/CD24^{+}$ therefore it expected that their phenotype would change in the presence of mycoplasma[51,153]. All of the cytotoxicity tests performed prior to mycoplasma testing were repeated three times following mycoplasma removal. Data shown represents one test, but the trend remains the same from experiment to experiment. The cytotoxicity of each stabilizer and the resulting nanoparticles were examined against BT-474 and BT-474m cells (Figure 4.13 A-D). CMHA does not have any inherent toxicity to either cell type (Figure 4.13 A). Darvan caused 50% cell death at its top concentration of 1 mg/mL. with BT-474m cells (Figure 4.13 B). Neither nanoparticle formulations were cytotoxic at concentrations tested which match the nCaP in nCaPxCDDP test groups (Figure 4.13 C & D).

The cytotoxicity of CDDP, Aq CDDP, Aq CDDP reacted with CMHA (Aq CDDP – CMHA), Aq CDDP reacted with D (Aq CDDP – D), nCaP^{CMHA}CDDP and nCaP^{D}CDDP were re-examined against BT-474 and BT-474m cells. The curve fits are shown in Figure 4.14 A-F for BT-474 cells. The IC50 values calculated from these curve fits are shown in Figure 4.15. nCaP^{CMHA}CDDP remained significantly more cytotoxic than CDDP alone, as did Aq CDDP ($P < 0.0001$). Additionally, nCaP^{D}CDDP was the most cytotoxic, which was not found in experiments with cells infected with mycoplasma. The curve fits for each group tested against BT-474m cells are shown in Figure 4.16 A-F. The IC50 values calculated from these curves are shown in Figure 4.17. Here there were no significant differences between groups tested compared to CDDP, with the exception of Aq CDDP – D, which was very significantly less cytotoxic ($P < 0.0001$).

4.3.7 BT-474m Tumor Take Rate

Two tumor take rate studies were conducted with BT-474m cells. Athymic nude mice were injected with 5 x 10^5 BT-474m cells per injection in 100 uL of BD Matrigel™ :cells in base media at a ratio of 60:40 subcutaneously. Seven days following cell inoculation, tumors were palpable and the Matrigel plug had visibly degraded from the time of injection. At this time tumors were quite small, 50 mm^3 on average. After approximately 12 days tumors were 100 mm^3 on average (Figure 4.18 A). Animals were monitored for 25 days following inoculation where tumors continued to grow steadily up to 500 mm^3 without necrosis.

4.3.8 nCaP^{CMHA}CDDP Maximum Tolerable Dose

A maximum tolerable dose study was conducted first in two 6-8 week old, J:Nu mice bearing BT-474m tumors at 150 mm^3, where each animal received nCaP^{CMHA}CDDP at 10 mg/kg (80-90

uL) intratumorally. Four days following treatment one mouse lost more than 15% of its weight at the time of treatment. The other mouse lost only 6.7% of its weight at treatment and fully recovered. The second MTD study was conducted using 6-8 week old, athymic nude mice bearing BT-474m tumors. Animals were treated at an average tumor volume of 170 mm^3, 14 days following cell inoculation. Four animals were treated with 7 mg/kg $nCaP^{CMHA}$CDDP (60-70 uL) intratumorally. Four additional animals were monitored as untreated controls. The results are shown in Figure 4.18 B, where a maximum weight loss was 5%, two to five days following treatment. This is an acceptable weight loss during treatment with chemotherapeutics, therefore this dose was deemed tolerable.

4.3.9 In Vivo *Anti-Tumor Efficacy and Toxicity Study*

The *in vivo* anti-tumor efficacy of the $nCaP^{CMHA}$CDDP was evaluated using BT-474m human xenograft tumors in 6 week old J:Nu mice. Mice were injected with $5x10^5$ BT-474m cells in 100 µL of 60% Matrigel™ 60% cells in base media subcutaneously. Tumors were treated once with: 2.8 mg/kg (60 uL) CDDP NT (8 mice), 60 uL of saline NT (4 mice), 60 µL of $nCaP^{CMHA}$ NT (4 mice), 7 mg/kg $nCaP^{CMHA}$CDDP NT (8 mice), when tumor volume reached 100 ± 10 mm^3. The change in tumor volume and mouse weight was evaluated for 30 days post treatment (Figure 4.19). No animal experience weight loss greater than 2% (data not shown). Near tumor delivery of 2.8 mg/kg CDDP was most effective at inhibiting tumor growth. No treatment caused toxicity to the animals as measured by weight loss and overall grooming/appearance. Survival over time post treatment was evaluated for each group. The results are shown in Figure 4.20.

4.4 Discussion

The addition of CMHA during precipitation of CaP resulted in successful stabilization of nCaP. TEM images reveal small 30-80 nm particles, agglomerated into larger particles, which likely accounts for the 200 nm size measured by DLS. The introduction of D or CMHA clearly restricts the crystallization of CaP, as can be seen by the broad peaks of nCaP XRD spectra. MicroCaP created by precipitation without the addition of stabilizer exhibits a crystalline pattern with major peaks comparable to brushite, (calcium hydrogen phosphate dehydrate, $CaHPO_4 \cdot 2H_2O$). This form of calcium phosphate naturally occurs and dissolves in the body as kidney stones and is therefore highly biocompatible[135]. The particle sizes obtained here made for a readily injectable nanoparticle suspension via a 25G needle.

It was shown in previous studies and Chapter 2, that D halts CaP crystal growth[16]. This is believed to be due in part to the repeating carboxylate groups throughout the polymer. There is significant literature showing the carboxylate groups of sodium citrate (3 carboxylate groups per molecule) interact with the Ca ions during CaP precipitation acting as a surfactant to halt nucleation[134,154–157]. The interaction of D and CaP created regularly shaped nCaP, with low polydispersity. This was also true for citrate. Unfortunately, these stabilizers inhibited the cytotoxicity of CDDP. Interestingly, it was recently shown that citrate nearly irreversibly binds CDDP and renders it unable to intercalate with DNA, making it biologically inactive[158]. This finding complements our findings in Chapter 3. Thus, a balance needs to be achieved between stable nCaP and their effective binding and release of biologically active CDDP. The findings of Chapters 2 & 3 led us to the utilization of a stabilizer that has biological targeting capability concurrent with nCaP stabilization. Here the approach was to use CMHA to enhance uptake of

nCaP^{CMHA}CDDP by cells expressing CD44. CMHA is HA with additional carboxylate groups, but in comparison to D and citrate there are fewer carboxylate groups per molecular weight.

To date, there is not a compendial *in vitro* release test for parenteral dosage forms. The current USP apparatus are specified to test release/dissolution of oral and transdermal dosage forms. As the development of liposomes and nanoparticles advances towards a commercial product, there is a desperate need to evaluate batch to batch quality by developing an *in vitro* release method that can discriminate between small variations in formulation. Published *in vitro* release testing methods for controlled release nanoparticles/liposomes include, flow through[22], dialysis sac[119,124,159], or sample and separate[15,16]. Major drawbacks exist for sample and separate as well as dialysis sac methods. Sample and separate methods involve the use of centrifugation and/or filtration where the liposomes can be disrupted causing erroneous release, additionally great variability exists from lab to lab with vessel size, agitation and centrifugation making the test not reproducible. Dialysis methods are limited by insufficient agitation within the dialysis sac, delayed diffusion of released drug through the dialysis membrane and high concentration of carrier within the sac limiting release[120,121]. Dr. Diane Burgess' lab at the University of Connecticut, has been working towards the development of a compendial release testing method/system to fill the current void for nanoparticle formulations. They developed a dialysis adapter to fit within the standard sample cell in the Sotax™ CE7 USP apparatus 4, where the dialysis membrane MWCO is chosen such that when the drug of interest releases, it can freely flow through the dialysis membrane and the carrier (liposome or nanoparticle) stays within the dialysis adapter[22]. They were able to discriminate between different liposomal formulations using the dialysis adapter modified USP 4 apparatus. Here we compared the *in vitro* release of CDDP from nCaP^{CMHA}CDDP and nCaP^{D}CDDP. In a side-by-side release test, nCaP^{CMHA}CDDP

released 73% of the CDDP bound compared to 45% from nCaP^{D}CDDP in 2 days. As release continued, nCaP^{CMHA}CDDP released a total of 86% while nCaP^{D}CDDP released 74.5%. Several papers have published the use of HA to create particles containing CDDP via ion complexes between the carboxylate groups of HA to aquated species of CDDP[160–162]. In each study it was shown that Aq CDDP that had been complexed with HA could subsequently be released both *in vitro* and *in vivo*. Release was enhanced in the presence of Cl^- ions[160]. This taken together with the cytotoxicity examinations of each stabilizer reacted with Aq CDDP may explain the enhanced release of CDDP from nCaP^{CMHA}CDDP over nCaP^{D}CDDP, where the interaction between Aq CDDP and CMHA is weaker than with D.

SPR analysis of targeted nanoparticles is challenging. SPR systems utilize expensive microfluidics that normally transport solutions containing ligands or proteins of interest, but generally not solid materials such as nCaP particles. Of additional concern is the ability to correct for bulk response due to the relatively large nanoparticles passing over the sensor. Here we were able to use nCaP^{D}CDDP as a comparably sized, non-specific nanoparticle control. The density of receptor (here CD44) immobilized on the chip is inherently related to the response measured, therefore we utilized a low density of CD44 on the chip surface[163]. After correcting for bulk nanoparticle response, it is clear that nCaP^{CMHA}CDDP does effectively bind CD44. The highest binding observed was for HA (60 kDa), followed by CMHA (34 kDa) alone. The chemical modification of HA to create CMHA occurs at 15 – 20% of the repeating 6'-OH groups of the N-acetylglucosamine residues. The interaction of CD44 and HA has low affinity but high avidity. A single HA disaccharide contains an N-acetyl-D-glucosamine and D-glucuronic acid, HA_2. It has been shown that HA_6 is necessary for binding CD44, but HA_{10} is more preferential[164]. Additionally, divalent binding occurs with HA_{20} and larger oligomers. This likely explains the

slight reduction in binding of CMHA to CD44, due to an interruption of sugar residues by the added carboxylate groups of CMHA compared to HA. This may also explain the significant time required for cellular uptake of nCaP$^{CMHA\text{-}AF488}$, where uptake was only found significantly at 18 hours post treatment. This was a preliminary test of cellular uptake. These were insufficient to prove that nCaP$^{CMHA\text{-}AF488}$ cellular uptake was mediated by CD44. To do so, at least two controls are necessary, a CD44- cell type and a CD44+ cell type pre-treated with HA to effectively saturate the CD44 receptors. nCaP^{CMHA}CDDP showed lower binding than CMHA, which is believed to be due to two factors. By utilizing fluorescently labeled CMHA, we were able to determine that during precipitation of nCaP^{CMHA} only 30% of the available CMHA is incorporated. Additionally, nCaP^{CMHA}CDDP is stored as a suspension which allows the CaP to undergo Ostwald ripening which could further trap the CMHA within the nCaP core[93,165].

Interestingly, nCaP^{CMHA}CDDP did not show preferential toxicity to cells with high CD44 expression (LMS and BT-474m) compared to those with low or negative CD44 expression (NIH-3T3 and BT-474). It was hypothesized that the CMHA would allow for preferential cytotoxicity to cells with high CD44 expression due to the targeting of CD44 via CMHA. It was expected that the BT-474m and LMS cells would be chemotherapy resistant, as it was shown that LMS cells were resistant to other chemotherapies (docetaxel and tamoxifen) [17,50]. When treated with CDDP alone, both BT-474m and LMS cells were relatively sensitive to CDDP. This is likely explained by the nature of CDDP toxicity, where it intercalates with DNA, causing DNA adducts that cannot be removed by DNA repair machinery prior to replication resulting in cell death. LMS and BT-474m cells divide at 2-3x the rate of their non-transformed counter-parts, MCF-7 and BT-474 cells, respectively. Importantly, nCaP^{CMHA}CDDP was as cytotoxic as CDDP alone against all cell types tested. This finding is not common for targeted nanoparticles

utilizing HA and may be due in part to released CDDP from the formulation. The controlled release of CDDP from nCaP^{CMHA}CDDP allowed for prolonged delivery of drug to the slower replicating BT-474 cells, which could explain the enhanced cytotoxicity of nCaP^{CMHA}CDDP over CDDP alone. HA bioconjugates with Taxol were less cytotoxic than free Taxol against cells expressing CD44 and had limited to no cytotoxicity against cells that did not express CD44[166,167]. Mesoporous silica nanoparticles targeted with HA carrying doxorubicin, were significantly more cytotoxic than doxorubicin alone against CD44 expressing cells, but were significantly less cytotoxic to CD44 negative cells[168]. This can be explained by specific CD44 mediated uptake that allowed drug to release intracellularly, where cells lacking CD44 did not take up the particles. nCaP^{CMHA}CDDP may not be as readily taken up as nanoparticles with HA on their surface, due to limited CMHA on the surface and the chemical modifications on HA to make CMHA.

This study was the first to create BT-474m cell based tumors in nude mice. BT-474m cells were developed following a previously reported method for transformation of human epithelial breast cancer cells, in the same lab at UCHC[50]. Within that research an animal model was developed, where 5 x 10^5 cells were injected orthotopically into athymic nude mice using Matrigel, where tumor volume reached 600 mm^3, 20 days following inoculation. Here, we also used 5 x 10^5 cells, but cells were injected subcutaneously in the flank of J:Nu mice. The BT-474m tumors created here showed high variability in tumor volume in the control groups as well as the treated groups. Due to the high variability in tumor volume, significant differences did not exist between treatment groups. From our experience with the FaDu tumor model in Chapter 3 of this dissertation, we found that 2 x 10^5 and 8 x 10^5 FaDu cells were insufficient for significant tumor growth beyond inoculation volume and 2 x 10^6 was sufficient with limited differences in

tumor volume from the 5 x 10^6 cell number inoculation. If we injected a higher number of BT-474m cells we may have found limited variability in tumor volume, because sufficient cells were injected such that all tumors grew beyond their inoculation volume.

Levy-Nissenbaum et al. recently showed that a local dose of polymer carrying CDDP administered near or surrounding the tumor significantly increased the anti-tumor efficacy compared to an intratumoral injection[169]. Tumor tissue is very dense with high interstitial fluid pressure[82] and therefore we have had difficulty administering even very small (60 uL) volumes directly into the tumor. These complications taken together with the results of Levy-Nissenbaum led us to change to a near tumor administration of treatment. To do so, the skin above each tumor was gently lifted away from the tumor surface and with a single injection drug was deposited on either side of the tumor. For some animals this was easy to achieve and others, this proved more difficult as the skin would not lift from the tumor surface. As this was our first attempt at near tumor treatment, we are unsure if this complication has any impact on the standard deviations within each treatment group. At the time of resection, depots of nCaP^{CMHA}CDDP were found. Animals with the largest tumor volumes had nCaP^{CMHA}CDDP located on just one side of the tumor, while animals with smaller tumor volumes had depots on opposing sides of the tumor. We believe the lack of even distribution nCaP^{CMHA}CDDP may have contributed to lack of anti-tumor efficacy observed in these animals. nCaP^{CMHA}CDDP does not freely diffuse throughout the tumor due to the density of the tumor and therefore only the areas of the tumor proximal to the nCaP^{CMHA}CDDP depot are treated with CDDP. The overall goal of this treatment modality is to cover more of the tumor area with drug, therefore if the drug deposited on just one side of the tumor, potentially fewer cancer cells we treated. Taken together

it is likely that, the ability of free CDDP to diffuse throughout the tumor enabled the tumor growth inhibition observed in the CDDP alone group.

4.5 Conclusions

CMHA is a novel and effective stabilizer for nCaP that can bind CD44 for potential targeting applications. Importantly, we determined that CMHA has no negative impact of the biological activity of CDDP *in vitro*, against human breast cancer cells. nCaP^{CMHA}CDDP allowed for efficient release of CDDP in neutral PBS which should be enhanced by CaP dissolution in lower pH environments, like that found in solid tumors. nCaP^{CMHA}CDDP had equivalent cytotoxicity to CDDP alone against both $CD44^+$ and $CD44^-$ cells. Tumors are very heterogeneous in cell surface expression and therefore non-exclusive cytotoxicity is important *in vivo*. Our *in vivo* efficacy study showed that near tumor delivery of 2.8 mg/kg CDDP was most effective at inhibiting tumor growth. This finding agrees with a recently published clinical trial showing neoadjuvant CDDP treatment was effective for patients with TNBC, though this treatment has not yet been adopted clinically. Here we locally administered less than a third of the typical systemic dose of CDDP for a mouse and found excellent tumor growth delay. Importantly, a higher dose of nCaP^{CMHA}CDDP should be examined *in vivo* to evaluate the targeting of therapy resistant CD44+ cells, which should increase the efficacy of locally delivered CDDP.

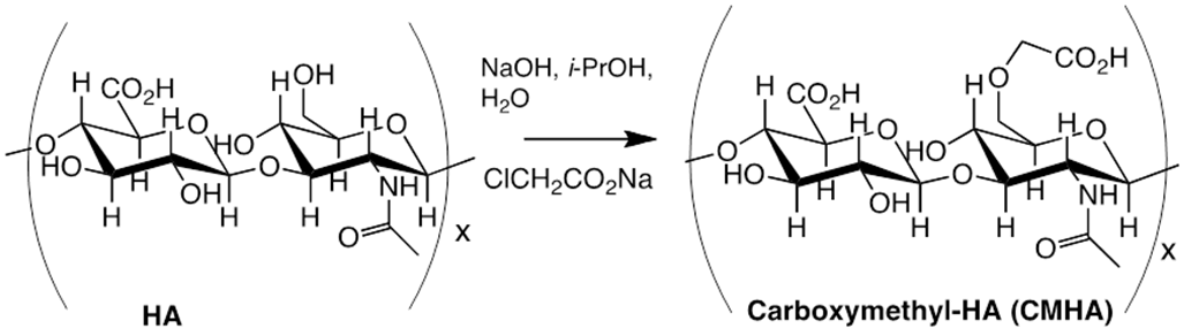

Figure 4.1 Chemical modification of hyaluronic acid (HA) to synthesize carboxymethyl hyaluronic acid (CMHA).

Table 4.1 Side by side comparison of nCaP^{CMHA}CDDP and nCaP^{D}CDDP batch characteristics. Ratio of components, precipitation volume, and stabilizer final concentration remain the same from batch to batch. Yield, CDDP concentration, drug loading, particle size and polydispersity represent averages and standard deviations from a minimum of three batches.

	nCaP^{CMHA}CDDP	**nCaP^{D}CDDP**
Ca : P : Stabilizer (v:v:v)	2:2:1	30:30:1
Total precipitation volume (mL)	250	1033
Stabilizer final concentration (mg/mL)	4	9
Yield (mg nCaP/ mL precipitation)	2.3 ± 0.4	0.3 ± 0.17
CDDP concentration (mg/mL)	4.1 ± 1.4	5.4 ± 1.2
Drug loading (ug CDDP/ mg nCaP)	140 ± 12	183 ± 37
Particle Size (nm)	204 ± 13 nm	149 ± 7 nm
Polydispersity	0.116	0.128
Zeta Potential (mV)	-43 ± 4	-34.3 ± 5

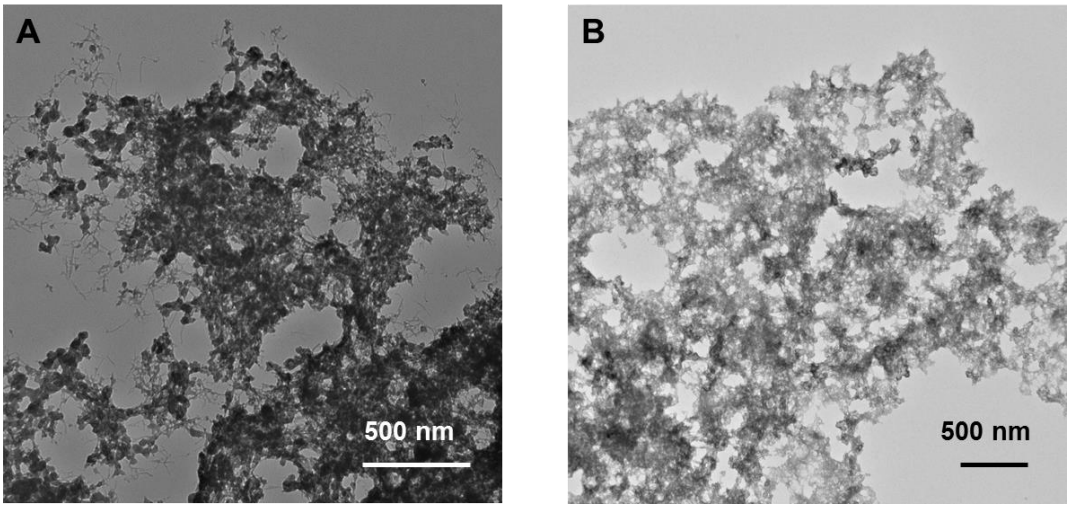

Figure 4.2 TEM images of (A) nCaP^{CMHA}CDDP and (B) nCaP^{D}CDDP, depicting small nCaP 20-50 nm agglomerated into larger groups of particles**.**

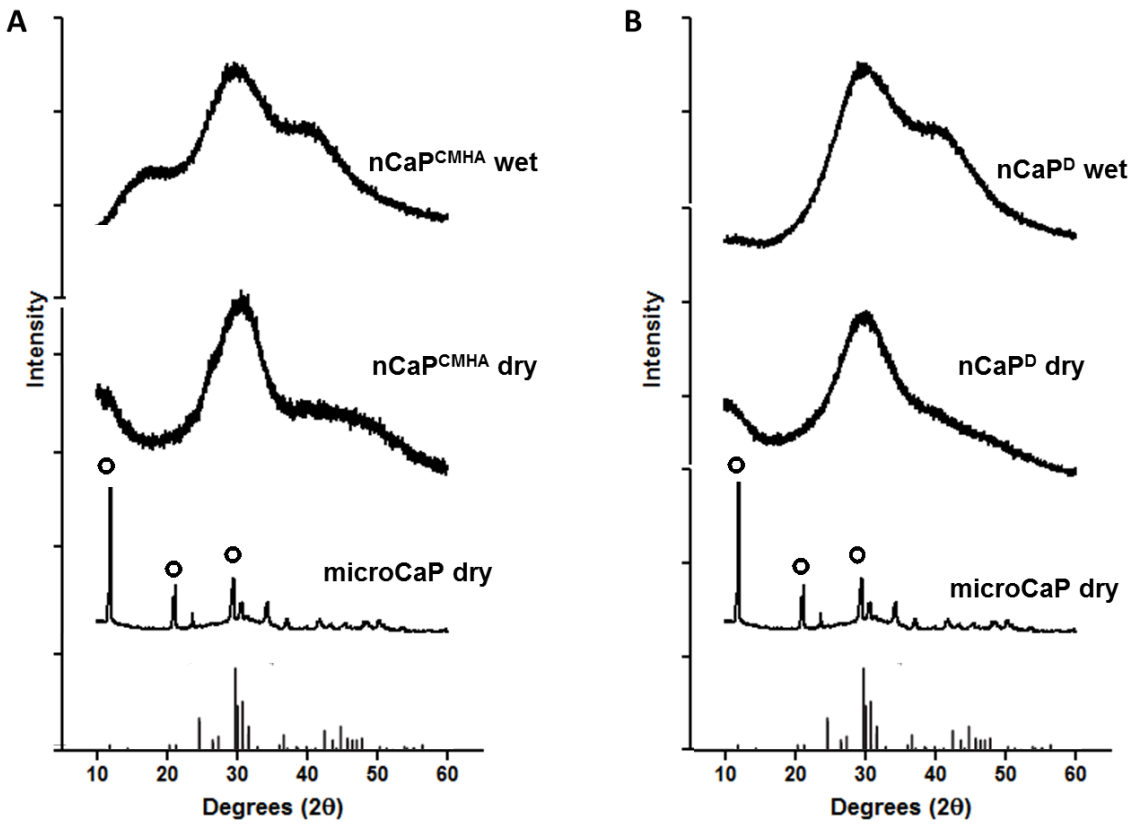

Figure 4.3 XRD spectra of (A) $nCaP^{CMHA}$ suspension ($nCaP^{CMHA}$ wet), lyophilized $nCaP^{CMHA}$ ($nCaP^{CMHA}$ dry) and lyophilized CaP without stabilizer added during precipitation (microCaP dry) (B) $nCaP^{D}$ suspension ($nCaP^{D}$ wet), lyophilized $nCaP^{D}$ ($nCaP^{D}$ dry) and lyophilized CaP without stabilizer added during precipitation (microCaP dry). Both plots show hydroxyapatite standard (JCPDS, #09-0432) (bars) for comparison. MicroCaP pattern has major peaks characteristic of Brushite (peaks denoted with open circles). MicroCaP was precipitated without a stabilizer and is crystalline. With a stabilizer present (CMHA or D) the crystallization is halted, depicted by broad peaks showing no long range crystal order.

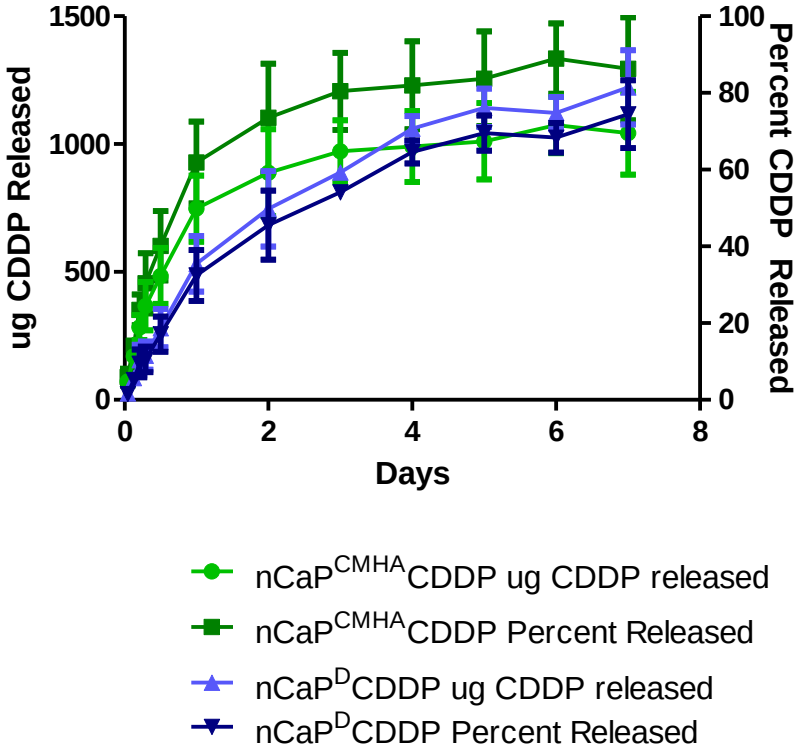

Figure 4.4 *In vitro* release testing using a modified USP Apparatus 4 (dialysis adapter molecular weight cut off 100 kDa) of nCaP^{CMHA}CDDP and nCaP^{D}CDDP. Cumulative CDDP released is plotted using the left y-axis, percent CDDP released using right y-axis. Both formulations provide sustained delivery of CDDP for 2 days. After 2 days nCaP^{CMHA}CDDP released 74% of bound CDDP available for release and release plateaus. nCaP^{D}CDDP released 45% of bound CDDP in 2 days. At study completion, nCaP^{CMHA}CDDP released more CDDP faster than nCaP^{D}CDDP with total percent release at 86% and 74%, respectively. Release in 10 mM PBS pH 7.4, 0.1% sodium azide at 37ºC.

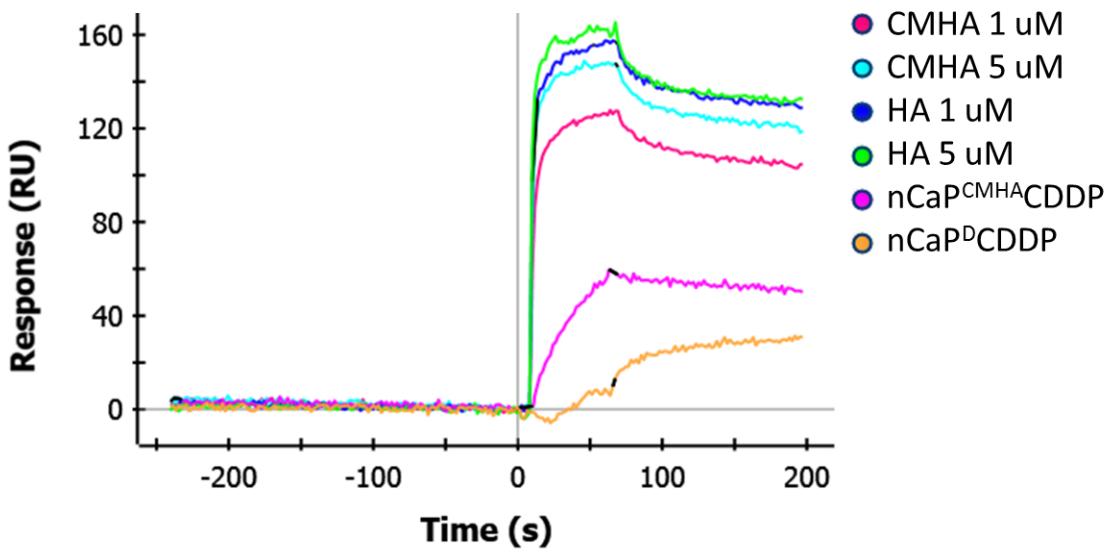

Figure 4.5 Surface plasmon resonance sensogram depicting binding of CMHA, HA and nCaP^{CMHA}CDDP with immobilized CD44. All data shown has been corrected for non-specific binding to blank channels of blocked NHS-EDC. nCaP^{D}CDDP was used as a comparable sized control, which does not have specific interactions with CD44. HA has the highest affinity for CD44, followed by CMHA then nCaP^{CMHA}CDDP.

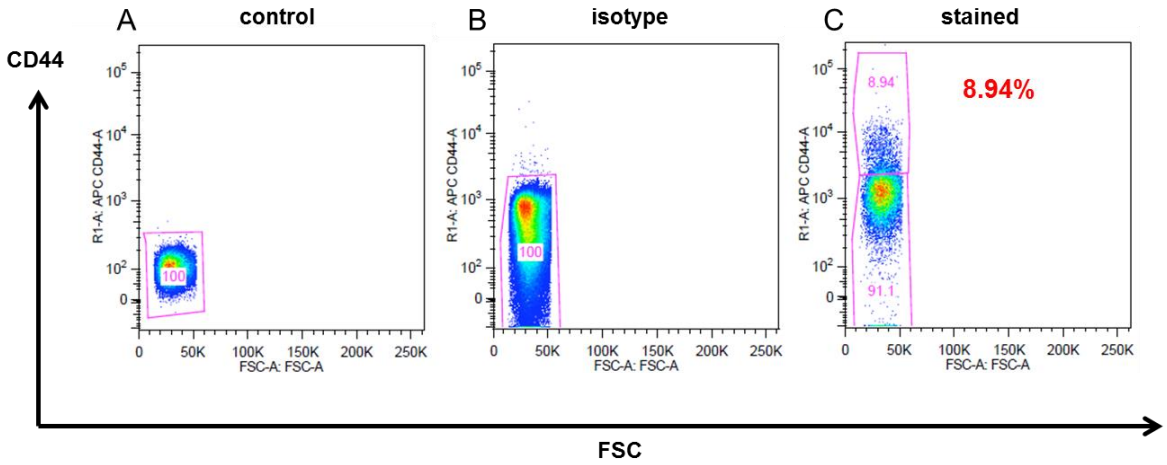

Figure 4.6 Flow cytometry data shows NIH-3T3 cells are CD44$^{-/low}$. These cells will serve as a negative control for CD44 targeting, as they have low CD44 expression. (A) Unstained control (B) isotype control (C) stained cells with CD44 – Alexa Fluor® 647 against forward scattered light (FSC, proportional to cell surface area).

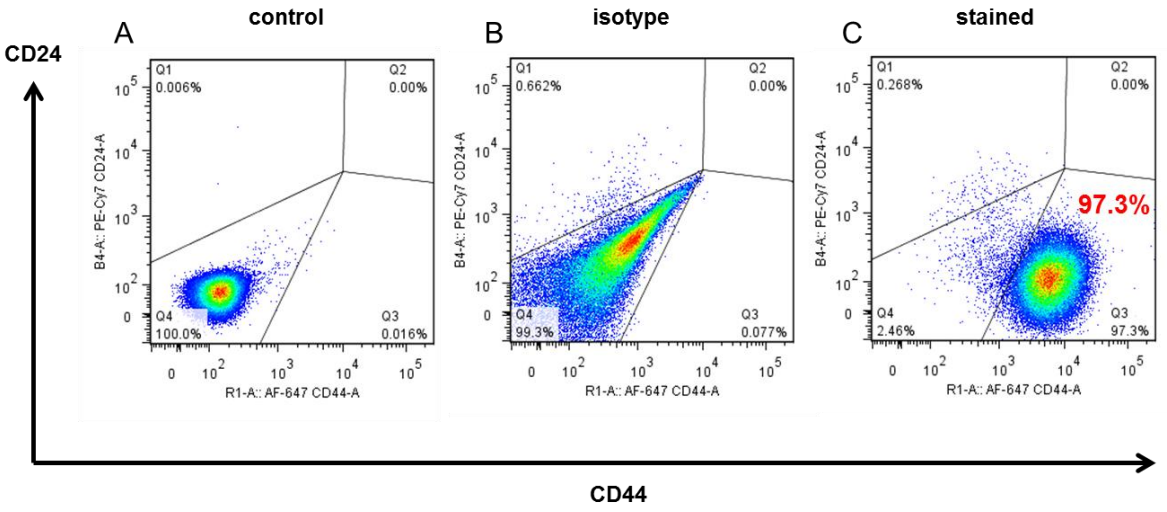

Figure 4.7 Flow cytometry data confirms that LMS cells are CD24$^{-/low}$/CD44^{high}. These cells will be the experimental group for CD44 targeting, as they have high CD44 expression. (A) Unstained control (B) isotype control (C) stained cells with CD44 – Alexa Fluor® 647 and CD24 – PE-Cy7.

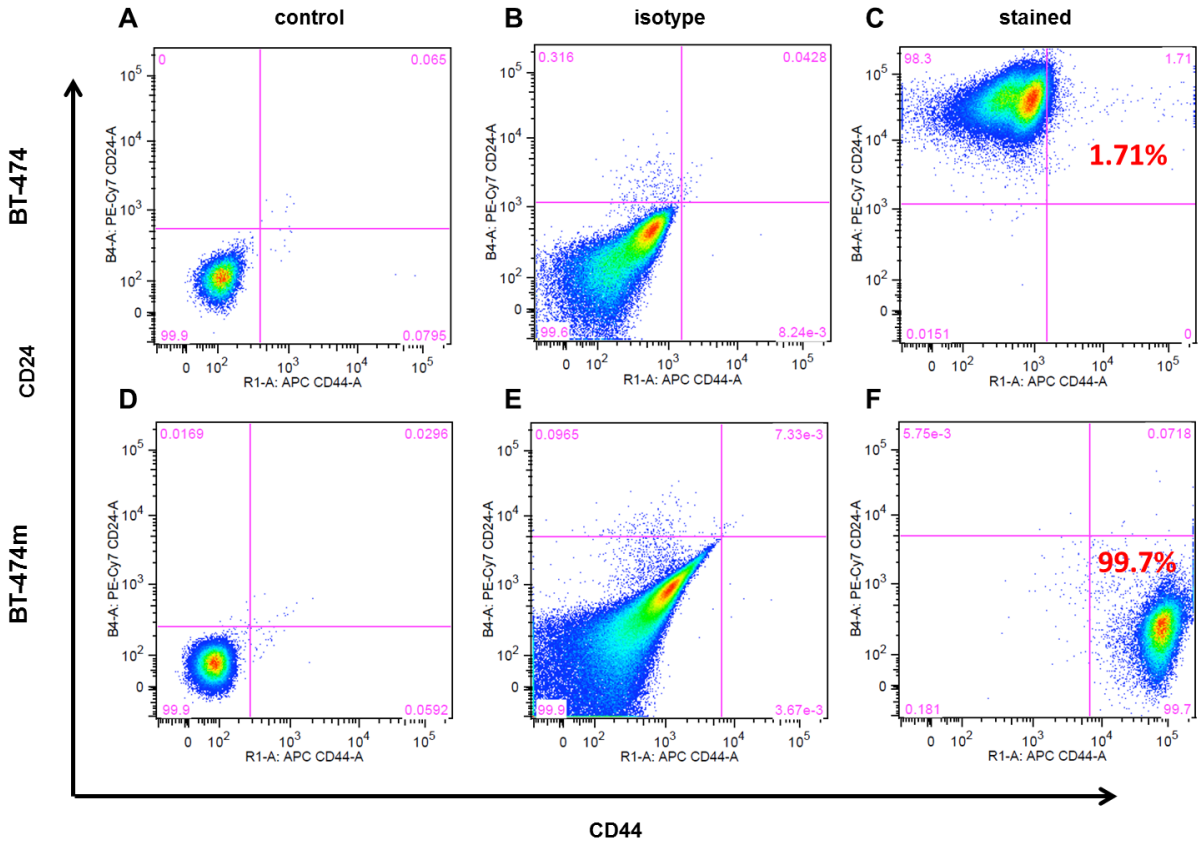

Figure 4.8 Flow cytometry data demonstrates that BT-474 cells are $CD24^{high}/CD44^{low}$. These cells will serve as the negative control for CD44 targeting, because they lack CD44 expression. (A) Unstained control, (B) isotype control, (C) stained cells with CD44 – Alexa Fluor® 647 and CD24 – PE-Cy7. BT-474m cells are $CD24^{low}/CD44^{high}$. These cells will serve as the experimental group to investigate CD44 targeting, as they have high CD44 expression. (D) Unstained control, (E) isotype control, (F) stained cells with CD44 – Alexa Fluor® 647 and CD24 – PE-Cy7.

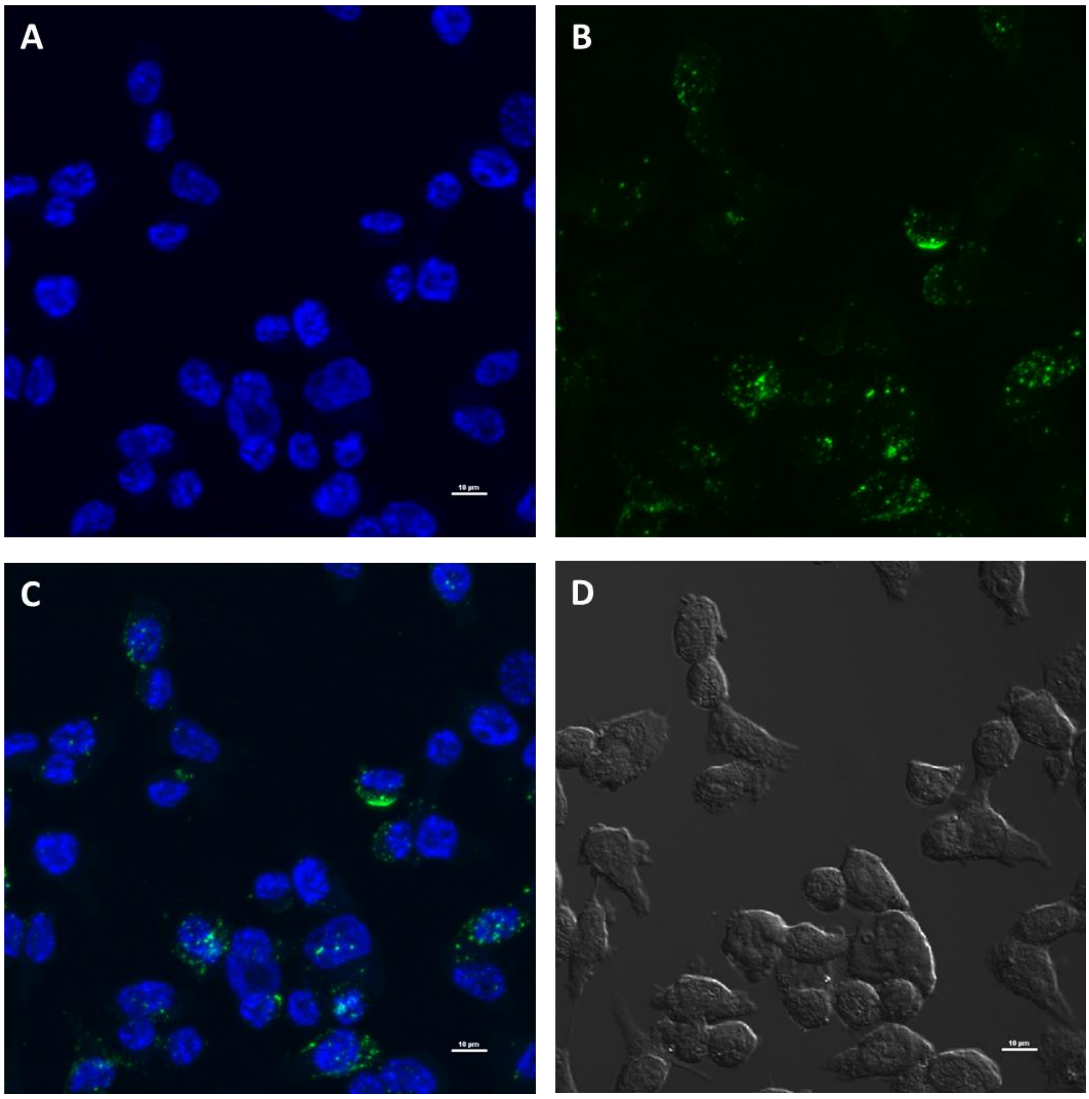

Figure 4.9 Cellular uptake study using BT-474m cells. Cells were plated and allowed to adhere for 24 hours, after which nCaP$^{CMHA\text{-}AF488}$ was added at a concentration of 2 mg/mL, in complete media. After 18 hours, nCaP$^{CMHA\text{-}AF488}$ can clearly be seen within cells as confirmed by z-stack images. (A) Cells stained with DAPI, (B) Cells imaged containing nCaP$^{CMHA\text{-}AF488}$, (C) Overlay of DAPI and AF488 images, showing nCaP$^{CMHA\text{-}AF488}$ uptake, and (D) Differential interference contrast (DIC) image.

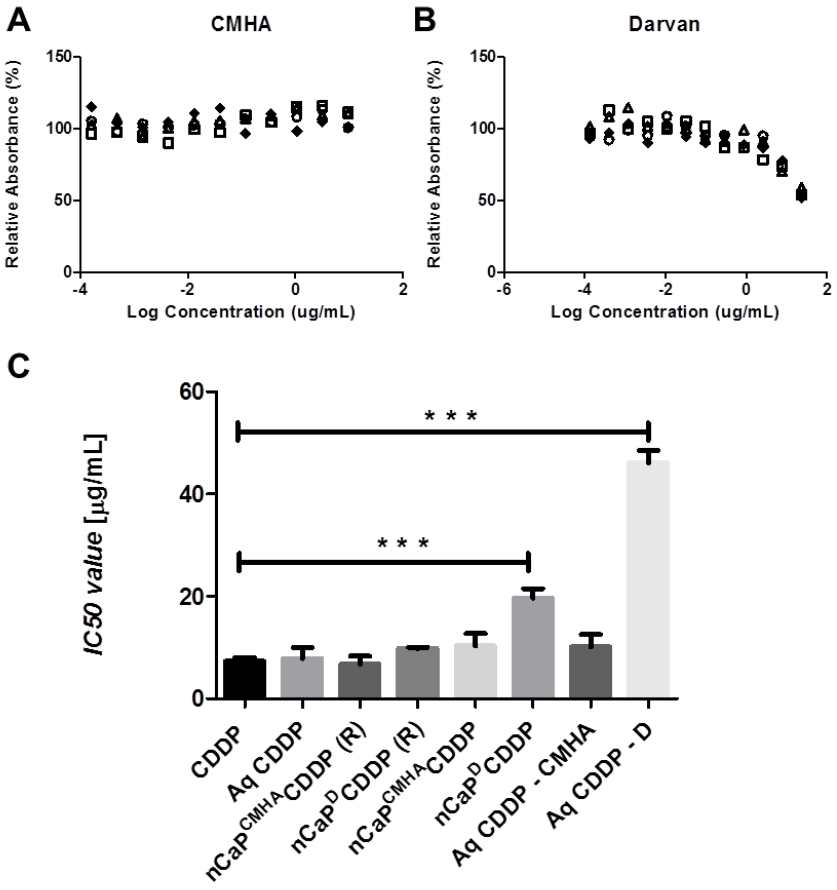

Figure 4.10 Mouse fibroblast cells, NIH-3T3, were used to examine the *in vitro* cytotoxicity of CMHA and D. (A) CMHA has no toxicity at a top concentration of 1 mg/mL. (B) D causes 50% cell death at a top concentration of 1 mg/mL. (C) Calculated IC50 values of: CDDP, Aq CDDP, CDDP released from nCaP^{CMHA}CDDP, CDDP released from nCaP^{D}CDDP, nCaP^{CMHA}CDDP, nCaP^{D}CDDP, Aq CDDP reacted with CMHA, and Aq CDDP reacted with D. Drug released from nCaP^{CMHA}CDDP has the same cytotoxicity as free CDDP and Aq CDDP. (One way ANOVA with Dunnet post-test, $P < 0.05$). Reacting D with Aq CDDP, significantly decreases the cytotoxicity of Aq CDDP. Reacting CMHA with Aq CDDP does not inhibit the cytotoxicity of Aq CDDP.

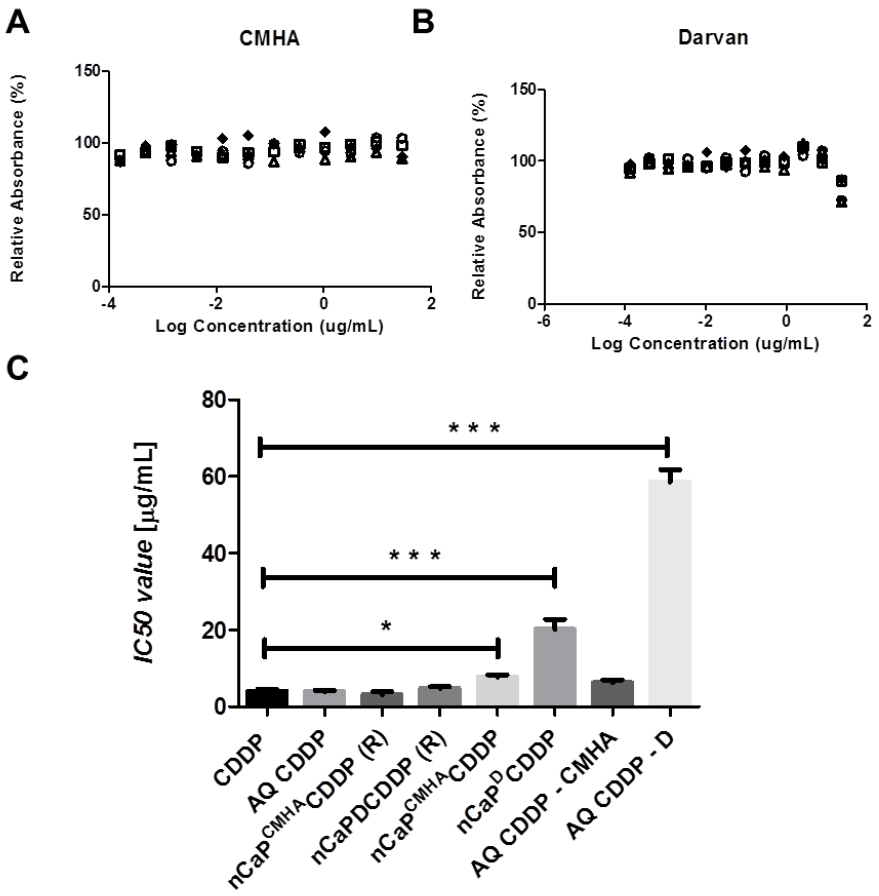

Figure 4.11 Cytotoxicity testing results in LMS cells. (A) CMHA has no toxicity at a top concentration of 1 mg/mL. (B) D causes 75% cell death at a top concentration of 1 mg/mL. (C) Calculated IC50 values of: CDDP, Aq CDDP, CDDP released from nCaP^{CMHA}CDDP, CDDP released from nCaP^{D}CDDP, nCaP^{CMHA}CDDP, nCaP^{D}CDDP, Aq CDDP reacted with CMHA, and Aq CDDP reacted with D. Drug released from nCaP^{CMHA}CDDP has the same cytotoxicity as free CDDP and Aq CDDP. nCaP^{CMHA}CDDP was significantly less cytotoxic than CDDP ($P<0.05$). nCaP^{D}CDDP and reacting D with Aq CDDP, are significantly less cytotoxic than CDDP ($P\leq0.001$). Reacting CMHA with Aq CDDP does not inhibit the cytotoxicity of Aq CDDP.

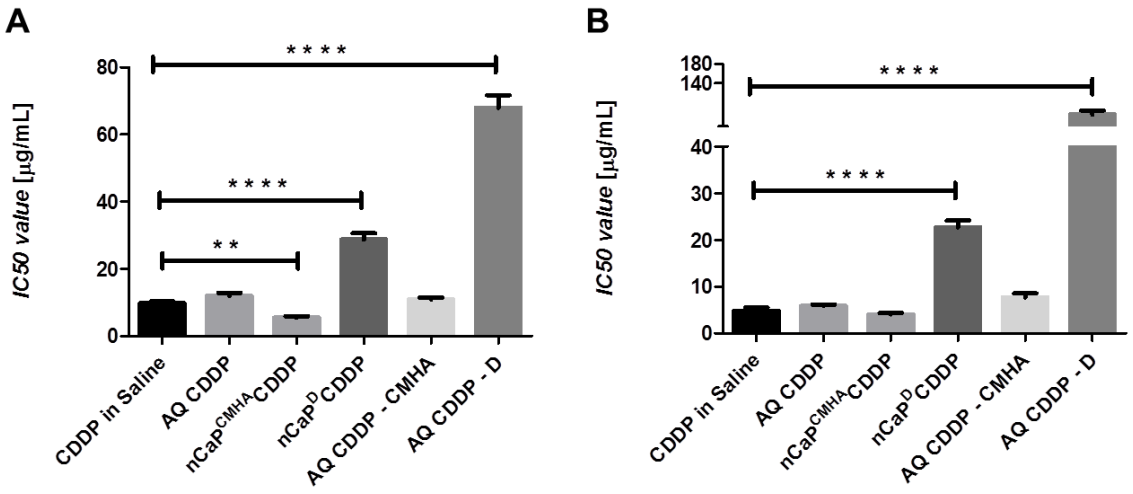

Figure 4.12 Cytotoxicity experiments were conducted using BT-474 (CD44-) and BT-474m (CD44+) cells. (A) Against BT-474 cells nCaP^{CMHA}CDDP is significantly more cytotoxic than CDDP ($P \leq 0.01$). nCaP^{D}CDDP and reacting D with Aq CDDP, are significantly less cytotoxic than CDDP ($P \leq 0.0001$). Reacting CMHA with Aq CDDP does not inhibit the cytotoxicity of Aq CDDP. (B) Against BT-474m cells nCaP^{D}CDDP and reacting D with Aq CDDP, are significantly less cytotoxic than CDDP ($P \leq 0.0001$). Reacting CMHA with Aq CDDP does not inhibit the cytotoxicity of Aq CDDP.

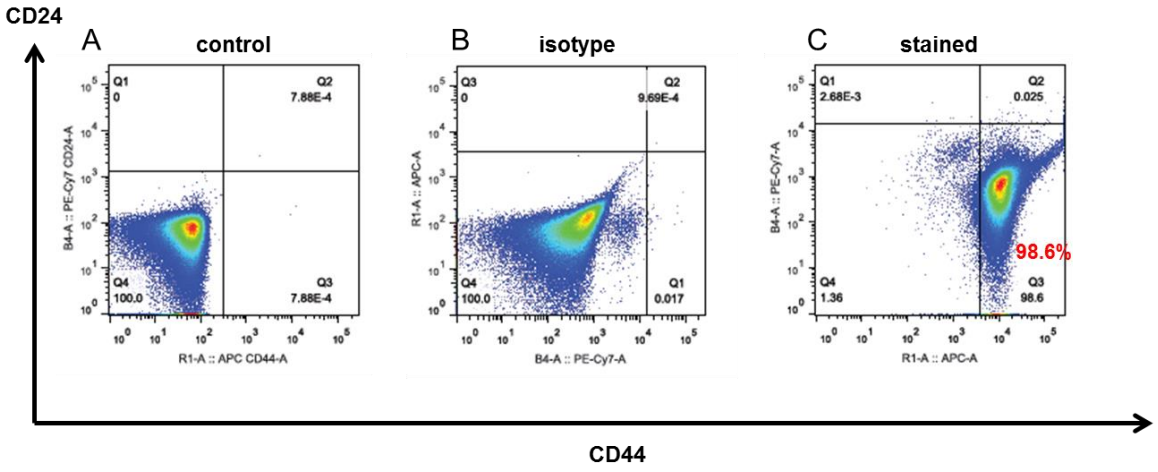

Figure 4.13 Flow cytometry data reveals BT 474m cells remain $CD24^{-/low}/CD44^{high}$ after mycoplasma removal. This ensured that the CD44 high status was maintained after mycoplasma removal. (A) Unstained control, (B) isotype controls, (C) stained cells with CD44 – Alexa Fluor® 647 and CD24 – PE-Cy7.

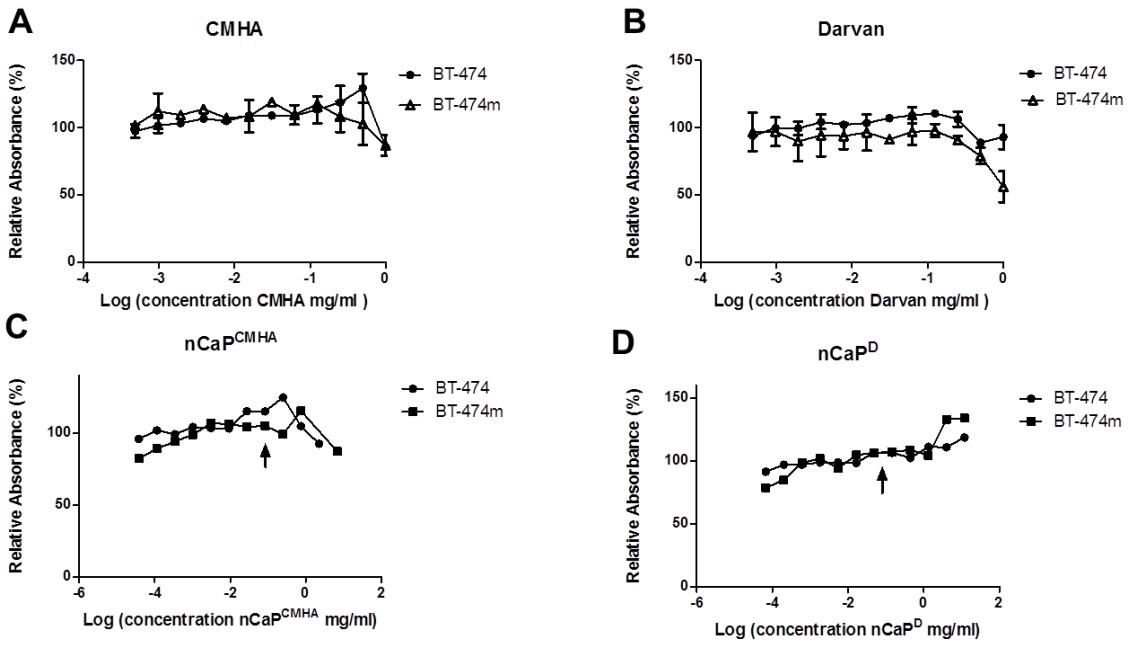

Figure 4.14 Cytotoxicity evaluations of nanoparticle components using BT-474 and BT-474m cells. (A) CMHA is not cytotoxic to either cell type. (B) D is cytotoxic to BT-474m cells at a top concentration of 1 mg/mL (C) $nCaP^{CMHA}$ is not cytotoxic, arrow indicates approximate $nCaP^{CMHA}$ concentration in IC50 of $nCaP^{CMHA}$CDDP. (D) $nCaP^{D}$ is not cytotoxic, arrow indicates approximate $nCaP^{D}$ concentration in IC50 of $nCaP^{CMHA}$CDDP.

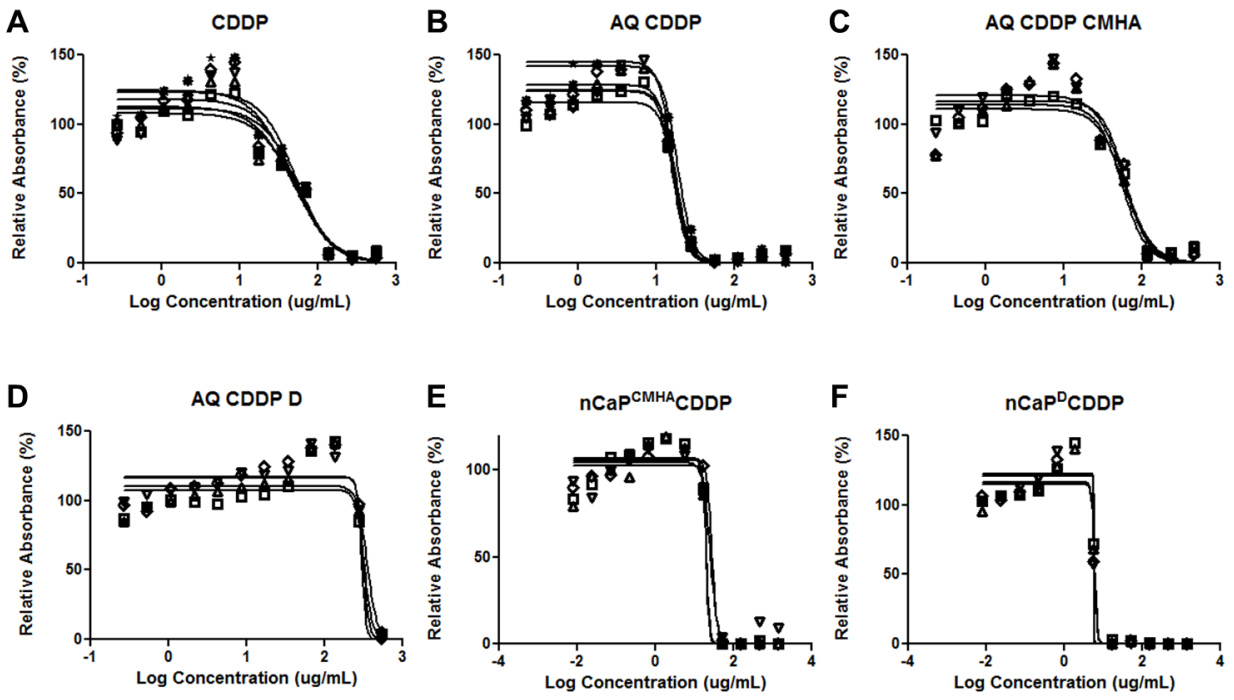

Figure 4.15 Cytotoxicity evaluation using BT-474 (CD44-) cells in an MTS assay. (A) CDDP, (B) Aq CDDP, (C) Aq CDDP reacted with CMHA, (D) Aq CDDP reacted with D, (E) nCaP^{CMHA}CDDP, and (F) nCaP^{D}CDDP.

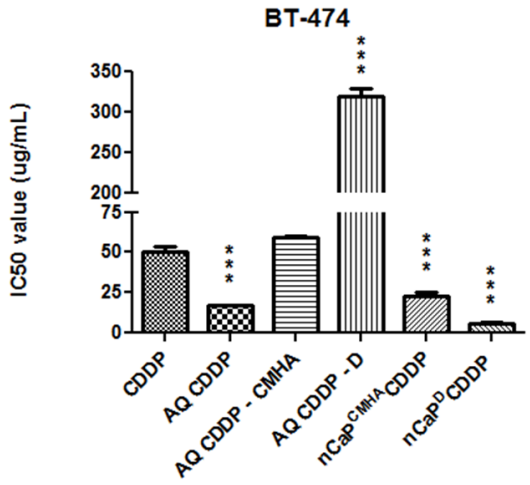

Figure 4.16 Calculated IC50 values against BT-474 (CD44-) cells, from curves shown in Figure 4.14. nCaP^{CMHA}CDDP is significantly more cytotoxic than CDDP ($P \leq 0.0001$). Reacting D with Aq CDDP (AQ CDDP D) is significantly less cytotoxic than CDDP ($P \leq 0.0001$). Reacting CMHA with Aq CDDP (AQ CDDP CMHA) does not inhibit the cytotoxicity of Aq CDDP. Aq CDDP is significantly more cytotoxic than CDDP ($P \leq 0.0001$).

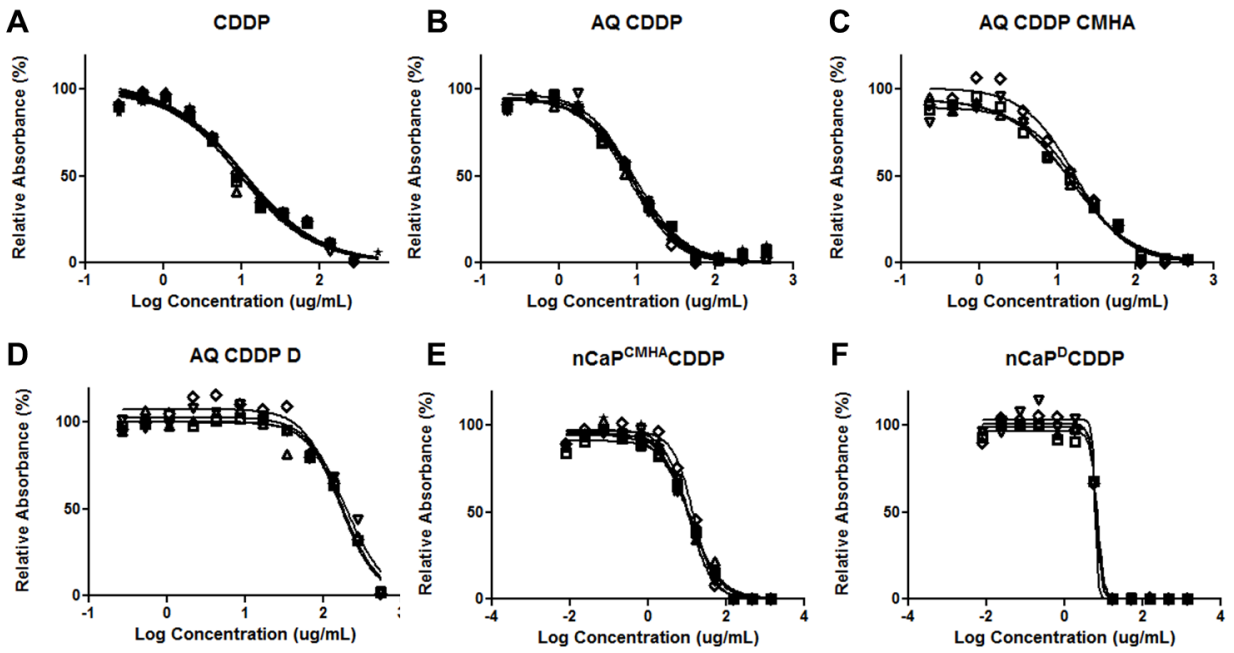

Figure 4.17 Cytotoxicity evaluation using BT-474m (CD44+) cells in an MTS assay. (A) CDDP, (B) Aq CDDP, (C) Aq CDDP reacted with CMHA, (D) Aq CDDP reacted with D, (E) nCaP^{CMHA}CDDP, and (F) nCaP^{D}CDDP.

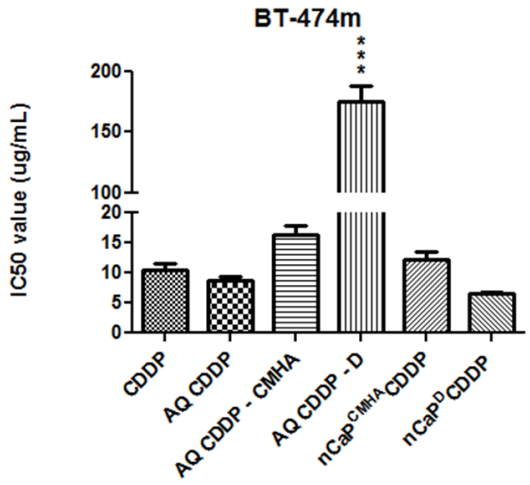

Figure 4.18 Calculated IC50 values against BT-474m (CD44+) cells, from curves shown in Figure 4.16. Reacting D with Aq CDDP (AQ CDDP D) is significantly less cytotoxic than CDDP ($P \leq 0.0001$). No other groups were significantly different from CDDP.

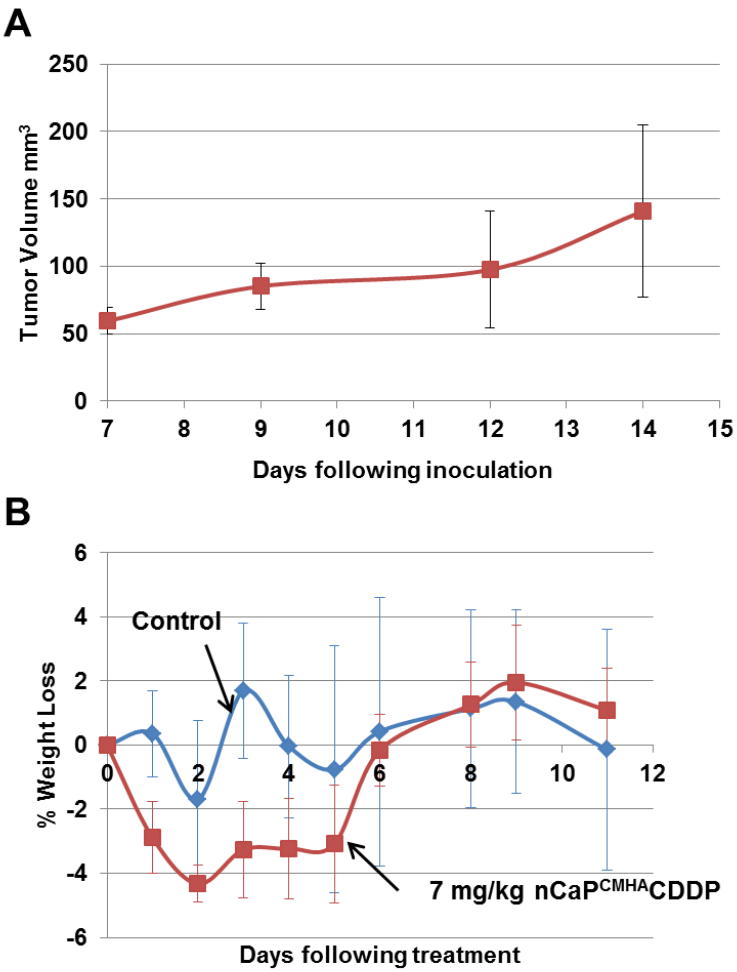

Figure 4.19 (A) Tumor take rate study performed in Athymic nude mice with 5 x 10^5 BT-474m cells injected subcutaneously in right rear flank of animals. Data represents average tumor volume vs days following inoculation with standard deviations. (B) Maximum tolerable dose study conducted with Athymic nude mice (6-8 weeks old) carrying BT-474m tumors. An intratumoral 7 mg/kg dose of nCaP^{CMHA}CDDP (4 mice/group) was compared to an untreated control (4 mice/group). nCaP^{CMHA}CDDP caused minimal weight loss at 7 mg/kg and all animals recovered.

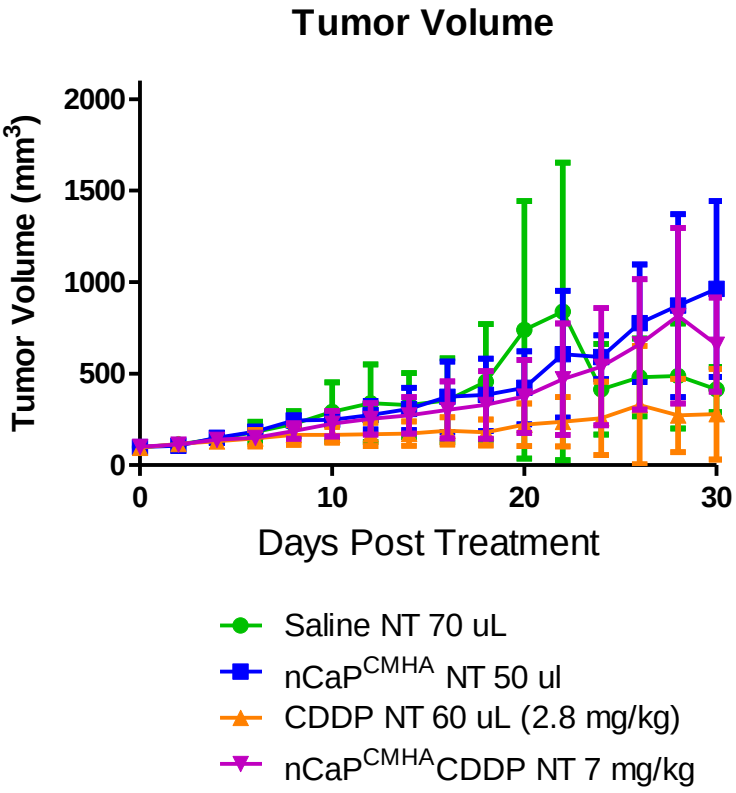

Figure 4.20 Efficacy study of nCaP^{CMHA}CDDP was conducted on J:Nu mice bearing BT-474m tumors. Animals were treated once when their tumor volume reached 100 ± 10 mm^3 and were compared to 2.8 mg/kg CDDP administered near the tumor. Tumor volume, grooming and weight loss were monitored every other day following treatment. The graph depicts average tumor volume (mm^3) per group versus days post treatment. The negative control Saline IT (70 uL) had no effect on tumor growth. nCaP^{CMHA} (60 uL) had no effect on tumor growth. CDDP at 2.8 mg/kg administered near the tumor delayed tumor growth.

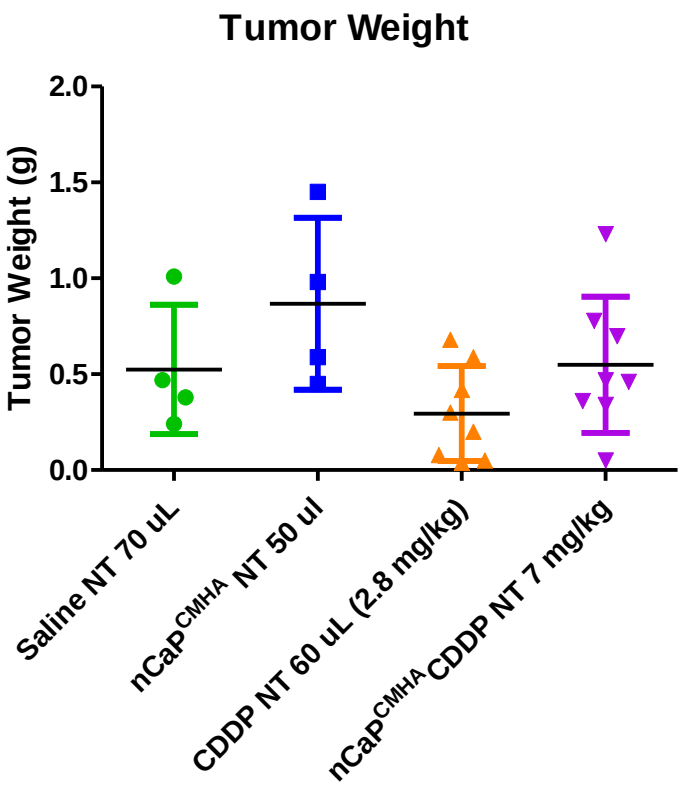

Figure 4.21 Tumor weight at the end of the study or at time of euthanasia for the efficacy study shown in Figure 4.19. The study was conducted on J:Nu mice bearing BT-474m tumors. Animals were treated once when their tumor volume reached 100 ± 10 mm^3. Tumors were resected at the end of the study and weighed. Animals were euthanized if tumor diameter was measured > 2 cm or at the completion of the study (Day 30). No significant differences were found between groups.

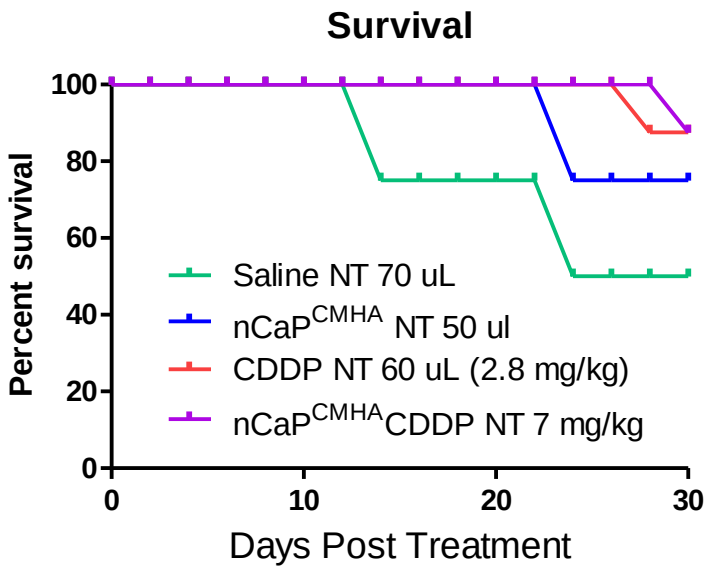

Figure 4.22 Survival was plotted for the efficacy study shown in Figure 4.19. The study was conducted on J:Nu mice bearing BT-474m tumors. Animals were treated once when their tumor volume reached 100 ± 10 mm^3 and compared to 2.8 mg/kg CDDP administered near tumor (NT). Tumor volume, grooming and weight loss were monitored every other day following treatment. Survival was defined as a tumor diameter > 2 mm or inability to groom. A treatment of 7 mg/kg $nCaP^{CMHA}$CDDP and 2.8 mg/kg CDDP (NT) were most effective at prolonging survival compared to control treatments of Saline or $nCaP^{CMHA}$ (NT).

Chapter 5

Suggested Future Directions and Conclusions

The goal of these studies was to develop a stabilized, injectable calcium phosphate nanoparticle system for the delivery of CDDP that releases biologically active drug and can furthermore be targeted to therapy resistant cancer cells. Using a systematic approach to understand the nano-molecular interactions of the stabilizer/drug/nanoparticle system and its resulting biological effect, we have revealed pitfalls in stabilizer-drug interactions that were previously unknown. These complex and inherently important interactions are crucial to define in order to develop an effective drug delivery system. By studying the interaction of each material component with the chemotherapy drug, cancer cells, and tumors, we identified a novel stabilizer for nCaP that has biological targeting capacity and importantly does not negatively impact the biological efficacy of CDDP. Sodium polyacrylate and sodium citrate were excellent stabilizers for nCaP, but negatively impacted the biological activity of CDDP. It is essential in future work to examine the components of each nanoparticle system as they interact with the drug to be delivered as it relates to anticipated biological effect. This process is not commonplace for current nanoparticle research and should be adopted to prevent complications moving forward.

This work highlighted a novel nCaP stabilizer candidate, carboxymethyl hyaluronic acid (CMHA). We showed that nCaP^{CMHA}CDDP does bind to CD44, but this binding was much lower than that of CMHA alone, which was lower than HA. The chemical modification of HA to create CMHA may contribute to the lower binding of CMHA with CD44. Additionally, the molecular weight of HA has been shown to significantly impact its binding with CD44, where

higher molecular weights have greater binding[170]. The CMHA used in these studies was ~34 kDa, compared to HA at 60 kDa during SPR experiments. This is a major factor that likely contributes to the enhanced binding of HA over CMHA observed. The incorporation of CMHA into $nCaP^{CMHA}$ likely lessens the number of available CD44 binding sites as well as the presentation of the molecule to CD44. With further funding, it would be of interest to study varied molecular weights of CMHA, to see if higher molecular weights have increased CD44 binding similar to HA. A higher molecular weight CMHA will likely change the stabilization of $nCaP^{CMHA}$, therefore a balance must be achieved between physical and biological properties of the resulting nanoparticle system.

More research is necessary to understand the interactions of $nCaP^{CMHA}$CDDP and CD44 expressed on the surface of cancer cells. The preliminary cell uptake study conducted here was able to show uptake of $nCaP^{CMHA\text{-}AF488}$ by CD44 positive BT-474m cells, but this is not sufficient to prove uptake was mediated by CD44. To do so, thorough cellular uptake studies combined with CD44 inhibition or saturation, via pretreatment with HA is necessary[171]. An additional control would be to examine $nCaP^{CMHA}$ uptake by cells that do not express CD44, like BT-474 cells. $nCaP^{CMHA}$CDDP had equivalent cytotoxicity in both $CD44^-$ and $CD44^+$ cells which is an excellent property for treating tumors *in vivo*, due to heterogeneity. This may be due to sufficient drug release from $nCaP^{CMHA}$CDDP or possibly cellular uptake is being mediated by a mechanism other than CD44 mediated uptake.

Each $nCaP^{x}$CDDP system that was synthesized was examined in an animal anti-cancer efficacy model. Each model utilized a different cell type to create tumors. We examined murine head and neck cancer (HNC), human head and neck cancer and human breast cancer, in order to demonstrate a broad range of activity. As a hypothesized negative control, we included a group

in each study that received an intratumoral injection of CDDP alone at the maximum tolerated volume. This was compared to an experimental group of an intratumoral dose of nCaP^{x}CDDP at the same volume, which delivered a significantly higher dose of CDDP, due to the high drug loading capacity of nCaP. In four out of five animal studies, local delivery of CDDP without nanoparticles was the most effective at delaying tumor growth. In Chapter 3, we utilized human HNC (FaDu) cells in a subcutaneous tumor model and found that a 1.4 mg/kg intratumoral dose of CDDP was sufficient to cause significant tumor growth delay. In that study, all animals in the CDDP IT treatment group survived the full length of the study, 30 days. This finding is completely novel and to our knowledge nothing comparable has been published. The efficacy of this treatment is likely due to the ability of CDDP to diffuse freely into the tumor with local administration. Each nCaP^{x}CDDP IT or NT treatment did not evenly distribute throughout the tumor as hypothesized. This was evident in the work performed in Chapter 4 with nCaP^{CMHA}CDDP. Tumors were resected at the time of euthanasia and those animals treated near tumor with nCaP^{CMHA}CDDP had obvious deposits of nanoparticles. Interestingly, tumors were smaller when two deposits of nCaP^{CMHA}CDDP were present versus larger tumors when only one deposit of nCaP^{CMHA}CDDP was found. When nCaP^{CMHA}CDDP was administered the goal was to deposit the nanoparticles in two locations opposite one another, but for some tumors this was not achieved. We believe the lack of distribution of nCaP^{CMHA}CDDP throughout the tumor contributed to the lack of efficacy observed because drug exposure was limited to one side of the tumor. Moving forward nCaP^{CMHA}CDDP could be given using intravenous (IV) administration to aid in distribution of nCaP^{CMHA}CDDP throughout the tumor. IV administration will allow nCaP^{CMHA}CDDP to passively target the tumor via the enhanced permeability and retention (EPR) effect[7,172–174] in addition to active targeting via CD44 expression in cancer cells. Once

nCaP^{CMHA}CDDP reaches the tumor, CD44 mediated uptake[175] and an acidic tumor microenvironment will enhance CDDP release locally.

Choice of animal model is essential to obtaining statistically significant, meaningful results. Within this dissertation we studied mouse HNC via SCCVII cells in CH3/HeJ mice, human HNC via FaDu cells in Nu/J mice and human TNBC via BT-474m cells in J:Nu mice. SCCVII cells are very aggressive, which is well published[63,128,176]. This model was chosen because of their aggressive phenotype, with the goal of overcoming the fast tumor growth with local delivery of CDDP via nCaP^{D}CDDP. We found that only local delivery of CDDP had a significant effect at delaying tumor growth and this was only found when all animals were treated when their tumor volume reached strictly within ±10% of one another, specifically 160 mm^3 for the second efficacy study (Figure 2.19). Due to the aggressive nature of these tumors only 20% of animals remained in the most effective treatment group, CDDP IT, at the 20 day completion of the study. All other animals had to be euthanized due to a tumor diameter > 2 cm, weight loss, or tumor necrosis, prior to day 20 following treatment. This model is too aggressive and consequently we moved to the use of a human HNC model, which employed FaDu cells. FaDu cells proved to be less aggressive, where animals treated with control treatments of saline or nCaP^{CIT} alone were able to survive for 16 to 27 days and all of the animals in the CDDP IT treatment group survived 30 days. This model proved to develop tumors that when left untreated, all grew within a close tumor volume range of one another, which limited variability within treatment groups. Additionally, necrosis and rapid tumor growth (diameter > 2 cm 10 days following treatment) was not an issue. In Chapter 4 of this dissertation, we aimed to target human, CD44 expressing, therapy resistant TNBC. BT-474m cells proved to be an excellent model for this *in vitro* but when these cells were inoculated in J:Nu mice their growth was highly

variable. This may be due to an insufficient number of cells injected, loss of aggressive phenotype *in vivo* or an immune response in the J:Nu mice. We chose to use this cell type because they uniquely represent a sub-set of transformed, triple negative breast cancer (TNBC) cells which are $CD44^{+}/CD24^{-}$. This type of cancer cell has not previously been examined for *in vivo* tumor take rate or anti-cancer efficacy using CDDP, but has excellent clinical relevance towards more effective treatment of TNBC. It is likely that moving forward with this cell line will require inoculating mice with a higher concentration of cells, where we injected 5×10^5 and something more comparable to what was used for FaDu tumors would be more appropriate, 2×10^6 cells. This can be evaluated using an additional tumor take rate study. It is essential to determine an appropriate animal model that will result in tumors that will grow beyond inoculation volume, but are not too aggressive causing necrosis and tumor diameters above limits set by Institutional Animal Care.

Overall, $nCaP^{CMHA}$CDDP shows great promise for the treatment of TNBC. CD44 expression is also common in HNC[37,177–180], therefore revisiting the HNC model *in vitro* and *in vivo* with the $nCaP^{CMHA}$CDDP formulation is of interest. A thorough maximum tolerable dose study with a wider range of doses of $nCaP^{CMHA}$CDDP should be performed prior to a repeat efficacy study. It is likely that a higher dose of $nCaP^{CMHA}$CDDP will be safe, as no animals lost more than 5% of their weight at time of treatment due to the 7 mg/kg dose used in Chapter 4. The cytotoxicity studies were very promising and thus we anticipated significant tumor growth delay *in vivo*. With thorough characterization and optimization $nCaP^{CMHA}$CDDP has excellent potential for localized treatment of CD44+ cancers, like TNBC and HNC.

References

1. Ries, L. A. G., Keel, G. E. & Horner, M. D. SEER Survival Monograph, Cancer Survival Among Adults : U.S. SEER Program , 1988 -2001 Patient and Tumor Characteristics. 1988–2001 (2007).

2. American Cancer Society. *Cancer Facts & Figures*. 1–64 (2013).

3. Byrne, J. D., Betancourt, T. & Brannon-Peppas, L. Active targeting schemes for nanoparticle systems in cancer therapeutics. *Adv. Drug Deliv. Rev.* **60,** 1615–26 (2008).

4. Hans, M. L. & Lowman, A. M. B iodegradable nanoparticles for drug delivery and targeting. **6,** 319–327 (2002).

5. Mahon, E., Salvati, A., Baldelli Bombelli, F., Lynch, I. & Dawson, K. Designing the nanoparticle-biomolecule interface for "Targeting and Therapeutic Delivery."*J. Control. Release* (2012). doi:10.1016/j.jconrel.2012.04.009

6. Eifler, A. & Thaxton, S. in *Biomed. Nanotechnol. Methods Mol. Biol.* (Hurst, S.) 325–338 (Humana Press, 2011). doi:10.1007/978-1-61779-052-2_21

7. Mcneil, S. E. Nanoparticle therapeutics : a personal perspective. *WIREs Nanomedicine and Nanobiotechnology* **1,** 264–271 (2009).

8. Nel, A. E. *et al.* Understanding biophysicochemical interactions at the nano-bio interface. *Nat. Mater.* **8,** 543–57 (2009).

9. Ganesan, K., Kovtun, A., Neumann, S., Heumann, R. & Epple, M. Calcium phosphate nanoparticles: colloidally stabilized and made fluorescent by a phosphate-functionalized porphyrin. *J. Mater. Chem.* **18,** 3655 (2008).

10. Kakizawa, Y., Furukawa, S. & Kataoka, K. Block copolymer-coated calcium phosphate nanoparticles sensing intracellular environment for oligodeoxynucleotide and siRNA delivery. *J. Control. Release* **97,** 345–56 (2004).

11. Dubowchik, G. M. & Walker, M. a. Receptor-mediated and enzyme-dependent targeting of cytotoxic anticancer drugs. *Pharmacol. Ther.* **83,** 67–123 (1999).

12. Cairns, R., Papandreou, I. & Denko, N. Overcoming physiologic barriers to cancer treatment by molecularly targeting the tumor microenvironment. *Mol. Cancer Res.* **4,** 61–70 (2006).

13. Nobs, L., Buchegger, F., Gurny, R. & Allémann, E. Current methods for attaching targeting ligands to liposomes and nanoparticles. *J. Pharm. Sci.* **93,** 1980–92 (2004).

14. Barroug, A. & Glimcher, M. J. Hydroxyapatite crystals as a local delivery system for cisplatin: adsorption and release of cisplatin in vitro. *J. Orthop. Res.* **20,** 274–80 (2002).

15. Barroug, a, Kuhn, L. T., Gerstenfeld, L. C. & Glimcher, M. J. Interactions of cisplatin with calcium phosphate nanoparticles: in vitro controlled adsorption and release. *J. Orthop. Res.* **22,** 703–8 (2004).

16. Cheng, X. & Kuhn, L. Chemotherapy drug delivery from calcium phosphate nanoparticles. *Int. J. Nanomedicine* **2,** 667 (2007).

17. Li, X. *et al.* Intrinsic resistance of tumorigenic breast cancer cells to chemotherapy. *J. Natl. Cancer Inst.* **100,** 672–9 (2008).

18. Visvader, J. E. & Lindeman, G. J. Cancer stem cells in solid tumours: accumulating evidence and unresolved questions. *Nat. Rev. Cancer* **8,** 755–68 (2008).

19. Lee, H. E. *et al.* An increase in cancer stem cell population after primary systemic therapy is a poor prognostic factor in breast cancer. *Br. J. Cancer* **104,** 1730–8 (2011).

20. Yang, G., Prestwich, G. D. & Mann, B. K. Thiolated Carboxymethyl-Hyaluronic-Acid-Based Biomaterials Enhance Wound Healing in Rats, Dogs, and Horses. *ISRN Vet. Sci.* **2011,** 1–7 (2011).

21. Leeuwenburgh, S. C. G., Ana, I. D. & Jansen, J. a. Sodium citrate as an effective dispersant for the synthesis of inorganic-organic composites with a nanodispersed mineral phase. *Acta Biomater.* **6,** 836–44 (2010).

22. Bhardwaj, U. & Burgess, D. J. A novel USP apparatus 4 based release testing method for dispersed systems. *Int. J. Pharm.* **388,** 287–94 (2010).

23. National Cancer Institute. Understanding Cancer Statistics. *Serv. People Cancer Stat.* (2010). at <http://www.cancer.gov/aboutnci/servingpeople/cancer-statistics>

24. Jemal, A., Bray, F. & Ferlay, J. Global Cancer Statistics. **61,** 69–90 (2011).

25. National Cancer Institute. *Incidence and Mortality Rate Trends Trends in NCI Funding for Head and Neck Cancers 2 Research Examples of NCI Activities Relevant to Head and Neck Cancers Selected Advances in Head and Neck Cancers Research*. 1–3 (2007).

26. Schlecht, N. F. *et al.* Gene expression profiles in HPV-infected head and neck cancer. 283–293 (2007). doi:10.1002/path

27. Vu, H. L., Sikora, A. G., Fu, S. & Kao, J. HPV-induced oropharyngeal cancer, immune response and response to therapy. *Cancer Lett.* **288,** 149–55 (2010).

28. Syrjänen, S. Human papillomavirus (HPV) in head and neck cancer. *J. Clin. Virol.* **32 Suppl 1,** S59–66 (2005).

29. Argiris, A., Karamouzis, M. V, Raben, D. & Ferris, R. L. Head and neck cancer. *Lancet* **371,** 1695–709 (2008).

30. Ringash, J. *et al.* Outcomes Toolbox for Head and Neck Cancer. *Head Neck* (2013).

31. Fromer, B. M. J. News from ODAC ODAC Votes No on IntraDose Injectible Cisplatin / Epinephrine Gel for Head and Neck Cancer. 57–58 (2001).

32. Burris, H. a *et al.* Intratumoral cisplatin/epinephrine-injectable gel as a palliative treatment for accessible solid tumors: a multicenter pilot study. *Otolaryngol. Head. Neck Surg.* **118,** 496–503 (1998).

33. Duvillard, C. *et al.* Epinephrine enhances penetration and anti-cancer activity of local cisplatin on rat sub-cutaneous and peritoneal tumors. *Int. J. Cancer* **81,** 779–84 (1999).

34. Malhotra, H. & Plosker, G. L. Cisplatin/epinephrine injectable gel. *Drugs Aging* **18,** 787–93; discussion 794–5 (2001).

35. Gel, I. FDA ODAC Briefing Document for NDA 21-236.

36. Ward, B. B. Targeted therapy in head and neck cancer. *Oral Maxillofac. Surg. Clin. North Am.* **25,** 83–92, vi–vii (2013).

37. Suh, Y., Amelio, I., Guerrero Urbano, T. & Tavassoli, M. Clinical update on cancer: molecular oncology of head and neck cancer. *Cell Death Dis.* **5,** e1018 (2014).

38. American Cancer Society. Breast Cancer. (2013). at <http://www.cancer.org/acs/groups/cid/documents/webcontent/003090-pdf.pdf>

39. American Cancer Society. *Cancer Facts & Figures*. (2012). at <http://www.cancer.org/acs/groups/content/@epidemiologysurveilance/documents/document/acspc-031941.pdf>

40. National Cancer Institute. Triple-Negative Breast Cancer. *Breast Cancer Treat.* (2014). at <http://www.cancer.gov/cancertopics/pdq/treatment/breast/healthprofessional/page8>

41. Liedtke, C. *et al.* Response to neoadjuvant therapy and long-term survival in patients with triple-negative breast cancer. *J. Clin. Oncol.* **26,** 1275–81 (2008).

42. Hermann, P. C., Bhaskar, S., Cioffi, M. & Heeschen, C. Cancer stem cells in solid tumors. *Semin. Cancer Biol.* **20,** 77–84 (2010).

43. Lock, F. E. *et al.* Targeting carbonic anhydrase IX depletes breast cancer stem cells within the hypoxic niche. *Oncogene* 1–10 (2012). doi:10.1038/onc.2012.550

44. Nagrath, S. *et al.* Isolation of rare circulating tumour cells in cancer patients by microchip technology. *Nature* **450,** 1235–9 (2007).

45. Van der Pluijm, G. Epithelial plasticity, cancer stem cells and bone metastasis formation. *Bone* **48,** 37–43 (2011).

46. Strewler, G. J. Cancer Stem Cells and Bone Metastasis. **5,** 308–322 (2008).

47. Idowu, M. O. *et al.* CD44(+)/CD24(-/low) cancer stem/progenitor cells are more abundant in triple-negative invasive breast carcinoma phenotype and are associated with poor outcome. *Hum. Pathol.* **43,** 364–73 (2012).

48. Giatromanolaki, A., Sivridis, E., Fiska, A. & Koukourakis, M. I. The CD44+/CD24- phenotype relates to "triple-negative" state and unfavorable prognosis in breast cancer patients. *Med. Oncol.* **28,** 745–52 (2011).

49. Silver, D. P. *et al.* Efficacy of neoadjuvant Cisplatin in triple-negative breast cancer. *J. Clin. Oncol.* **28,** 1145–53 (2010).

50. Guttilla, I. K. *et al.* Prolonged mammosphere culture of MCF-7 cells induces an EMT and repression of the estrogen receptor by microRNAs. *Breast Cancer Res. Treat.* **132,** 75–85 (2012).

51. Murohashi, M. *et al.* Gene set enrichment analysis provides insight into novel signal pathways in breast cancer stem cells. *Br. J. Cancer* **102,** 206–212 (2010).

52. Sheridan, C. *et al.* CD44+/CD24- breast cancer cells exhibit enhanced invasive properties: an early step necessary for metastasis. *Breast Cancer Res.* **8,** R59 (2006).

53. American Cancer Society. Chemotherapy. *Ovarian Cancer, Bl. Cancer, Ovarian Cancer* (2013). at <http://www.cancer.org/cancer/ovariancancer/detailedguide/ovarian-cancer-treating-chemotherapy>

54. Jamieson, E. R. & Lippard, S. J. Structure, Recognition, and Processing of Cisplatin-DNA Adducts. *Chem. Rev.* **99,** 2467–98 (1999).

55. Goldberg, E. P., Hadba, A. R., Almond, B. a & Marotta, J. S. Intratumoral cancer chemotherapy and immunotherapy: opportunities for nonsystemic preoperative drug delivery. *J. Pharm. Pharmacol.* **54,** 159–80 (2002).

56. Penn, R. D., Kroin, J. S., Harris, J. E., Chiu, K. M. & Braun, D. P. Chronic Intratumoral Chemo of Rat Tumor with Cisplatin and FLuorouracil. *Proc. Am. Soc. Stereotact. Funct. Neurosurg.* **46,** 240–244 (1983).

57. Muchmore, J. H. & Wanebo, H. J. Regional chemotherapy: overview. *Surg. Oncol. Clin. N. Am.* **17,** 709–30, vii (2008).

58. Beasley, G. M., Kahn, L. & Tyler, D. S. Current clinical and research approaches to optimizing regional chemotherapy: novel strategies generated through a better understanding of drug pharmacokinetics, drug resistance, and the development of clinically relevant animal models. *Surg. Oncol. Clin. N. Am.* **17,** 731–58, vii–viii (2008).

59. Brincker, H. Direct intratumoral chemotherapy. *Crit. Rev. Oncol. Hematol.* **15,** 91–8 (1993).

60. Chen, F.-A., Kuriakose, M. A., Zhou, M.-X., DeLacure, M. D. & Dunn, R. L. Biodegradable polymer-mediated intratumoral delivery of cisplatin for treatment of human head and neck squamous cell carcinoma in a chimeric mouse model. *Head Neck* **25,** 554–60 (2003).

61. Begg, a C., Deurloo, M. J., Kop, W. & Bartelink, H. Improvement of combined modality therapy with cisplatin and radiation using intratumoral drug administration in murine tumors. *Radiother. Oncol.* **31,** 129–37 (1994).

62. Cemazar, M. *et al.* Improved therapeutic effect of electro chemotherapy with cisplatin by intratumoral drug administration and changing of electrode orientation for electropermeabilization on EAT tumor model in mice. 121–127 (1995).

63. Ning, S., Yu, N., Brown, D. M., Kanekal, S. & Knox, S. J. Radiosensitization by intratumoral administration of cisplatin in a sustained-release drug delivery system. *Radiother. Oncol.* **50,** 215–23 (1999).

64. Celikoglu, F., Celikoglu, S. I. & Goldberg, E. P. Techniques for intratumoral chemotherapy of lung cancer by bronchoscopic drug delivery. **6,** 545–552 (2008).

65. Al-Kattan, A. *et al.* Biomimetic nanocrystalline apatites: Emerging perspectives in cancer diagnosis and treatment. *Int. J. Pharm.* (2011). doi:10.1016/j.ijpharm.2011.07.005

66. Drouet, C. *et al.* Nanocrystalline apatites: From powders to biomaterials. *Powder Technol.* **190,** 118–122 (2009).

67. Gómez-Morales, J., Iafisco, M., Delgado-López, J. M., Sarda, S. & Drouet, C. Progress on the preparation of nanocrystalline apatites and surface characterization: Overview of fundamental and applied aspects. *Prog. Cryst. Growth Charact. Mater.* **59,** 1–46 (2013).

68. Emoto, M. *et al.* Novel chemoembolization using calcium-phosphate ceramic microsphere incorporating TNP-470, an anti-angiogenic agent. *Cancer Sci.* **101,** 984–90 (2010).

69. Tanzawa, Y. *et al.* Potentiation of the antitumor effect of calcium phosphate cement containing anticancer drug and caffeine on rat osteosarcoma. *J. Orthop. Sci.* **16,** 77–84 (2011).

70. Holback, H. & Yeo, Y. Intratumoral drug delivery with nanoparticulate carriers. *Pharm. Res.* **28,** 1819–30 (2011).

71. Greco, F. & Vicent, M. J. Combination therapy: opportunities and challenges for polymer-drug conjugates as anticancer nanomedicines. *Adv. Drug Deliv. Rev.* **61,** 1203–13 (2009).

72. Wiedeman, M. P. Dimensions of Blood Vessels from Distributing Artery to Collecting Vein. *Circ. Res.* **12,** 375–378 (1963).

73. Janssen Products, L. Doxil (doxorubicin HCl liposome injection). *All about Doxil* 1 (2014). at <https://www.doxil.com/>

74. Singh, R. & Lillard, J. W. Nanoparticle-based targeted drug delivery. *Exp. Mol. Pathol.* **86,** 215–23 (2009).

75. Celgene Corporation. Abraxane. *Abraxane Inject. Suspens.* (2014). at <http://www.abraxane.com/>

76. Petros, R. a & DeSimone, J. M. Strategies in the design of nanoparticles for therapeutic applications. *Nat. Rev. Drug Discov.* **9,** 615–27 (2010).

77. Gregoriadis, G. Engineering liposomes for drug delivery: progress and problems. *Trends Biotechnol.* **13,** 527–37 (1995).

78. Seetharamu, N., Kim, E., Hochster, H., Martin, F. & Muggia, F. Phase II study of liposomal cisplatin (SPI-77) in platinum-sensitive recurrences of ovarian cancer. *Anticancer Res.* **30,** 541–5 (2010).

79. Vokes, E. E. *et al.* A phase II study of STEALTH cisplatin (SPI-77) and vinorelbine in patients with advanced non small-cell lung cancer. *Clin. Lung Cancer* **2,** 128–32 (2000).

80. Ye, M., Kim, S. & Park, K. Issues in long-term protein delivery using biodegradable microparticles. *J. Control. Release* **146,** 241–60 (2010).

81. Angelova, N. & Hunkeler, D. Rationalizing the design of polymeric biomaterials. *Trends Biotechnol.* **17,** 409–21 (1999).

82. Jain, R. K. & Stylianopoulos, T. Delivering nanomedicine to solid tumors. *Nat. Rev. Clin. Oncol.* **7,** 653–64 (2010).

83. Zhang, M. *et al.* PEGylated Calcium Phosphate Nanocomposites as Smart Environment-Sensitive Carriers for siRNA Delivery. *Adv. Mater.* **21,** 3520–3525 (2009).

84. Wang, J. *et al.* Peptide decorated calcium phosphate/carboxymethyl chitosan hybrid nanoparticles with improved drug delivery efficiency. *Int. J. Pharm.* **446,** 205–10 (2013).

85. Lee, K. *et al.* Stabilized calcium phosphate nano-aggregates using a dopa-chitosan conjugate for gene delivery. *Int. J. Pharm.* **445,** 196–202 (2013).

86. Chernousova, S., Klesing, J., Soklakova, N. & Epple, M. A genetically active nano-calcium phosphate paste for bone substitution, encoding the formation of BMP-7 and VEGF-A. *RSC Adv.* (2013). doi:10.1039/c3ra23450a

87. Dorozhkin, S. V. Biocomposites and hybrid biomaterials based on calcium orthophosphates. *Biomatter* **1,** 3–56 (2011).

88. Gbureck, U., Barralet, J. E., Spatz, K., Grover, L. M. & Thull, R. Ionic modification of calcium phosphate cement viscosity. Part I: hypodermic injection and strength improvement of apatite cement. *Biomaterials* **25,** 2187–2195 (2004).

89. Sokolova, V. V, Radtke, I., Heumann, R. & Epple, M. Effective transfection of cells with multi-shell calcium phosphate-DNA nanoparticles. *Biomaterials* **27,** 3147–53 (2006).

90. Kester, M. *et al.* Calcium phosphate nanocomposite particles for in vitro imaging and encapsulated chemotherapeutic drug delivery to cancer cells. *Nano Lett.* **8,** 4116–21 (2008).

91. He, Q. *et al.* Calcium phosphate nanoparticle adjuvant. *Clin. Diagn. Lab. Immunol.* **7,** 899–903 (2000).

92. Al-Kattan, A., Dufour, P., Dexpert-Ghys, J. & Drouet, C. Preparation and Physicochemical Characteristics of Luminescent Apatite-Based Colloids. *J. Phys. Chem. C* **114,** 2918–2924 (2010).

93. Sokolova, V. & Epple, M. Inorganic nanoparticles as carriers of nucleic acids into cells. *Angew. Chem. Int. Ed. Engl.* **47,** 1382–95 (2008).

94. Viktoriya Sokolova, Olga Rotan, Jan Klesing, Perihan Nalbant, Jan Buer, Torben Knuschke, A. M. W. and M. E. Calcium phosphate nanoparticles as versatile carrier for small and large molecules across cell membranes. *J. Mater. Chem.* (2011).

95. Sokolova, V. *et al.* An outer shell of positively charged poly(ethyleneimine) strongly increases the transfection efficiency of calcium phosphate/DNA nanoparticles. *J. Mater. Sci.* **45,** 4952–4957 (2010).

96. Sokolova, V., Kovtun, A., Heumann, R. & Epple, M. Tracking the pathway of calcium phosphate/DNA nanoparticles during cell transfection by incorporation of red-fluorescing tetramethylrhodamine isothiocyanate-bovine serum albumin into these nanoparticles. *J. Biol. Inorg. Chem.* **12,** 174–9 (2007).

97. Rey, C., Combes, C., Drouet, C. & Glimcher, M. J. Bone mineral: update on chemical composition and structure. *Osteoporos. Int.* **20,** 1013–21 (2009).

98. Kovtun, A. *et al.* Nanoparticle-mediated gene transfer from electrophoretically coated metal surfaces. *J. Phys. Chem. B* **117,** 1550–5 (2013).

99. Banik, M. & Basu, T. Calcium phosphate nanoparticles: a study of their synthesis, characterization and mode of interaction with salmon testis DNA. *Dalton Trans.* **43,** 3244–59 (2014).

100. Urch, H., Vallet-Regi, M., Ruiz, L., Gonzalez-Calbet, J. M. & Epple, M. Calcium phosphate nanoparticles with adjustable dispersability and crystallinity. *J. Mater. Chem.* **19,** 2166 (2009).

101. Klesing, J., Wiehe, a, Gitter, B., Gräfe, S. & Epple, M. Positively charged calcium phosphate/polymer nanoparticles for photodynamic therapy. *J. Mater. Sci. Mater. Med.* **21,** 887–92 (2010).

102. Iafisco, M. *et al.* Cell Surface Receptor Targeted Biomimetic Apatite Nanocrystals for Cancer Therapy. *Small* **17,** (2013).

103. Palazzo, B. *et al.* Biomimetic Hydroxyapatite–Drug Nanocrystals as Potential Bone Substitutes with Antitumor Drug Delivery Properties. *Adv. Funct. Mater.* **17,** 2180–2188 (2007).

104. Mahoney, B. P., Raghunand, N., Baggett, B. & Gillies, R. J. Tumor acidity, ion trapping and chemotherapeutics. *Biochem. Pharmacol.* **66,** 1207–1218 (2003).

105. Lee, E. S., Gao, Z. & Bae, Y. H. Recent progress in tumor pH targeting nanotechnology. *J. Control. Release* **132,** 164–70 (2008).

106. Li, J., Yang, Y. & Huang, L. Calcium Phosphate Nanoparticles with an Asymmetric Lipid Bilayer Coating for siRNA Delivery to the Tumor. *J. Control. Release* **158,** 108–114 (2013).

107. Tannock, I. F., Rotin, D. & Hot, D. Acid pH in Tumors and Its Potential for Therapeutic Exploitation Perspectivesin CancerResearch Acid pH in Tumors and Its Potential for Therapeutic Exploitation1. 4373–4384 (1989).

108. Detsch, R. *et al.* The resorption of nanocrystalline calcium phosphates by osteoclast-like cells. *Acta Biomater.* **6,** 3223–33 (2010).

109. Epple, M. *et al.* Application of calcium phosphate nanoparticles in biomedicine. *J. Mater. Chem.* **20,** 18 (2010).

110. Yang, X.-Z. *et al.* Rational design of polyion complex nanoparticles to overcome cisplatin resistance in cancer therapy. *Adv. Mater.* **26,** 931–6 (2014).

111. Hecht, J. R. *et al.* A Phase I / II Trial of Intratumoral Endoscopic Ultrasound Injection of ONYX-015 with Intravenous Gemcitabine in Unresectable Pancreatic Carcinoma Advances in Brief A Phase I / II Trial of Intratumoral Endoscopic Ultrasound Injection of ONYX-015 with Intr. 555–561 (2003).

112. Wolinsky, J. B., Colson, Y. L. & Grinstaff, M. W. Local drug delivery strategies for cancer treatment: gels, nanoparticles, polymeric films, rods, and wafers. *J. Control. Release* **159,** 14–26 (2012).

113. Andres, C., Sinani, V., Lee, D., Gun'ko, Y. & Kotov, N. Anisotropic calcium phosphate nanoparticles coated with 2-carboxyethylphosphonic acid. *J. Mater. Chem.* **16,** 3964 (2006).

114. Products, L. D. Guidance for Industry Liposome Drug Products Guidance for Industry Liposome Drug Products. (2002).

115. Burgess, D. J., Crommelin, D. J. ., Hussain, A. S. & Chen, M.-L. Assuring quality and performance of sustained and controlled release parenterals. *Eur. J. Pharm. Sci.* **21,** 679–690 (2004).

116. Siewert, M., Dressman, J., Brown, C. K. & Shah, V. P. FIP/AAPS guidelines to dissolution/in vitro release testing of novel/special dosage forms. *AAPS PharmSciTech* **4,** E7 (2003).

117. Dutt, M. & Khuller, G. K. Liposomes and PLG microparticles as sustained release antitubercular drug carriers--an in vitro-in vivo study. *Int. J. Antimicrob. Agents* **18,** 245–52 (2001).

118. Avgoustakis, K. *et al.* PLGA-mPEG nanoparticles of cisplatin: in vitro nanoparticle degradation, in vitro drug release and in vivo drug residence in blood properties. *J. Control. Release* **79,** 123–35 (2002).

119. Cho, H.-J. *et al.* Polyethylene glycol-conjugated hyaluronic acid-ceramide self-assembled nanoparticles for targeted delivery of doxorubicin. *Biomaterials* **33,** 1190–200 (2012).

120. Zambito, Y., Pedreschi, E. & Di Colo, G. Is dialysis a reliable method for studying drug release from nanoparticulate systems?-A case study. *Int. J. Pharm.* **434,** 28–34 (2012).

121. Xu, X., Khan, M. a & Burgess, D. J. A two-stage reverse dialysis in vitro dissolution testing method for passive targeted liposomes. *Int. J. Pharm.* **426,** 211–8 (2012).

122. Dorozhkin, S. Medical Application of Calcium Orthophosphate Bioceramics. *Bio* **1,** 1–51 (2011).

123. Desai, N. Challenges in development of nanoparticle-based therapeutics. *AAPS J.* **14,** 282–95 (2012).

124. Kowalczuk, A. *et al.* Star-shaped nano-conjugates of cisplatin with high drug payload. *Int. J. Pharm.* **404,** 220–30 (2011).

125. Meerum Terwogt, J. M. *et al.* Phase I and pharmacokinetic study of SPI-77, a liposomal encapsulated dosage form of cisplatin. *Cancer Chemother. Pharmacol.* **49,** 201–10 (2002).

126. Veal, G. J. *et al.* A phase I study in paediatric patients to evaluate the safety and pharmacokinetics of SPI-77, a liposome encapsulated formulation of cisplatin. *Br. J. Cancer* **84,** 1029–35 (2001).

127. Zisman, N. *et al.* Optimizing Liposomal Cisplatin Efficacy through Membrane Composition Manipulations. *Chemother. Res. Pract.* **2011,** 213848 (2011).

128. Hainfeld, J. F. *et al.* Gold nanoparticles enhance the radiation therapy of a murine squamous cell carcinoma. *Phys. Med. Biol.* **55,** 3045–59 (2010).

129. Denaro, N., Russi, E. G. & Merlano, M. C. Strategies for non-resectable head and neck cancer. *Curr. Treat. Options Oncol.* **14,** 492–504 (2013).

130. Barroug, A. Lemaitre, J. Rouxhet, P. G. Lysozyme on Apatites. *Colloids and Surfaces* **37,** (1989).

131. Combes, C. & Rey, C. Amorphous calcium phosphates: synthesis, properties and uses in biomaterials. *Acta Biomater.* **6,** 3362–78 (2010).

132. Bose, S., Tarafder, S., Edgington, J. & Bandyopadhyay, A. Calcium phosphate ceramics in drug delivery. *Jom* **63,** 93–98 (2011).

133. Li, C. Crystalline behaviors of hydroxyapatite in the neutralized reaction with different citrate additions. *Powder Technol.* **192,** 1–5 (2009).

134. Jiang, W. *et al.* Atomic force microscopy reveals hydroxyapatite-citrate interfacial structure at the atomic level. *Langmuir* **24,** 12446–51 (2008).

135. Dosen, a. & Giese, R. F. Thermal decomposition of brushite, CaHPO4{middle dot}2H2O to monetite CaHPO4 and the formation of an amorphous phase. *Am. Mineral.* **96,** 368–373 (2011).

136. Yang, W.-L. *et al.* Development of cross-resistance between heat and cisplatin or hydroxyurea treatments in fadu squamous carcinoma cells. *J. Surg. Res.* **111,** 143–151 (2003).

137. Cullen, K. J., Newkirk, K. A., Schumaker, L. M. & Haddad, B. R. Glutathione S -Transferase π Amplification is Associated with Cisplatin Resistance in Head and Neck Squamous Cell Carcinoma Cell Lines and Primary Tumors Advances in Brief Glutathione S-Transferase Amplification is Associated with Cisplatin Resistance i. *Pathology* 8097–8102 (2003).

138. Iakovlev, V. V *et al.* Effect of distributional heterogeneity on the analysis of tumor hypoxia based on carbonic anhydrase IX. *Lab. Invest.* **87,** 1206–17 (2007).

139. Burgess, D. J., Crommelin, D. J. a, Hussain, A. S. & Chen, M.-L. Assuring quality and performance of sustained and controlled release parenterals: EUFEPS workshop report. *AAPS J.* **4,** 1–11 (2002).

140. Martinez, M. N., Rathbone, M. J., Burgess, D. & Huynh, M. Breakout session summary from AAPS/CRS joint workshop on critical variables in the in vitro and in vivo performance of parenteral sustained release products. *J. Control. Release* **142,** 2–7 (2010).

141. Brown, C. K. *et al.* FIP/AAPS joint workshop report: dissolution/in vitro release testing of novel/special dosage forms. *AAPS PharmSciTech* **12,** 782–94 (2011).

142. Li, X. *et al.* Superior antitumor efficiency of cisplatin-loaded nanoparticles by intratumoral delivery with decreased tumor metabolism rate. *Eur. J. Pharm. Biopharm.* **70,** 726–34 (2008).

143. Shikanov, A., Shikanov, S., Vaisman, B., Golenser, J. & Domb, A. J. Cisplatin tumor biodistribution and efficacy after intratumoral injection of a biodegradable extended release implant. *Chemother. Res. Pract.* **2011,** 175054 (2011).

144. Hu, D. *et al.* A novel modular polymer platform for the treatment of head and neck squamous cell carcinoma in an animal model. *Arch. Otolaryngol. Head. Neck Surg.* **138,** 412–7 (2012).

145. Lana, S. E. *et al.* SLOW RELEASE CISPLATIN COMBINED WITH RADIATION FOR THE TREATMENT OF CANINE NASAL TUMORS. *Vet. Radiol. Ultrasound* **38,** 474–478 (1997).

146. Yapp, D. T. T., Lloyd, D. K., Zhu, J. & Lehnert, S. M. TUMOR TREATMENT BY SUSTAINED INTRATUMORAL RELEASE OF CISPLATIN: EFFECTS OF DRUG ALONE AND COMBINED WITH RADIATION. *Int. J. Radiat. Oncol.* **39,** 497–504 (1997).

147. Yapp, D. T. T., Lloyd, D. K., Zhu, J. & Lehnert, S. M. THE POTENTIATION OF THE EFFECT OF RADIATION TREATMENT BY INTRATUMORAL DELIVERY OF CISPLATIN. *Int. J. Radiat. Oncol.* **42,** 413–420 (1998).

148. Almond, B. a *et al.* Efficacy of mitoxantrone-loaded albumin microspheres for intratumoral chemotherapy of breast cancer. *J. Control. Release* **91,** 147–55 (2003).

149. Epps, B. Y. H. L. V. A. N. Triple-Negative Breast Cancer : Divide and Conquer. (2010).

150. Luo, Y. & Prestwich, G. D. Synthesis and selective cytotoxicity of a hyaluronic acid-antitumor bioconjugate. *Bioconjug. Chem.* **10,** 755–63 (1999).

151. Bionique Testing Laboratories. What are Mycoplasmas ? *Mycoplasma Resour. Cent.* 1–2 (2011). at <http://www.bionique.com/files/whataremycoplasma.pdf>

152. Bionique Testing Laboratories. What are the consequences of mycoplasma contamination? *Mycoplasma Resour. Cent.* (2011). at <http://www.bionique.com/mycoplasma-resources/faq/consequences-of-mycoplasma-contamination.html>

153. Charafe-Jauffret, E. *et al.* Gene expression profiling of breast cell lines identifies potential new basal markers. *Oncogene* **25,** 2273–84 (2006).

154. Giocondi, J. L., El-Dasher, B. S., Nancollas, G. H. & Orme, C. a. Molecular mechanisms of crystallization impacting calcium phosphate cements. *Philos. Trans. A. Math. Phys. Eng. Sci.* **368,** 1937–61 (2010).

155. Hu, Y.-Y., Rawal, a & Schmidt-Rohr, K. Strongly bound citrate stabilizes the apatite nanocrystals in bone. *Proc. Natl. Acad. Sci. U. S. A.* **107,** 22425–9 (2010).

156. Martins, M. a, Santos, C., Almeida, M. M. & Costa, M. E. V. Hydroxyapatite micro- and nanoparticles: nucleation and growth mechanisms in the presence of citrate species. *J. Colloid Interface Sci.* **318,** 210–6 (2008).

157. Bleek, K. & Taubert, A. New developments in polymer-controlled, bioinspired calcium phosphate mineralization from aqueous solution. *Acta Biomater.* **9,** 6283–321 (2013).

158. Wang, F., Huang, P.-J. J. & Liu, J. Citrate inhibition of cisplatin reaction with DNA studied using fluorescently labeled oligonucleotides: implication for selectivity towards guanine. *Chem. Commun. (Camb).* **49,** 9482–4 (2013).

159. Han, S.-Y. *et al.* Mineralized hyaluronic acid nanoparticles as a robust drug carrier. *J. Mater. Chem.* **21,** 7996 (2011).

160. Cai, S., Xie, Y., Bagby, T. R., Cohen, M. S. & Forrest, M. L. Intralymphatic chemotherapy using a hyaluronan-cisplatin conjugate. *J. Surg. Res.* **147,** 247–52 (2008).

161. Jeong, Y. *et al.* Cisplatin-Incorporated Hyaluronic Acid Nanoparticles Based on Ion-Complex Formation. *Pharm. Nanotechnol.* **97,** 1268–1276 (2008).

162. Choi, K. Y. *et al.* Self-assembled hyaluronic acid nanoparticles for active tumor targeting. *Biomaterials* **31,** 106–14 (2010).

163. Tassa, C. *et al.* Binding affinity and kinetic analysis of targeted small molecule-modified nanoparticles. *Bioconjug. Chem.* **21,** 14–9 (2010).

164. Lesley, J., Hascall, V. C., Tammi, M. & Hyman, R. Hyaluronan binding by cell surface CD44. *J. Biol. Chem.* **275,** 26967–75 (2000).

165. Kumar, S., Xu, X., Gokhale, R. & Burgess, D. J. Formulation parameters of crystalline nanosuspensions on spray drying processing: a DoE approach. *Int. J. Pharm.* **464,** 34–45 (2014).

166. Luo, Y. & Prestwich, G. D. Synthesis and Selective Cytotoxicity of a Hyaluronic Acid−Antitumor Bioconjugate. *Bioconjug. Chem.* **10,** 755–763 (1999).

167. Luo, Y., Ziebell, M. R. & Prestwich, G. D. A hyaluronic acid-taxol antitumor bioconjugate targeted to cancer cells. *Biomacromolecules* **1,** 208–18 (2000).

168. Chen, Z. *et al.* Biomineralization inspired surface engineering of nanocarriers for pH-responsive, targeted drug delivery. *Biomaterials* **34,** 1364–71 (2013).

169. Levy-Nissenbaum, E. *et al.* Pharmacokinetic and efficacy study of cisplatin and paclitaxel formulated in a new injectable poly(sebacic-co-ricinoleic acid) polymer. *Eur. J. Pharm. Biopharm.* **82,** 85–93 (2012).

170. Mizrahy, S. *et al.* Hyaluronan-coated nanoparticles: the influence of the molecular weight on CD44-hyaluronan interactions and on the immune response. *J. Control. Release* **156,** 231–8 (2011).

171. Qhattal, H. S. S. & Liu, X. Characterization of CD44-mediated cancer cell uptake and intracellular distribution of hyaluronan-grafted liposomes. *Mol. Pharm.* **8,** 1233–46 (2011).

172. Platt, V. M. & Szoka, F. C. Anticancer Therapeutics : Targeting Macromolecules and Nanocarriers to Hyaluronan or CD44 , a Hyaluronan Receptor. *Mol. Pharm.* **5,** 474–486 (2008).

173. Albanese, A., Tang, P. S. & Chan, W. C. W. The effect of nanoparticle size, shape, and surface chemistry on biological systems. *Annu. Rev. Biomed. Eng.* **14,** 1–16 (2012).

174. Brannon-Peppas, L. & Blanchette, J. O. Nanoparticle and targeted systems for cancer therapy. *Adv. Drug Deliv. Rev.* **56,** 1649–59 (2004).

175. Wang, L. *et al.* CD44 antibody-targeted liposomal nanoparticles for molecular imaging and therapy of hepatocellular carcinoma. *Biomaterials* **33,** 5107–14 (2012).

176. Li, S., Zhang, X. & Xia, X. Regression of tumor growth and induction of long-term antitumor memory by interleukin 12 electro-gene therapy. *J. Natl. Cancer Inst.* **94,** 762–8 (2002).

177. Gurtner, K. *et al.* Combined treatment of the immunoconjugate bivatuzumab mertansine and fractionated irradiation improves local tumour control in vivo. *Radiother. Oncol.* **102,** 444–9 (2012).

178. Tijink, B. M. *et al.* A phase I dose escalation study with anti-CD44v6 bivatuzumab mertansine in patients with incurable squamous cell carcinoma of the head and neck or esophagus. *Clin. Cancer Res.* **12,** 6064–72 (2006).

179. Rupp, U. *et al.* Safety and pharmacokinetics of bivatuzumab mertansine in patients with CD44v6-positive metastatic breast cancer: final results of a phase I study. *Anticancer. Drugs* **18,** 477–85 (2007).

180. Sauter, A. *et al.* Pharmacokinetics, immunogenicity and safety of bivatuzumab mertansine, a novel CD44v6-targeting immunoconjugate, in patients with squamous cell carcinoma of the head and neck. *Int. J. Oncol.* **30,** 927–35 (2007).